Summer 2023

Diversity, Function, and Phenotypic Plasticity of Cryptophyte Phycobiliproteins

Kristiaän Merritt

DIVERSITY, FUNCTION, AND PHENOTYPIC PLASTICITY OF CRYPTOPHYTE PHYCOBILIPROTEINS

by

Kristiaän Merritt

Bachelor of Science
Clemson University, 2013

Submitted in Partial Fulfillment of the Requirements

For the Degree of Doctor of Philosophy in

Biological Sciences

College of Arts and Sciences

University of South Carolina

2023

Accepted by:

Tammi Richardson, Major Professor

Jeffry Dudycha, Committee Member

Brian Hollis, Committee Member

Daniel Speiser, Committee Member

Erin Meyer-Gutbrod, Committee Member

Ann Vail, Dean of the Graduate School

DEDICATION

This dissertation is dedicated to Marci Fish, who loved me long before I was born and whose love lasts long after her passing.

"How lucky I am to have something that makes saying goodbye so hard." A. A. Milne

ACKNOWLEDGEMENTS

I am so grateful for all the support I have received over the 4 years I've been at University of South Carolina. I would not be here without Dr. Tammi Richardson giving me the opportunity to work in her lab as a PhD student. I'm eternally grateful for her mentorship and the many ways she's both challenged me and supported me over the years. I am also grateful to Dr. Jeff Dudycha for encouraging me to relate the lessons learned from cryptophytes to broader evolutionary concepts. Thank you to Dr. Brian Hollis, Dr. Dan Speiser, and Dr. Erin Meyer-Gutbrod for serving on my committee and providing helpful feedback that has shaped this dissertation.

I also thank Dr. Amanda Ziegler for her mentorship as an educator and for the opportunity to develop my own teaching lab as a graduate student. I'm grateful to the many lab technicians and undergraduate research assistants whose hard work made my largest projects possible. I'm thankful for funding from the Slocum-Lunz Foundation and the USC SPARC graduate research grant that supported parts of this project. Thank you to the Department of Biological Sciences for fostering community, insightful conversations, and the best working environment I've ever been a part of.

I'm so thankful to the team at Lexington Neurology for working so hard to help me manage my chronic migraine disorder. I would not be able to finish this dissertation without their compassion and dedication to their patients.

Thank you to my dad and brother for setting the bar for success in our family so high. I especially thank my dad for telling me to go consider the complexity in a blade of

grass any time I was bored. I don’t think he realized then that I would eventually spend 4 years considering the complexity of algal photosynthesis. I will forever be grateful to my mom for genuinely believing there isn’t a single thing in the world I’m incapable of. Thank you to all my incredible friends, whose encouragement I envision as bleachers full of cheering fans. I’m thankful to Megan Thee Stallion, Trixie Mattel, and Barbra Striesand for inspiring the confidence it takes to share my work with the world. Thank you to the family members who supported me so much that they let me put them to work in the lab. Most of all, thank you to person whose love and support rivals that of my mom—Mark Merritt.

ABSTRACT

Cryptophytes are a group of unicellular eukaryotic algae that can be found in a wide range of underwater habitats. Part of their ecological success can be attributed to their diverse array of cryptophyte phycobiliproteins (Cr-PBPs), a pigment class that captures wavelengths of light that are poorly absorbed by chlorophylls. Cryptophytes gained photosynthesis via secondary endosymbiosis in which their ancestor engulfed a red algal endosymbiont. Following endosymbiosis, they deconstructed the red algal photosynthetic machinery to form the Cr-PBP. Since then, the Cr-PBPs have diversified into at least 9 spectrally distinct forms. I investigated the diversity of Cr-PBP light absorption across 76 cryptophyte strains and found that there were many overlooked differences within the commonly accepted Cr-PBP "types." I also found that adding criteria beyond the commonly used wavelength of maximum absorption can help distinguish between similar Cr-PBPs.

While cryptophytes are generally found in low-light intensity environments that are spectrally limited, little work has been done to determine whether they are low-light adapted and unable to live in environments with high light intensities. I constructed photosynthesis versus irradiance curves for 3 cryptophyte species in white, green, and red light using a ^{14}C radiolabel. I found that all three species had low (less than 100 μmol photons m^{-2} s^{-1}) compensation irradiance, but there was only photoinhibition in white light.

Finally, I used experimental evolution to determine whether 2 cryptophyte species in the genus *Hemiselmis* (*Hemiselmis rufescens* and *Hemiselmis tepida*) could adapt their Cr-PBP absorption spectra when grown in white, blue, green, or red light for hundreds of generations. Not only did *H. tepida* evolve in green light to use a Cr-PBP that resembles that of *H. rufescens*—it also evolved plasticity that allowed it to quickly switch between its ancestral Cr-PBP and the evolved Cr-PBP depending on the light environment. This finding may explain the diversity in Cr-PBP found in the genus *Hemiselmis*.

TABLE OF CONTENTS

LIST OF TABLES

LIST OF FIGURES

LIST OF SYMBOLS

α	Parameter describing the linear portion of the photosynthesis vs. irradiance curve at irradiance values less than compensation irradiance.
α-subunit	Smaller of two subunits in cryptophyte phycobiliproteins
β	Photoinhibition parameter describing the linear portion of the photosynthesis vs irradiance curve at irradiance values greater than compensation irradiance
β-subunit	Larger of two subunits in cryptophyte phycobiliprotein
λ	Wavelength
λ_{max}	Wavelength of maximal light absorption
μ	Growth rate
E_k	Compensation irradiance: the irradiance at which photosynthesis rate is maximal
P_{max}	Maximum photosynthetic rate

LIST OF ABBREVIATIONS

ANOVA ..... Analysis of variance

AP ..... Allophycocyanin

B-584 ..... Bilin 584

B-618 ..... Bilin 618

CCA ..... Complementary chromatic acclimation

CDOM ..... Colored dissolved organic matter

Chl ..... Chlorophyll

Chl-*a* ..... Chlorophyll *a*

Chl-*c* ..... Chlorophyll *c*

Cr-PBP ..... Cryptophyte phycobiliprotein

Cr-PC ..... Cryptophyte phycocyanin

Cr-PE ..... Cryptophyte phycoerythrin

DBV 15,16-dihydrobiliverdin

E ..... Irradiance

MBV ..... Mesobiliverdin

PBP ..... Phycobiliprotein

PC ..... Phycocyanin

PCB ..... Phycocyanobilin

PE ..... Phycoerythrin

PEB ..... Phycoerythrobilin

CHAPTER 1

INTRODUCTION

Light is a critical resource for phytoplankton, but light color in water can be highly variable depending on what's in the water. Depth, particulate organic matter, and colored dissolved organic matter (CDOM) change both the amount and spectrum of light available (Kirk 2011). Blue light reaches the lowest depths of the photic zone in clear, oligotrophic environments, while red light reaches the deepest in CDOM-rich waters (Kirk 2011, Blough and Del Vecchio 2002, Lawrenz et al. 2010). In eutrophic environments, green light reaches the lowest depths of the photic zone. As depth increases, light environments become more monochromatic (Stomp et al. 2007b). Differences in light spectra is one way that the water column is partitioned into many niches (Stomp et al 2007b).

Pigment composition determines the wavelengths of light that can be efficiently absorbed and used for photosynthesis by phytoplankton. Cryptophytes are a group of phytoplankton that gained their photosynthetic machinery from a secondary endosymbiosis event in which an ancient eukaryote engulfed a red algal cell (Archibald & Keeling 2002). Following this event, cryptophytes broke down a complex light harvesting antenna from red algae and used some of its components to evolve a simpler antenna known as the cryptophyte-phycobiliprotein (Cr-PBP) (Apt et al. 1995, Rathbone et al. 2021). Cr-PBPs are used to absorb wavelengths of light that are poorly absorbed by

chlorophylls. These Cr-PBPs come in a wide variety of colors ranging from red cryptophyte-phycoerythrins (Cr-PEs) to blue cryptophyte-phycocyanins (Cr-PCs). Historically, cryptophytes have been thought to only have a single Cr-PBP per species (e.g. Hill & Rowan 1989, Wedemayer et al. 1996, Hoef-Emden 2008).

There are nine spectrally distinct Cr-PBP types described in the literature, each named for the approximate wavelength of maximum absorption: Cr-PE 545, Cr-PE 555, Cr-PE 566, Cr-PC 564, Cr-PC 569, Cr-PC 577, Cr-PC 612, Cr-PC 630, and Cr-PC 645 (Hoef-Emden 2008; Overkamp, et al. 2014; Magalhães et al. 2021). While most cryptophyte genera only contain one or two Cr-PBP types, the genus *Hemiselmis* contains six of the nine types (Hoef-Emden 2008, Cunningham et al. 2019, Greenwold et al. submitted). *Hemiselmis* is the only genus to contain both Cr-PEs and Cr-PCs (Hoef-Emden 2008, Cunningham et al. 2019). The spectral diversity within *Hemiselmis* suggests a complicated evolutionary history regarding Cr-PBPs that involves multiple state changes between Cr-PEs and Cr-PCs (Hoef-Emden 2008, Greenwold 2019). On top of being especially evolutionarily labile with regard to Cr-PBP, some species in *Hemiselmis* have also been shown to have some degree of phenotypic plasticity in their Cr-PBP absorption spectra (Heidenreich & Richardson 2020, Spangler et al. 2022). *Hemiselmis cryptochromatica* and *Hemiselmis pacifica* can change their Cr-PBP absorption spectra depending on the spectral environment. These short-term, reversible changes are a type of phenotypic plasticity commonly referred to as complementary chromatic acclimation (Heidenreich & Richardson 2020).

Absorption characteristics of Cr-PBPs are derived from each of the two Cr-PBP components: the chromophores and the proteins to which they are covalently bound. The

chromophores found in Cr-PBPs are linear tetrapyrroles called phycobilins. Two of the phycobilins used by cryptophytes are present in red algae and cyanobacteria: phycoerythrobilin (PEB) and phycocyanobilin (PCB) (Glazer 1989, Glazer & Wedemayer 1995). Four of the phycobilins are only used by cryptophytes: dihydrobiliverdin (DBV), mesobiliverdin (MBV), bilin 584, and bilin 618 (Glazer & Wedemayer 1995). The protein component of Cr-PBPs consists of a dimer of two αβ monomers that form a ring-like quaternary structure (Doust et al. 2004). The quaternary structure is a tightly packed "closed form" in most cryptophyte species, but *Hemiselmis* species produce a donut-shaped "open form" quaternary structure resulting from an amino acid insertion on the α subunits (Harrop et al. 2014). The α subunits each bind a single chromophore at a conserved location, and the β subunits each bind 3 chromophores at conserved locations (Glazer & Wedemayer 1995). Cryptophytes can express up to 23 different α subunits, depending on the species (Kieselbach et al. 2018, Michie et al. 2023). The α subunits can interact with the bound chromophores to influence the Cr-PBP absorption spectrum (Michie et al. 2023).

In Chapter 2, I trace the evolutionary history of the Cr-PBP components from their roots in cyanobacterial and red algal phycobilisomes. I examine the ways cryptophytes evolved to have such a diverse range of phycobilins and Cr-PBPs since the secondary endosymbiosis event with red algae. I also contrast mechanisms of complementary chromatic acclimation in cyanobacterial PBPs to potential mechanisms of complementary chromatic acclimation in Cr-PBPs.

Chapter 3 highlights the diversity of Cr-PBP absorption characteristics within the 9 Cr-PBP types described in cryptophyte literature. Much what's written regarding Cr-

PBPs revolves around two major assumptions: 1) cryptophytes only have a single Cr-PBP type per species, and 2) Cr-PBP types are distinct, categorical traits (e.g. Hoef-Emden 2008, Cunningham et al. 2019, Greenwold et al. 2019). Under these two assumptions, there is an implicit third assumption that there should not be spectral variation in Cr-PBP absorption spectra. I examine this assumption by comparing extracted Cr-PBP absorption spectra within each Cr-PBP type using data from 76 cryptophyte species. While some Cr-PBP spectra from certain Cr-PBP types are similar across multiple species, others differ greatly within a single species.

In Chapter 4, I investigate how cryptophytes with different Cr-PBPs photosynthesize in white, green, and red light. I also determine the effect of historical light environment on photosynthesis in novel light environments. I constructed photosynthesis versus irradiance curves using *Proteomonas sulcata* with Cr-PE 545 and *Chroomonas mesostigmatica* with Cr-PC 645. I also used *Hemiselmis tepida* that had been grown in white, green, or red light. When grown white or red light, *H. tepida* uses Cr-PC 612. After growing in green light for 22 months, *H. tepida* uses a novel Cr-PBP with an absorption maximum at 560 nm. I found that whether cryptophytes are photoinhibited depends on species, light color, and historical light environment. I also found that each species in each color has a compensation irradiance that is less than 100 μmol photons m^{-2} s^{-1}.

Chapter 5 presents results from an experimental evolution project that was carried out over hundreds of generations in white, blue, green, and red light. After 3 years of growth (~370-540 generations) in each color of light *Hemiselmis rufescens* showed little change in its Cr-PBP absorption spectrum. In contrast *Hemiselmis tepida* gradually

changed its Cr-PBP absorption spectrum when growing in green light. It started with Cr-PC 612. Between 6-12 months it had a Cr-PBP spectrum that resembled that of Cr-PC 564 from *Hemiselmis aquamarina*. By the end of the experiment, it had a Cr-PBP with an absorption maximum near that of Cr-PE 555 from *Hemiselmis rufescens*. Additionally, *H. tepida* growing in green light evolved phenotypic plasticity, allowing it to change Cr-PBP spectra quickly (within 13 days/~5 generations) and reversibly in response to its light environment.

Finally, I conclude this dissertation in Chapter 6 by highlighting the importance of constantly reevaluating scientific frameworks in light of new evidence. I present a classic case study demonstrating how adherence to a flawed framework can impede scientific progress. I then present a case against the widely accepted framework that cryptophytes only have a single Cr-PBP per species. Rejecting this framework based on evidence in the literature and evidence presented in this dissertation, I propose that phenotypic plasticity in Cr-PBP absorption has greatly contributed to the diversity in Cr-PBPs in *Hemiselmis*.

CHAPTER 2

MAKING DO WITH LESS: THE EVOLUTIONARY HISTORY OF THE CRYPTOPHYTE PHYCOBILIPROTEINS

Abstract

Cryptophytes evolved via a secondary endosymbiosis event in which a eukaryotic ancestor engulfed a red algal endosymbiont. The red algal endosymbiont had a structurally complex and efficient light harvesting antenna called a phycobilisome inherited from their cyanobacterial endosymbiont. The phycobilisome is composed of a variety of pigment-protein complexes called phycobiliproteins (PBPs). Cryptophytes retained only a fraction of a single red algal PBP and modified it to create a simple but novel cryptophyte-PBP (Cr-PBP) antenna. While simple in structure, the Cr-PBP antenna achieves nearly the same energy transfer efficiency as the more complex phycobilisome. An advantage of the phycobilisome is that many organisms can modify the PBP content to suit their light environment in a process called complementary chromatic acclimation. Yet even without the phycobilisome, some cryptophytes are also capable of modifying their Cr-PBP absorption spectra to capture more light. This review gives an overview of the complicated evolutionary history of the Cr-PBP by tracing its roots back to the three major components of the phycobilisome (phycobilin chromophores, PBPs, and linker proteins). It will also compare complementary chromatic acclimation between organisms

that use a phycobilisome and cryptophytes and explore possible mechanisms in light of a potential paradigm shift in what we know about Cr-PBP content.

Introduction

Photosynthesis has undeniably shaped the atmosphere on Earth as well as the evolution of the organisms that inhabit it. The advent of oxygenic photosynthesis has led to a 100 to 1,000-fold increase in global organic productivity (Des Marais 2000). Oxygenic photosynthesis likely originated in cyanobacteria or their predecessors over 2 billion years ago (Buick 1992, Brocks et al. 2003, Dutkiewicz et al. 2006).

The phycobilisome is a major component of the photosynthetic machinery for most cyanobacteria. It evolved over 1 billion years ago in cyanobacteria before the last common ancestor of modern cyanobacteria and before primary endosymbiosis (the process by which an ancient cyanobacterium became a eukaryotic plastid) occurred (Apt et al. 1995). The phycobilisome is a structure made up of multiple phycobiliprotein (PBP) rods that sits on the outside of the thylakoid membrane and shuttles light energy to the photosystems (Figure 2.1) (MacColl 1998). Light is captured by tetrapyrrole chromophores called phycobilins that are covalently bound to the PBPs. Light energy captured by phycobilins is shuttled through the phycobilisome terminal energy acceptor to chlorophyll-*a* (chl-*a*) in the photosystems with over 95% efficiency *in vivo* (Glazer 1989).

PBPs absorb wavelengths of light in the middle of the photosynthetically available radiation (PAR) spectrum—the region that is most poorly absorbed by chl-*a* (MacColl & Guard-Friar 1987, Apt et al. 1995). By absorbing light that is poorly absorbed by chlorophylls, PBPs allow organisms to exploit more of the

photosynthetically available light spectrum than organisms that rely on chlorophylls alone (Stomp et al. 2007a). In cyanobacteria with phycobilisomes, the cell absorption spectrum can be modified in a process known as complementary chromatic acclimation (CCA) (reviewed by Kehoe & Gutu 2006, Sanfilipo et al. 2019). While this process is often referred to as complementary chromatic *adaptation*, complementary chromatic *acclimation* may be more appropriate, as these are short term, reversible shifts in absorption spectra. In any case, CCA allows organisms to change their absorption spectra in a way that allows for greater light capture when the spectral environment has changed.

All eukaryotic phototrophs gained their photosynthetic abilities from cyanobacteria through the process of endosymbiosis approximately 1 billion years ago (Shih & Matze 2013). Primary plastids were derived directly from the initial cyanobacterial endosymbiont. From one primary endosymbiosis event, the descendants of the first photosynthetic eukaryote quickly diverged into three distinct lineages: the red algae (rhodophytes), the green algae (chlorophytes), and the glaucophytes (reviewed by Keeling 2004, Oborník 2019). Of the three lineages, only rhodophytes and glaucophytes retained the phycobilisome. The chlorophyte lineage, which includes all land plants and green algae, has completely lost the phycobilisome.

Primary endosymbiosis initially brought photosynthesis to eukaryotes, but secondary and tertiary endosymbioses brought incredible diversity to the algae. Secondary endosymbiosis is the acquisition of a plastid by means of engulfing a phototrophic eukaryote from one of the three primary linages (Archibald & Keeling 2002). This has allowed for lateral spread of plastids between far removed eukaryotic lineages. Despite the incredible efficiency and the widening of spectral niches attributable

to the phycobilisome, no algal groups that originated from secondary endosymbiosis have retained the phycobilisome in its entirety (Green 2019).

While most algal lineages derived from secondary or tertiary endosymbiosis completely lost the phycobilisome, cryptophytes retained a part of it: the phycoerythrin (PE) β-subunit from the red algal phycobilisome (Apt et al. 1995). From this PE subunit, cryptophytes constructed a novel cryptophyte-PBP-based light harvesting antenna made up of two distinct α-subunits and two β-subunits (Wilk et al. 1999). (Note: much of the cryptophyte literature refers to cryptophyte-PBPs as PBPs, but because this review is also covering cyanobacterial/rhodophyte PBPs, which are structurally distinct from PBPs in cryptophytes, I will refer to cryptophyte-PBPs as Cr-PBPs throughout.) While the cryptophyte β-subunit is closely related to those found in red algae, the cryptophyte α-subunits are completely unrelated to those found in any phycobilisome (Wilk et al. 1999). This original PE has evolved and diversified over time within Cryptophyta, resulting in 9 spectroscopically distinct Cr-PBP pigments (Hoef-Emden & Archibald 2017, Magalhães et al. 2021). In addition to their novel Cr-PBP antennae, cryptophytes have also evolved to use multiple phycobilins not found in any other organism (Wedemayer et al. 1992). The innovations that cryptophytes have made to the original Cr-PBP have allowed them to diversify and occupy a multitude of spectral habitats.

While they did not retain the complete phycobilisome, cryptophytes are able to reap many of the benefits with a much simpler light harvesting antenna. Like the phycobilisome, the Cr-PBP antennae can capture light and shuttle light energy to the photosystems with nearly 100% efficiency (Doust, et al. 2004, Doust, et al. 2006). Cryptophytes also have more spectral niches available to them than algae that primarily

rely on chl-*a*. Recent work has shown that some cryptophytes are capable of CCA, despite the fact that most mechanisms of CCA in cyanobacteria rely on the phycobilisome (Heidenreich & Richardson 2019, Sanfilipo et al. 2019, Spangler, et al. 2022). This review will trace the evolution of the Cr-PBP antenna from the cyanobacterial phycobilisome and consider possible mechanisms of CCA in cryptophytes.

Phycobilisome Overview

Phycobilisomes are very large water-soluble complexes comprised of PBPs covalently bound to chromophores called phycobilins (MacColl 1998). The phycobilisome is situated like a satellite dish on the thylakoid membrane, in close proximity to the photosystems to allow for efficient energy transfer. PBP-based antenna rods radiate from a central core made up of a PBP called allophycocyanin (AP), in a hemi-discoidal shape (as seen in most cyanobacteria) (e.g.), hemi-ellipsoidal shape (as seen in most rhodophytes) (e.g.), and sometimes in such a way that rods are parallel to each other but perpendicular to the AP core (as in the cyanobacterial species *Gloeobacter violaceus*) (Gantt & Lipschultz 1972, Glazer et al. 1979, Gugliemi et al. 1981). The antenna rods are composed of stacked PBPs arranged from those that absorb high energy (low wavelength) light at the distal end to those that absorb lower energy photons at the proximal end.

Optimal intermolecular transfer of light energy occurs when the fluorescence of the excitation donor overlaps with the absorption spectrum of the excitation recipient (Förster 1948). This is why the PBPs are stacked from high energy absorbing at the ends of the antenna rods to low energy absorbing at the base: it is a physical arrangement that

provides optimal intermolecular transfer (Glazer 1989) (Fig. 2.1a). The same principle that applies to the PBPs also applies to phycobilins on the PBPs—phycobilins that absorb higher energy light fluoresce to pass excitation energy to phycobilins that absorb lower energy light (Fig. 2.1b). The energy donor phycobilins are arranged along the outside of a PBP hexamer ring and send the excitation energy to the acceptor phycobilins located on the inside of the ring. These then shuttle the light energy down to the next PBP ring on a rod.

The PBPs are brightly colored and get their light absorption properties from the covalently bound phycobilin chromophores. A single PBP monomer may be bound to 2-6 chromophores, depending on PBP type (Stadnichuk 1995). There are four types of phycobilin that may be present in cyanobacteria: phycocyanobilin (PCB), phycourobilin (PUB), phycoerythrobilin (PEB), and phycoviolobilin (PXB) (Reviewed in Stadnichuk 1995, MacColl 1998). These phycobilins are structurally very similar, differing only in number of double bonds and spectroscopic properties (Glazer 1989). Phycobilins are bound to the PBPs using thioether cysteine bonds. Like chlorophylls, phycobilins are also tetrapyrrole chromophores. Unlike chlorophylls, which have closed tetrapyrrole ring structures bound to a central magnesium atom, phycobilins are open chain tetrapyrroles without any metal atoms (Stadnichuk et al. 2015).

The linker proteins bind the PBP discs together and determine the structure of the phycobilisome. These proteins make up approximately 12-15% of the phycobilisome protein content (de Marsac & Cohen-Bazire 1977). Although the linker proteins are colorless, they can determine the absorption characteristics of the phycobilisome by changing the shapes and angles of the PBP rods (Watanabe & Ikeuchi 2013). They also

control interactions between the phycobilisome and the thylakoid membrane (Liu et al. 2005). The PBP rods may be visualized as beads on a wire, where each bead is a trimer $(\alpha\ \beta)_3$ or a hexamer $(\alpha\ \beta)_6$ of one PBP type and the linker proteins represent the wire holding a set of beads together from the inside and connecting them to a core structure.

Evolution of phycobilins

Phycobilins are the chromophoric component of the phycobilisome and Cr-PBPs. The similarities between chlorophylls and phycobilins do not stop at light absorption properties or structural similarities—both chromophores share the same biochemical pathway and, likely, evolutionary history. The Granick Hypothesis states that the biosynthesis pathway of a molecule recapitulates the evolution of that molecule (1965). Every intermediate molecule in a pathway was likely the end of the pathway at some point. Therefore, each step would have served a useful purpose that would later be improved upon. The biosynthetic pathways that are in place also allow for ease in development of new molecules. If a pathway is conceptualized as a large highway, new molecules can be interpreted as new exits being added to that highway. Like a highway, one major biosynthesis pathway may lead to multiple end points. Although proposed as something broadly applicable to biochemical evolution, Granick came to this hypothesis by studying the pathway that produces chlorophyll, heme, and phycobilins.

The phycobilin biosynthesis pathway follows the same steps as the chlorophyll biosynthesis pathway until protophorphyrin IX and the heme pathway until protoheme (Figure 2.2) (Stadnichuck et al. 2015). Use of oxygen in the removal of iron from protoheme implies that phycobilins likely evolved after the emergence of chl-*a* containing oxygenic phototrophs (Stadnichuck & Tropin 2014).

While cyanobacteria and rhodophytes only use 4 types of phycobilin, cryptophytes have 6 types: PCB and PEB (as in cyanobacteria and rhodophytes); 15,16-dihydrobiliverdin (DBV), bilin 584 (B-584), bilin 618 (B-618), and mesobiliverdin (MBV) (Glazer & Wedemayer 1995). The same biosynthesis pathway that may explain the evolution of the cyanobacterial and red algal phycobilins also helps explain the emergence of the novel cryptophyte phycobilins (Figure 2.2). DBV is a precursor to PEB as well as PUB and PXB (Frankenberg et al. 2001). PEB and MBV can be precursors to PCB (Beale 1993, Frankenberg & Lagarias 2003). While Granick considered evolution to be a "one-way road" (1965), it seems cryptophytes found a way to make use of multiple useful molecules in the biosynthesis pathway.

B-584 and B-618 are unique in that they have acryloyl groups at ring C of the tetrapyrrole (Wedemayer et al. 1992). These phycobilins are not found in any stage of any biosynthesis pathway outside of cryptophytes, but some have speculated that they could have evolved along their own pathway stemming from acrylo-porphyrin (Scholes et al. 2012).

Evolution of PBPs

While spectral qualities of cyanobacteria, rhodophytes, and cryptophytes primarily come from their phycobilins, they are also influenced by the protein portion of the PBPs. PBPs differ in which phycobilins are bound and how those phycobilins are arranged spatially. Cyanobacteria and rhodophytes contain AP, PE, and PC, where cryptophytes only contain Cr-PEs and Cr-PCs derived from a red algal PE. PBPs are further classified based on the type of organism in which they were discovered and, in the case of cryptophytes, the wavelength where their absorption is maximal (MacColl &

Guard-Friar 1987). Cyanobacteria and rhodophytes with phycobilisome always have AP, usually have cyanobacterial PC, and can have phycoerythrocyanin, rhodophyte-II PC, rhodophyte-III PC, cyanobacterial-PE, or urobilin-containing cyanobacterial-PE (Stadnichuk et al. 2015). Although the cyanobacterial and rhodophyte PBPs are named for the type of organism they were originally found in, they are not exclusive to one type of organism (Stadnichuk et al. 2015). Cryptophytes can contain Cr (for "cryptophyte")-PE 545, Cr-PE 555, Cr-PE 566, Cr-PC 564, Cr-PC 569, Cr-PC 577, Cr-PC 612, Cr-PC 630, or Cr-PC 645 (Hoef-Emden 2008, Overkamp et al. 2014, Magalhães et al. 2021). This section will explore the origins of PBPs in general and examine how the Cr-PBP evolved from pieces of the ancestral phycobilisome.

The homology between the α and β-subunits in cyanobacterial, red algal, and glaucophyte PBPs was recognized as evidence of gene duplication and diversification almost two decades before a phylogeny of PBP proteins across taxa was created (Glazer et al. 1976). A PBP phylogeny was inferred from amino acid sequences from 100 PBP subunits, including the terminal energy acceptor (TEA), a large polypeptide with a PBP-like domain at the base of the phycobilisome that funnels energy to the photosystems; AP; PC; PE; Cr-PC; and Cr-PE from cyanobacteria, rhodophytes, and cryptophytes (Apt et al. 1995). Ultimately this analysis suggests that all PBP subunits originated from a common ancestor that was likely most closely related to the TEA. The tree also shows the close relationship between the α and β subunits, suggesting that they've been coevolving for a long period of time. This scheme proposes that duplication of the ancestral gene gave rise to a pair of tandem PBP genes, which then diverged into the first α and β subunits. A duplication of the heterodimer pair may have then given rise to two

more lines of descent: the core (AP) and the rod (PE and PC) phycobiliproteins. The number of attachment sites for the phycobilins increased over time. Where there is variability in the number of phycobilins that can be attached to the PBP in cyanobacteria and red algae, all Cr-PBPs bind exactly 4 phycobilins—1 on the α-subunit and 3 on the β-subunit (Glazer & Wedemayer 1995). The attachment positions of the phycobilins on the apoprotein are conserved in cryptophyte PBPs: α-Cys 18 (or 19), β-Cys 50,61 (doubly linked bilin), β-Cys 82, and β-Cys 158 (Glazer & Wedemayer 1995). In cyanobacteria and rhodophytes, an increase in capacity to absorb shorter wavelengths of light evolved over time with the AP evolving first, then PCs, PEs, and PECs.

In Apt et al.'s PBP phylogeny, the amino acid sequences from eukaryotic PBPs were grouped together to the exclusion of cyanobacteria, suggesting that eukaryotic PBPs were derived from the same ancestral symbiont cyanobacteria (Apt et al. 1995). The β-subunits of Cr-PBPs were closely clustered with each other within the red algal PE β group, suggesting that all Cr-PBPs evolved from a red algal PE. Cryptophyte α-subunits did not share sequence similarity to any other subunits, including α-subunits from other organisms. This was not completely surprising as cryptophyte α-subunits, unlike cyanobacterial or rhodophyte α-subunits, are not homologous with β-subunits and are much smaller.

Following endosymbiosis of the rhodophyte cell by the cryptophyte ancestor, the phycobilisome was lost, and the structure of the PBP changed from an $(\alpha\beta)_6$ hexamer to an $\alpha_1\alpha_2\beta\beta$ tetramer (Glazer & Wedemayer 1995). The location of the PBP also changed drastically—while the phycobilisome is situated on the exterior of the thylakoid

membrane, the Cr-PBP antennae are located in the intrathylakoidal lumen (Gantt et al. 1971).

In red algae and cyanobacteria, the terminal energy acceptor phycobilin is always located at β-Cys 82 and is always a PEB for PEs or a PCB for PCs and APs (Ong & Glazer 1987, 1991). Cr-PBPs also only have PEB at β-Cys 82 for Cr-PE or PCB at the same site for Cr-PCs (Wedemayer et al. 1996). However, this site is not always the terminal energy acceptor site in Cr-PBPs. In fact, the terminal acceptor sites, and therefore the excitation transfer pathways, are variable across Cr-PBP types (Wedemayer, et al. 1996). The constraint in terminal energy acceptor site in cyanobacteria and red algae could be due to the high degree of structure and organization of the phycobilisome as well as its location on the thylakoid membrane. Perhaps Cr-PBPs are less constrained with respect to their energy pathways due to their placement within the thylakoid lumen. It's been shown for Cr-PE 545 that PBPs are densely packed in the lumen and don't have any apparent constraints on orientation with regard to other Cr-PBPs or to the thylakoid membrane (Hiller, et al. 1992). Thus, the Cr-PBPs could be spatially arranged in a way that accommodates different locations of the terminal energy acceptor. This flexibility could have allowed cryptophytes more opportunities to experiment with different chromophore compositions and placements during their evolution than cyanobacteria or red algae would have.

While cyanobacteria and red algae are usually capable of producing multiple PBPs per species, cryptophytes are generally thought to only have 1 Cr-PBP type per species (Hill & Rowan 1989, Wedemayer et al. 1996). In light of this, it's useful to match Cr-PBP types to organisms in a phylogeny to determine the order in which Cr-PBPs

evolved. Constructing cryptophyte phylogenies is particularly challenging because they have four genomes (cryptophyte nuclear, red algal nucleomorph, plastid, and mitochondrial genomes) which have undergone extensive intracellular horizontal gene transfer since the secondary endosymbiosis event (Douglas et al. 2001, Keeling 2004, Archibald 2020).

When phylogenies have been constructed previously, the trees imply multiple state reversals and an assortment of Cr-PBP types within multiple clades (e.g. Hoef-Emden 2008, Greenwold et al. 2019). While placement of some organisms differs across phylogenies based on the genes used, a few key features of Cr-PBP evolution stand out. Cr-PE 545 can be found in multiple clades. Cr-PE 566 is only found in the freshwater species from the genus, *Cryptomonas*. The *Chroomonas/Komma* (many species are named "*Chroomonas*" incorrectly, per Hoef-Emden 2018, and are closely related to *Komma*) and *Hemiselmis* genera tend to be grouped together, to the exclusion of non-*Hemiselmis*, Cr-PE containing cryptophyte species. *Chroomonas/Komma* species contain either Cr-PC 630 or Cr-PC 645 (although "true" *Chroomonas* only contain Cr-PC 630 per Hoef-Emden 2018). In the ultra-conserved element phylogeny in Figure 2.3, it appears that lineages within *Chroomonas/Komma* have switched between Cr-PC 630 and Cr-PC 645 over the course of their evolutionary history. These two Cr-PBPs share the same chromophore composition, but their spectra differ due to interactions between N-terminal amino acids on the α-subunit and the PCB on β-cys 82 that dictate the twist of the PCB (Michie et al. 2023). The situation is similar for Cr-PC 577 and Cr-PC 612, which are found in the *Hemiselmis* genus, except that 6 α-subunit amino acid residues in the middle of the α-subunit interact with the PCB on α-cys 20 (Michie et al. 2023). *Hemiselmis* is

the most diverse genus with regard to Cr-PBP type. It contains Cr-PE 545, Cr-PE 555, Cr-PC 564, Cr-PC 569, Cr-PC 577, Cr-PC 612 (Cunningham et al. 2019, Magalhães et al. 2021, Greenwold et al. submitted).

Some changes in Cr-PBP type between different cryptophyte species have relatively simple explanations like a change in protein conformation while keeping the same chromophores (Michie et al. 2023). However, Cr-PBP changes that involve changes to chromophore composition are difficult to resolve parsimoniously. For example, if a cryptophyte containing Cr-PE 566 evolved from a cryptophyte containing Cr-PE 545, every phycobilin except for the PEB on β-cys-82 would need to change to B-584 or B-618 (Table 2.1). This change would involve the creation of a biosynthesis pathway for B-584 and B-618 and the replacement of a DBV on the α-subunit and two PEBs on the β-subunit. The change from Cr-PE 545 to any Cr-PC requires recreating a biosynthesis pathway to create PCB that happens to have the same structure as cyanobacterial PCB. Of the cryptophyte phycobilin attachment sites, the α-Cys-19 site appears to be the easiest site to change as it has 6 possible phycobilins depending on the Cr-PBP type. β-cys-82 is only ever used to attach PEB or PCB, while β-Cys 50,61 and β-Cys-158 have 3 and 4 possibilities, respectively.

Unlike cyanobacteria, which began with a long-wavelength-absorbing PBP (AP) and later evolved short-wavelength-absorbing PEs (Apt, et al. 1995), cryptophytes most likely began their Cr-PBP evolution with Cr-PE 545 from the endosymbiont ancestor (Greenwold et al. 2019). This conclusion aligns with results from Apt et al. (1995) which demonstrate that Cr-PBPs evolved from a rhodophyte PE. Interestingly, the ancestral Cr-PE has the shortest wavelength of maximum absorption compared to the other Cr-PBPs.

This means that the direction of evolution of light absorption spectra in PBPs is reversed in cryptophytes as compared to cyanobacteria **(**Fig. 2.4**)**. Assuming that cryptophytes reduced the red algal phycobilisome to the ancestral Cr-PE 545 early in their evolution, Cr-PC would have to have evolved in cryptophytes from Cr-PE. Thus Cr-PC is an interesting case of convergent evolution towards an absorption spectrum and chromophore composition that is similar to cyanobacterial PC.

While the order of evolution of PBP types is reversed in cryptophytes compared to cyanobacteria (i.e. AP → PE in cyanobacteria versus Cr-PE → Cr-PC in cryptophytes), the evolution towards a more generalist strategy regarding light capture can be considered parallel. Cyanobacteria evolved the ability to produce multiple PBP types in one cell and change their absorption spectrum by modifying their phycobilisome (more details in section on complementary chromatic acclimation). This widened their spectral niche by allowing them to efficiently capture light in many types of spectral environments (e.g. a blue open ocean, a green eutrophic environment, or a red CDOM-rich environment). While cryptophytes do not seem able to change Cr-PBP type based on their environment, some have evolved a more generalist strategy compared to using the ancestral PE-545. Greenwold et al. (2019) found that as the wavelength of maximum absorption in Cr-PBPs increased, so too did photosynthetically usable radiation (PUR) in white light. This means that cryptophytes with Cr-PCs can efficiently capture a wider range of wavelengths of light than cryptophytes with Cr-PEs. The increase in PUR is attributable to the shape of Cr-PC absorption spectra, which have a larger full-width at half max compared to PEs (Fig. 2.5 and Table 2.2).

Linker Proteins

Linker proteins make up approximately 15% of the cyanobacterial phycobilisome protein content (de Marsac & Cohen-Bazire 1977). These proteins are the molecular skeleton of the phycobilisome, and changes to the conformation of the linker proteins can change the absorption properties of the phycobilisome (Reviewed by Watanabe & Ikeuchi 2013, Sui 2021). Although they are generally colorless, linker proteins aid in transfer of light energy through the phycobilisome, stabilize phycobilisome structure, and determine the position of PBPs within the phycobilisome. There are several classifications of linker protein depending on their location within the phycobilisome and their size: L_{CM} between the AP core and the thylakoid membrane (70-120 kDa), L_C in the phycobilisome core (7.7-7.8 kDa), L_R in the PBP rods (27-35 kDa), and L_{RC} between the core and rods (25-27 kDa).

L_Rs are specific to the PBP type in a cyanobacterial rod (MacColl 1998). Thus, in order to change PBP composition in response to a changing light environment, it's also necessary to change the corresponding L_Rs. In addition to changing the PBP composition, linker proteins in some cyanobacteria can change the shape of the phycobilisome in a way that captures more light (Westermann & Wehrmeyer 1995). L_Rs are arranged in a precise order within the phycobilisome rod, assuring that PBPs are arranged in order of highest energy light absorption to lowest energy light absorption (Watanabe & Ikeuchi 2013). This allows for the most efficient flow of light energy from the distal PBPs to the AP core and into the photosystems.

While nearly all PBP genes remained in the plastid genome following primary endosymbiosis, many of the linker protein genes were moved to the red algal nuclear

genome through the process of endosymbiotic gene transfer (Lee et al. 2019). The L_R genes were all moved to the red algal nucleus and greatly diversified following this event (Lee et al. 2019). Although most linker proteins are colorless, some red algal L_Rs can bind directly to phycobilins (e.g. Zhang et al. 2017). The chromophorylated L_Rs in red algae have been called γ subunits and tend to be associated with red algal PE (Klotz & Glazer 1985; Nagy et al. 1985).

Since cryptophytes do not have a phycobilisome, it's understandable that the connection between cryptophytes and linker proteins has generally not been explored in depth. Recently, however, Rathbone et al. (2021) noticed that part of a red algal L_R in published phycobilisome structures from *Porphyridium purpureum* (Ma et al. 2020) and *Griffithsia pacifica* (Zhang et al. 2017) bears striking resemblance to the cryptophyte α subunit. Strangely, the tail of the red algal linker, L_R6, was bound to a PE β-subunit that was not bound to a corresponding α-subunit. A structural comparison of the PE β-subunit bound to the L_R6 tail and the cryptophyte αβ protomer found striking similarity (Rathbone et al. 2021). Rathbone et al. (2021) found multiple cryptophyte α-like motifs (dubbed CALM domains) in red algal protein sequences. The sequence similarity between CALM domains in red algae and cryptophyte α-subunits was comparable to the sequence similarity between different cryptophyte α subunits.

Based on structural similarities, Rathbone et al. (2021) proposed that the cryptophyte α subunit evolved from CALM domains that were previously coded for in the red algal nucleus. They hypothesize that CALM domains and the red algal α-subunits would have competed within the cell to bind to the PE β-subunits. Eventually the proto-cryptophyte α outcompeted the red algal α and led to the current cryptophyte antenna.

Over time the cryptophyte α would gain a chromophore binding loop containing cysteine to attach a fourth phycobilin to the Cr-PBP antenna. This solution neatly resolves the issue of nonhomology between the cryptophyte α and red algal/cyanobacterial α-subunit put forth by Apt et al. (1995). It also highlights the importance of studying the protein structures and biology of endosymbionts in order to understand the biology of the modern host.

Similar to the way many linker protein genes from cyanobacteria moved to the red algal nucleus following endosymbiosis, the genes that encode the cryptophyte α-subunits moved from the red algal endosymbiont to the cryptophyte nucleus (Curtis et al. 2012). Unlike the β-subunit, which is encoded by a single, highly conserved plastid gene, the cryptophyte α-subunits are encoded by a large gene family (Curtis et al. 2012). A single cryptophyte species can transcribe as many as 20 distinct α-subunits, including α-subunits that would yield varying spectral absorption characteristics of the Cr-PBP (Kieselbach et al. 2018, Michie et al. 2023). Michie et al. (2023) built on Rathbone's (2021) model for evolution of the α-subunit. They proposed that once inside the cryptophyte nucleus, the gene for the α-subunit progenitor underwent multiple rounds of gene duplication and diversification to form the extant multigene families.

Complementary Chromatic Acclimation

The variation that has evolved in cyanobacterial, red algal, and cryptophyte pigmentation allows these organisms to capture light in a wide range of habitats. Phytoplankton with PE or Cr-PE can photosynthesize efficiently in eutrophic environments where green light penetrates the deepest (Stomp et al. 2007a). Phytoplankton with PC or Cr-PC can efficiently capture red light which is most abundant

in lakes with high amounts of colored dissolve organic matter (CDOM). However, light color in water is not just variable across habitats, but also in the same habitat over time (e.g. seasonal changes in CDOM input, surface algae blooms, or high rainfall events). To cope with this, cyanobacteria have evolved multiple strategies to change their absorption spectra to complement their spectral environment. Broadly, this is referred to as complementary chromatic acclimation/adaptation (CCA). It should be noted that in the literature the terminology is inconsistent—some authors refer to temporary changes in phytoplankton absorption spectrum as complementary chromatic *adaptation* rather than *acclimation*. Because adaptation often refers to long-term, permanent changes, this paper will use CCA to mean complementary chromatic acclimation and to refer to short-term, reversible changes.

CCA has been extensively studied in cyanobacteria for over a century (Engalmann 1902, Gaidukov 1902, Gaidukov 1903). Six types of CCA have been described in cyanobacteria (reviewed in Sanfilipo et al. 2019):

- CA1: A change in L_{RC} converts a phycobilisome that contains a typical AP core in red light to a phycobilisome with no core in green light
- CA2: PBP rods are longer and contain more PE discs in green light and are shorter with fewer PE discs in red light
- CA3: PBP rods are primarily composed of PEB-rich PE in green light but switch to rods primarily composed of PCB-rich PC in red light
- CA4: Phycobilin composition on PBP rods is PUB dominated in blue environments and PEB dominated in green environments

- CA5: PC rods are present in red light (~660 nm), but deleted and replaced with Chl-*d* based antennae in far-red (>700 nm)
- CA6: Typical AP core and photosystems using Chl-*a* in red light (~660 nm) are replaced with far-red shifted AP and far-red shifted photosystem using Chl-*d, f* in far-red light (>700 nm)

A few key similarities in all types of CCA stand out. Unsurprisingly, they all involve modifications to the chromophore composition either directly (CA3 and CA4) or indirectly (CA1, CA2, CA5, and CA6). All changes serve to increase photon capture, and therefore energy, in the corresponding light environment. CCA is reversible if the light environment changes. Finally, all changes depend on the ability to modify the phycobilisome structure and/or the ability to synthesize multiple types of PBP.

Because cyanobacteria use modifications to the phycobilisome for most types of CCA, it would be reasonable to assume that cryptophytes wouldn't be capable of CCA. In fact, early investigations into whether cryptophytes were capable of CCA showed such underwhelming results that one author wondered if Cr-PBPs were used to store nitrogen more than they were used for photosynthesis (Ojala 1993). However, more recent studies used different species of cryptophytes and incubated them for longer time periods in different colors of light (Heidenreich & Richardson 2019, Spangler et al. 2022). These studies found that some cryptophytes could modify their Cr-PBP absorption spectra in certain light conditions.

Peak shifts of 4-5 nm in cryptophytes in different colors of light have previously been associated with differences in thylakoid stacking within the chloroplast (Vesk & Jeffrey 1977). Another CCA mechanism in cryptophytes is changing the whole cell

absorption spectrum by changing the pigment composition—i.e. producing more or less Cr-PBP relative to Chl-*a* (Scholes et al. 2012, Heidenreich & Richardson 2020, Latsos et al. 2021, Spangler et al. 2022). While those mechanisms allow for CCA without modifying the Cr-PBP, it is also possible for CCA to occur in cryptophytes via the Cr-PBP.

Interestingly, the clearest examples of cryptophyte CCA were found in the genus *Hemiselmis* with Cr-PC (*Hemiselmis cryptochromatica* in Heidenreich and Richardson 2020 and *Hemiselmis pacifica* in Spangler et al. 2022). This genus not only appears to be the most evolutionarily labile with respect to Cr-PBP type, but also shows the most phenotypic plasticity in its Cr-PBP absorption spectra.

When the aptly named *H. cryptochromatica* was initially described, its Cr-PBP was classified as Cr-PC 630 and its color was described as faint gray (Lane and Archibald 2008). It was later described as having Cr-PC 569 with a secondary peak at 630 nm (Cunningham et al. 2019). As Heidenreich & Richardson (2020) discovered, the peak wavelength for *H. cryptochromatica*'s Cr-PC depends on its light environment. The absorption spectrum for Cr-PC extracted from *H. cryptochromatica* has two clear peaks: one in the 568-574 nm range and one in the 610-630 nm range. The dominant peak is defined as the wavelength with the highest absorption. In white (full spectrum) and green light, *H. cryptochromatica* has a dominant peak at 568-573 nm (Table 2.3), but in blue light the peak is at approximately 611 nm, and in red light the peak is at 625 nm (Heidenreich & Richardson 2020). Not only do the dominant and secondary peak switch, but the position of the peak changes based on light environment. The changes to the Cr-PBP absorption spectrum had a clear impact on the visual appearance of the cells as well

(Figure 5 from Heidenreich & Richardson 2020). In white and red light, *H. cryptochromatica* is a yellowish green color. In green light, it's orange, and in blue light, it's a bluish green color.

Given the variability in the Cr-PBP absorption spectra of *H. cryptochromatica* based on light environment, it's not surprising that authors have disagreed on which Cr-PBP *H. cryptochromatica* actually contains. This finding calls into question the utility of classifying cryptophytes based on their Cr-PBP. Interestingly, *H. cryptochromatica* in blue light has a combination of primary and secondary peak that matches the peaks found in extracted Cr-PC 612 from *Hemiselmis tepida* (Table 2.1). Did *H. cryptochromatica* change its Cr-PBP to Cr-PC 612 in blue light? This change would require changing B-584 on the β-50,61-Cys to DBV and the B-584 on β-Cys-158 to PCB. Confoundingly, this change doesn't increase blue light absorption and narrows the range of Cr-PBP light absorption (Fig. 2.6). So why did *H. cryptochromatica* change in this way? How did these changes happen in just over 10 generations?

In contrast to the seemingly non-complementary changes in blue light, *H. cryptochromatica* changed its Cr-PBP to absorb green light more efficiently in green light (Heidenreich & Richardson 2020). The primary peak in green light shifted approximately 4 nm towards the green part of the light spectrum. More dramatically, it increased the magnitude of this peak relative to the secondary peak. In full spectrum, blue, and red light, the primary peak is only 5-12% taller than the secondary peak (Table 2.3). In green light, the primary peak is 55% larger than the secondary peak. If a Cr-PBP's absorption is based on chromophore composition and cryptophytes only have one type of Cr-PBP in a species, how could a cryptophyte adjust the magnitude of one of its peaks?

Spangler et al. (2022) found that another Cr-PC-containing cryptophyte, *H. pacifica*, is also capable of modifying its Cr-PBP absorption spectrum in green light, shifting the leading and falling edges of spectrum in the direction of the green light emission spectrum. They also found that this change is reversible when the light environment returns to full spectrum light. Spangler et al. (2022) hypothesized that the change in Cr-PBP absorption spectrum could be caused by a change in Cr-PBP conformation due to an amino acid insertion ("open" vs. "closed" as shown in Harrop et al. 2014, Corbella et al. 2019) or due to changing phycobilin composition similarly to CA4 in cyanobacteria. X-ray crystallography and electrospray ionization mass spectroscopy revealed that there were no changes in mass or conformation of the apoprotein when grown in green light as compared to white light. By eliminating the hypothesis that changes to the protein conformation or tertiary structure caused the Cr-PBP spectrum shift, the authors concluded that changes in the phycobilin composition are the likely cause.

Based on the parts of the spectrum that were modified and the phycobilins with the most likely contribution to those areas, Spangler et al. (2022) propose that *H. pacifica* produced more DBV than PCB. They also separated the α and β subunits and evaluated the spectrum of each after being grown in green and white light. They found the same shifts in the β subunit spectrum as in the full PBP spectrum, indicating that *H. pacifica* likely substituted DBV for a PCB somewhere on the β subunit. Based on the modest shifts in Cr-PBP spectra and assuming cryptophytes only have the capacity to produce one Cr-PBP type per species and that it's unlikely they'd maintain biosynthetic pathways for other phycobilins, the authors conclude that the only two phycobilins at play are DBV

and PCB. Finally, they demonstrate that the binding site that has been shown to bind PCB has a geometry that is compatible with DBV.

Changes in phycobilin composition neatly resolves the changes in Cr-PBP absorption spectra for *H. pacifica* and *H. cryptochromatica* in green light, but what about the change in blue light? While the phycobilin composition has not been determined for *H. cryptochromatica* specifically, it has been determined for *Falcomonas daucoides*, which has Cr-PC 569 with peaks in the same location as *H. cryptochromatica* grown in white, green, and red light. Cr-PC 569 has PCB on the α-Cys-19 and β-Cys-82 positions and B-584 at β-Cys-50,61 and β-Cys-158 (Wedemayer et al. 1996). If changes in the proportion of B-584: PCB in Cr-PC 569 could reasonably account for the change in peak magnitude while maintaining peak locations for the *H. cryptochromatica* PCr-BP spectrum, then a larger jump in the location of a peak should not have the same explanation. Could *H. cryptochromatica* be switching two of its phycobilins (and replacing one with a phycobilin not observed in Cr-PC 569) to create Cr-PC 612? Could this change be due to a conformational change due to amino acid insertion? Is there a third mechanism that hasn't been explored?

Conclusion

Tracing the evolutionary history of the Cr-PBPs from their roots in cyanobacterial phycobilisomes through cryptophytes answers some questions but raises many more. Did cryptophytes reinvent a PCB that's identical to cyanobacterial PCB after only keeping Cr-PE? Why would cryptophytes only keep one subunit of red algal PE when it has the least amount of overlap with chl-*a* absorption? How is cryptophyte light energy transfer nearly as efficient as cyanobacterial light energy transfer without the phycobilisome?

Why do cryptophytes begin with a Cr-PE and evolve Cr-PCs later when cyanobacteria started with AP and later evolved PC and PE? Why is *Hemiselmis* so diverse with regard to Cr-PBP type when most other cryptophyte genera only have 1-2 Cr-PBP types and no other genus has both Cr-PE and Cr-PC? Why and how can only some cryptophytes change their PBP absorption spectrum to suit their light environment?

Much of the confounding nature of the evolution of Cr-PBPs can be linked to the assumption that cryptophytes only retained a single Cr-PBP. What if this assumption has been incorrect? Recently, it was discovered that a strain of *Hemiselmis andersenii* (CCMP 1180) has at least 3 distinct Cr-PBP types (Rathbone 2021). In addition to Cr-PE 555, Rathbone found a Cr-PBP with a peak at 560 nm, and a third with a peak at 560 nm and another at 645 nm. He names these "spectrotypes" with the prefix *Ha* to indicate that the Cr-PBPs came from *Hemiselmis andersenii* and distinguish them from each other since they have previously been analyzed as a single Cr-PBP. *Ha*PE555 comprised the vast majority of the Cr-PBP content in *H. andersenii*, with the other spectrotypes making up a much smaller fraction. This fraction would have been easy to discount as noise by investigators who lived by the dogma that cryptophytes only have one Cr-PBP.

The *Ha*PE555 absorption spectrum (Fig. 2.7) does not overlap well with chl-*a* or chl-*c*, which means that it should not be able to transfer energy to the photosystems particularly efficiently. However, using excitation-emission maps, Rathbone (2021) was able to demonstrate that *Ha*PE555 can transfer energy back and forth with *Ha*PE560. *Ha*PE555 and *Ha*PE560 can then transfer excitation energy to *Ha*PE645. Critically, *Ha*PE645 can efficiently pass excitation energy to the chlorophylls in the photosystems. Rathbone proposes that *Ha*PE645 is linked to the photosystems inside the thylakoid with

the other two spectrotypes filling the rest of the thylakoid lumen. If this finding is broadly applicable to cryptophytes, it would neatly answer the question of how cryptophytes have such efficient energy transfer to the photosystems. Rather than a PBP rod that requires a fixed proportion of distinct PBPs to satisfy the Förster (1948) model of excitation energy transfer, cryptophytes can invest in making much more of the Cr-PBP type that suits the light environment while making less of a Cr-PBP that exists to serve as a bridge between the main Cr-PBP and the photosystems.

The existence of a 645 nm peak on *Ha*PE645 prompted Rathbone (2021) to investigate the chromophore composition. Strangely, not only does *Ha*PE645 contain a PCB, it also contains asymmetrical β subunits—one with a PEB at β-Cys-82 and the other with PCB at β-Cys-82. This is the first time PEB and PCB have been found in the same cryptophyte AND the first time they've both been found on a cryptophyte $\alpha_1\alpha_2\beta\beta$ tetramer. As strange as this finding is, it does mean that if this is in any way indictive of a Cr-PBP the first cryptophyte ancestor had, cryptophytes would not have had to reinvent PCB.

If ancient cryptophytes had a pigment similar to *Ha*PE645 that could efficiently transfer energy to the photosystems, there's less of a paradox surrounding which Cr-PBP they "started" with. Rather than inferring that they began with Cr-PE 545 alone and evolved Cr-PCs later, opposite to the direction of evolution of cyanobacterial PBPs, it could be that cryptophytes have always had multiple Cr-PBPs. In fact, Michie et al. (2023) found that 11 cryptophyte species across multiple clades each expressed between 13 and 23 distinct α-subunit genes. They also demonstrated that differences in α-subunit amino acid sequences account for major differences in Cr-PBP spectra. If the same

cryptophyte is producing multiple α-subunits that, when paired with a β-subunit, produce different Cr-PBP absorption spectra, are they not, by definition producing multiple Cr-PBPs? In addition to retaining many α-subunit genes, it's possible cryptophytes retained the genes involved in the biosynthesis pathways for more than just PEB and DBV following secondary endosymbiosis.

Finally, if cryptophytes have multiple Cr-PBPs, maybe the ones capable of CCA are simply changing the proportions of their existing Cr-PBPs in response to light environments. Michie et al. (2023) showed that species in *Hemiselmis* produce α-subunits for both open and closed Cr-PBP conformations. Maybe these species are more capable of CCA than other cryptophytes because they're able to control the expression of their α subunits differentially. This possibility is not mutually exclusive with phycobilin swapping, and in fact, expands the possibilities. In order to produce the three Cr-PBP types found in Rathbone 2021, *Hemiselmis andersenii* had to synthesize PEB, DBV, and PCB. Depending on geometric fit in the Cr-PBP binding pocket, this expands the combinations of chromophore and binding site and, therefore, Cr-PBP absorption spectrum possibilities. On the other hand, if so many cryptophytes have multiple Cr-PBPs and potentially more phycobilins available, why do so few change their Cr-PBP absorption spectrum complementarily to their environment?

It will be important to replicate Rathbone's work in *H. andersenii* in a wide variety of cryptophytes in the future. It's worth pointing out that this work was on a species in the *Hemiselmis* genus. As this paper has discussed, *Hemiselmis* is particularly evolutionarily labile and shows particularly high phenotypic plasticity with regard to its Cr-PBP absorption spectrum. It will also be important to follow up on the work of Michie

et al. (2023). It will be important to determine how the many forms of α-subunit they found change the Cr-PBP absorption spectrum within the same cryptophyte species. Other authors have modeled cryptophyte light energy transfer while operating under the assumption that cryptophytes only have one Cr-PBP type (e.g. Doust et al. 2006, van der Wiej-De wit et al. 2006).

Tables

Table 2.1. Cr-PBP chromophore composition and absorption maxima in white light. Modified from Richardson 2022 with permission. Cr-PC 564 added from Magalhães et al. 2021. Bilin 618 on α-Cys-19 added from Wedemayer et al. 1992—some strains of *Cryptomonas ovata* have Bilin 584 in this position while others have Bilin 618 at this position. Chromophore on β-Cys-158 of Cr-PC 577 corrected to PCB based on Michie et al. 2023.

Cr-PBP	***Chromophore binding site***				***1° and 2° (if applicable) λ of maximum absorption (nm)***	***Species used***
	α-Cys-19	**β-Cys-50,61**	**β-Cys-82**	**β-Cys-158**		
Cr-PE 545	DBV	PEB	PEB	PEB	545	*Rhodomonas salina*
Cr-PE 555	PEB	DBV	PEB	PEB	555	*Hemiselmis rufescens*
Cr-PE 566	bilin 584 or bilin 618	bilin 584	PEB	bilin 584	566	*Cryptomonas ovata*
Cr- PC 564	Unknown	Unknown	Unknown	Unknown	564, 618	*Hemiselmis aquamarina*
Cr-PC 569	PCB	bilin 584	PCB	bilin 584	569, 625	*Falcomonas daucoides*
Cr-PC 577	PCB	DBV	PCB	DBV	577, 612	*Hemiselmis pacifica*
Cr-PC 612	PCB	DBV	PCB	PCB	612, 577	*Hemiselmis virescens*
Cr-PC 630	MBV	DBV	PCB	PCB	630, 583	*Chroomonas* sp.
Cr-PC 645	MBV	DBV	PCB	PCB	645, 585	*Chroomonas mesostigmatica*

Table 2.2. Full width at half max (FWHM) measurements for Cr-PBPs extracted from representative cryptophyte strains.

Cr-PBP Type	FWHM (nm)	Representative Strain
Cr-PE 545	68	*Rhodomonas salina* CCMP 1319
Cr-PE 555	55	*Hemiselmis rufescens* CCMP 440
Cr-PE 566	63	*Cryptomonas ovata* CCAC 1633B
Cr-PC 564	110	*Hemiselmis aquamarina* RCC 4102
Cr-PC 569	106	*Hemiselmis cryptochromatica* CCMP 1181
Cr-PC 577	96	*Hemiselmis pacifica* CCMP 706
Cr-PC 612	88	*Hemiselmis tepida* CCMP 443
Cr-PC 630	101	*Chroomonas vectensis* K-0432
Cr-PC 645	103	*Chroomonas mesostigmatica* CCMP 1168

Table 2.3. Unpublished data from Heidenreich and Richardson 2020, shared with permission. 1st peak is defined here as the Cr-PBP absorption peak with the smaller wavelength, and 2nd peak is defined as the Cr-PBP absorption peak with the larger wavelength. % difference in peak absorption was calculated by taking the difference between the two peak absorptions and dividing by the absorption at the dominant peak. Dominant peak is defined as the wavelength with the highest absorption.

Light treatment	*1st Peak (nm)*	*2nd Peak (nm)*	*% difference in peak absorption*	*Dominant peak (nm)*
White	572 ± 0.5	625 ± 0	12 ± 0%	572 ± 0.5
Blue	571 ± 0.6	611 ± 0.8	5 ± 0%	611 ± 0.8
Green	568 ± 0.5	626.5 ± 1	55 ± 2%	568 ± 0.5
Red	574 ± 0	625 ± 0	9 ± 1 %	625 ± 0

Figures

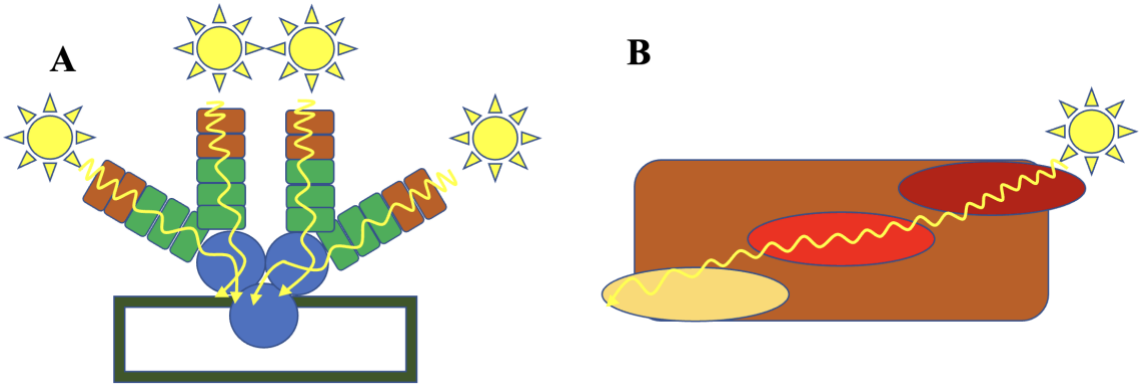

Figure 2.1. A. Cartoon representation of a phycobilisome attached to a photosystem on the thylakoid membrane (dark green box). Outermost orange blocks represent phycoerythrin hexamers, green blocks represent phycocyanin hexamers, and blue circles represent allophycocyanin. Suns and arrows represent incoming light and the flow of light energy. B. Cartoon representation of phycobilins attached to a phycoerythrin subunit. Each oval represents a unique phycobilin. Suns and arrows represent incoming light and the flow of light energy.

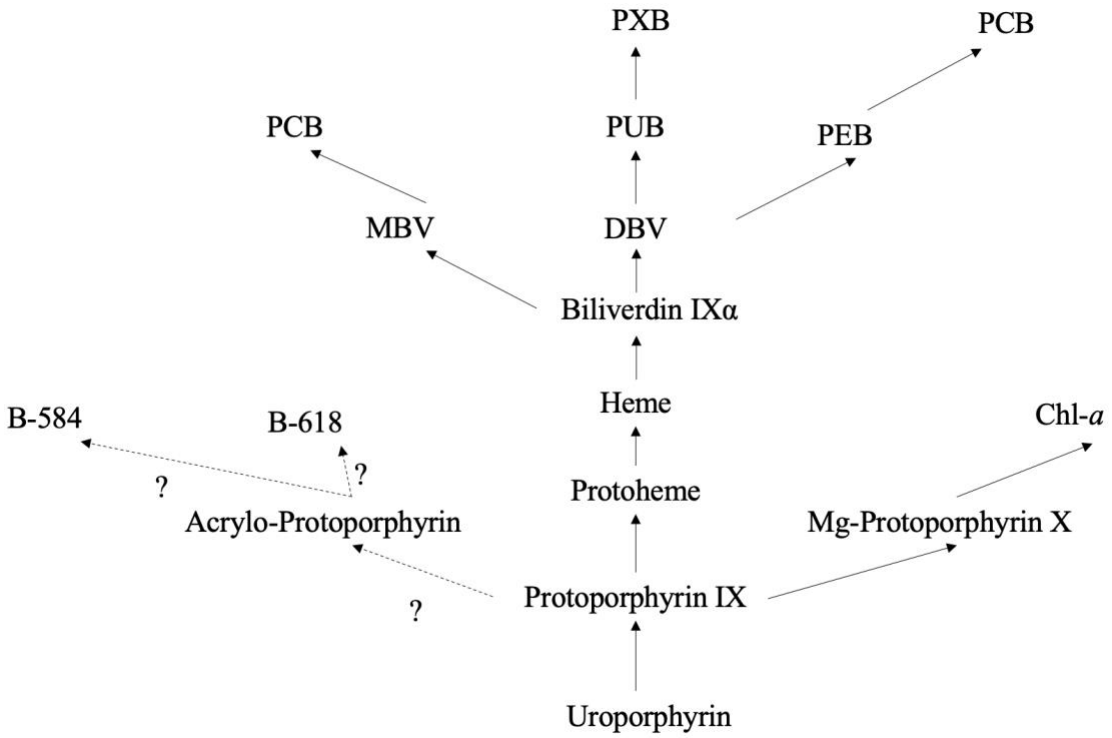

Figure 2.2. Abbreviated biosynthesis pathway for all phycobilins. Solid lines indicate steps in the pathway that are generally agreed upon. Dashed lines indicate plausible, but not confirmed steps in the pathway. Based on work by Granick 1965; Beale 1993; Scholes, et al. 2012; and Ledermann, et al. 2016.

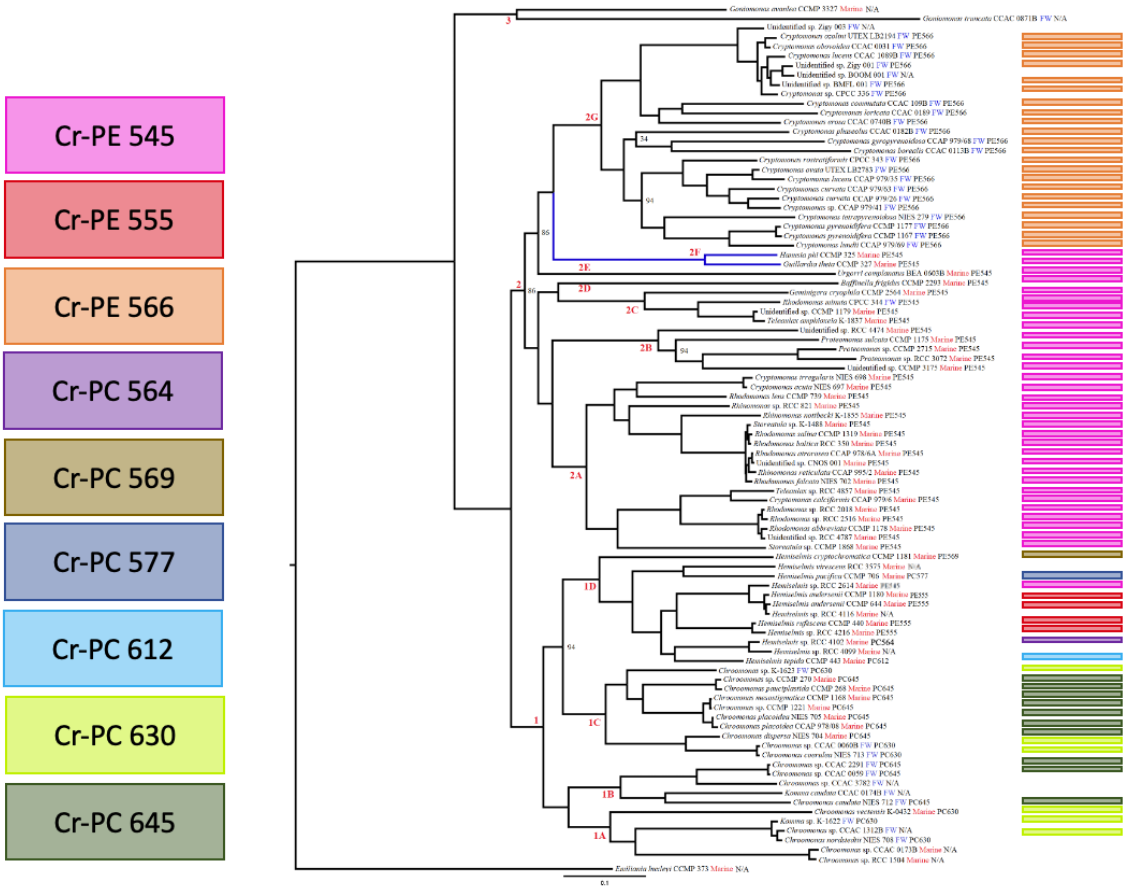

Figure 2.3. Ultra-conserved element phylogeny. Bootstrap support values are listed for nodes with less than 100% bootstrap support. Clade designations are listed for major nodes in the phylogeny according to Greenwold et al. (submitted, used with permission). Species names as well as the habitat and primary Cr-PBP type are listed for each taxon. Cr-PBP types are shown in color coded boxes.

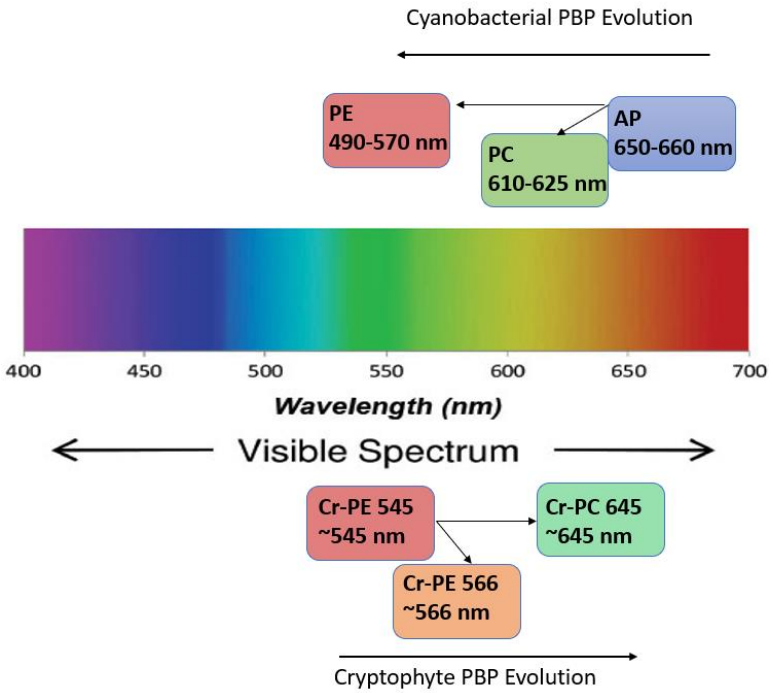

Figure 2.4. Schematic of the direction of PBP/Cr-PBP evolution based on the wavelength of maximum absorption in cyanobacteria versus cryptophytes

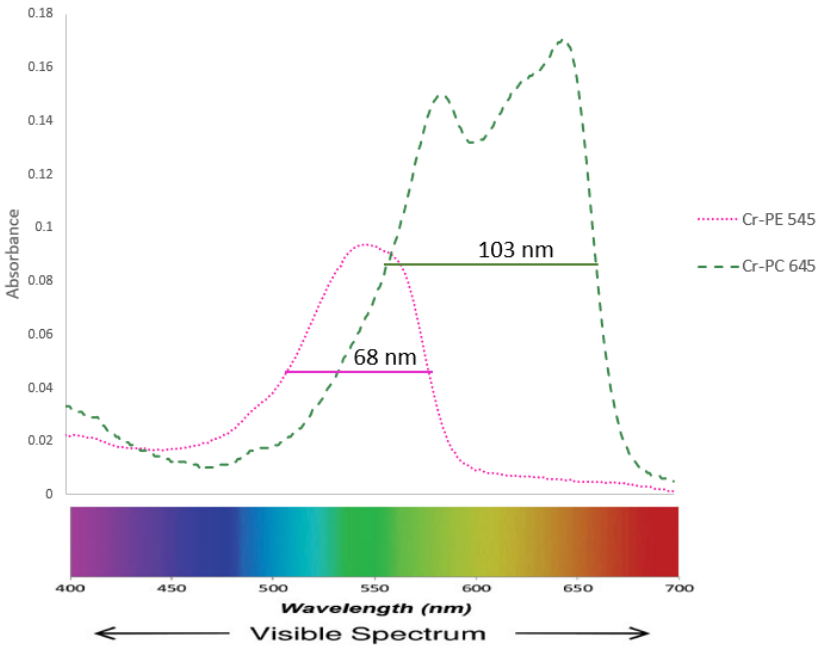

Figure 2.5 Comparison of absorption spectra of Cr-PE 545 extracted from *Rhodomonas salina* CCMP 1319 (pink dotted line) and Cr-PC 645 extracted from *Chroomonas mesostigmatica* CCMP 1168 (green dashed line). Spectra are not normalized, so differences in magnitude are attributed to differences in cell density at time of Cr-PBP extraction. Solid horizontal lines indicate full-width at half max, an indication of the breadth of wavelengths of light efficiently absorbed by the Cr-PBP.

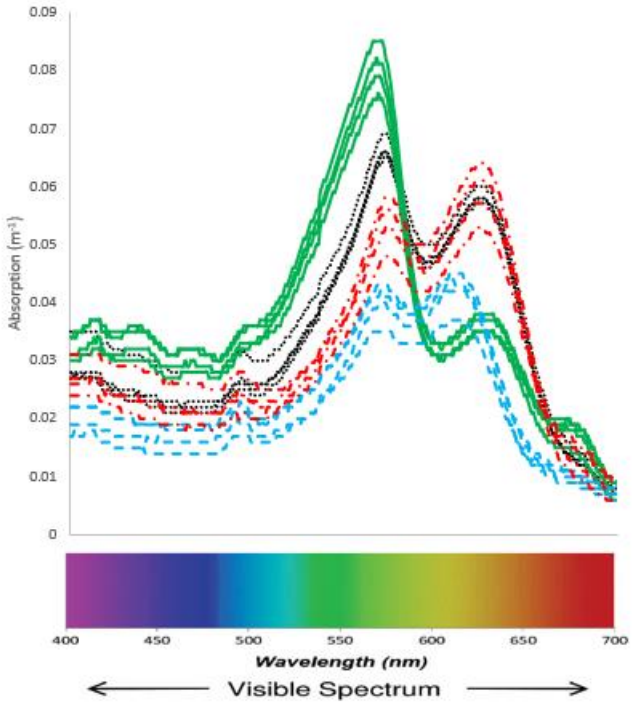

Figure 2.6. Cr-PBP absorption spectra from *H. cryptochromatica* (CCMP 1181) grown in full spectrum light (black dotted lines), blue light (blue dashed lines), green light (green solid lines), and red light (red dot and dashed lines). Raw data from Heidenreich and Richardson 2020, used with permission.

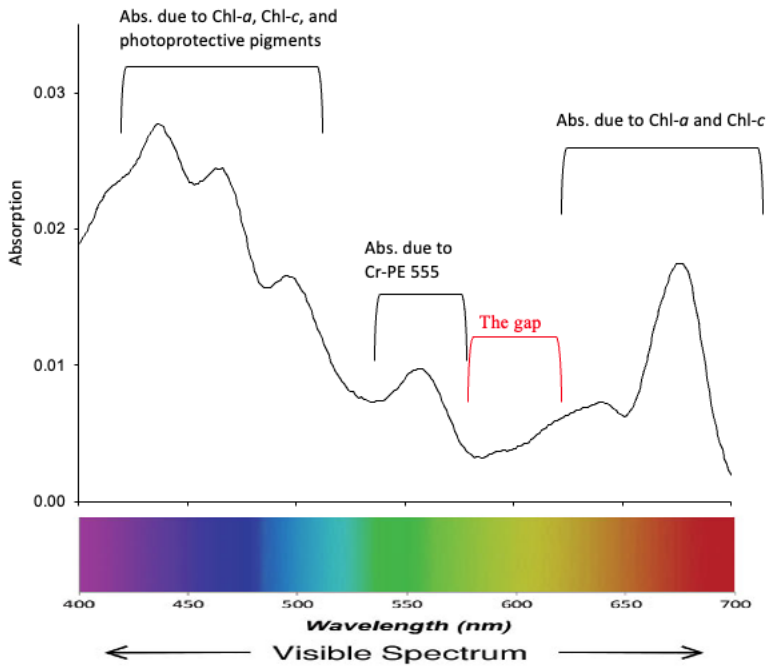

Figure 2.7. Whole cell absorption spectrum from *H. andersenii* CCMP 1180. Black brackets indicate pigments responsible for absorption peaks. Red bracket indicates apparent absorption gap between Cr-PE 555 and Chl-*a* and Chl-*c* absorption.

CHAPTER 3

DIVERSITY IN SPECTRAL ABSORPTION OF CRYPTOPHYTE PHYCOBILIPROTEINS

Abstract

Cryptophytes are known to vary widely in coloration across species. The differences in color come primarily from their cryptophyte phycobiliproteins (Cr-PBPs). There are 9 defined Cr-PBPs, named for the wavelength of maximal absorption, and cryptophytes are thought to only have one Cr-PBP per species. Because Cr-PBP type is usually regarded as a categorical trait, there tends to be a paucity of information about spectral absorption characteristics of Cr-PBPs or variation thereof across species. Here I present primary and secondary peak wavelengths and relative absorptions, shoulder wavelengths and relative absorptions, and full-width-at-half-max (FWHM) measurements of extracted Cr-PBP absorption spectra from 76 cryptophyte strains. This approach demonstrates spectral diversity between Cr-PBP types and allows for the development for more classification criteria when wavelength of maximal absorption alone is insufficient. I found that there is a wider range in primary peak wavelength for Cr-PE 545 than for Cr-PE 566. I also found that there is variability in Cr-PC peak shape even within species in the genus *Hemiselmis*.

Introduction

Cryptophytes are a group of unicellular, eukaryotic algae that are ubiquitous in freshwater, marine, and estuarine environments (Klaveness 1989, Hoef-Emden and Archibald 2017). Part of their ecological success is due to their unique cryptophyte phycobiliprotein (Cr-PBP) accessory pigments, which capture wavelengths of light not efficiently captured by chlorophylls (Doust et al. 2006), thus allowing them to occupy distinct vertical niches the water column (Stomp et al. 2007a, b). Cryptophytes are important primary producers, and their size range (~5 to 50 μm), digestibility, and generally high nutritional value make them attractive prey for grazers (Klaveness 1989, Pedrós-Alió et al. 1995, Pastoureaud et al. 2003, Adolf et al. 2008, Kiili et al. 2009, Gallegos et al. 2009).

Cryptophytes evolved as the result of a secondary endosymbiosis between an unknown eukaryotic host and a red algal symbiont (Archibald & Keeling 2002). The general structure of the Cr-PBP is an $\alpha_1\alpha_2\beta\beta$ tetramer with phycobilin chromophores attached to the subunits (Guard-Friar & MacColl 1986). The β subunits are believed to have evolved from the β-subunit of a red algal phycoerythrin molecule (Apt et al. 1995). The α-subunits are smaller and are not analogous to any phycobilisome subunit (Wilk et al. 1999) but are instead believed to be derived from a red algal linker protein (Rathbone et al. 2021). The β-subunits bind three chromophores at conserved locations on the protein, and the α-subunits bind one phycobilin at a conserved location (Glazer & Wedemayer 1995). Cr-PBPs have six possible phycobilin types. Phycoerythrobilin (PEB) and phycocyanobilin (PCB) are both found in red algae and cyanobacteria. Four additional phycobilins, 15,16-dihydrobiliverdin (DBV), bilin 584, bilin 618, and

mesobiliverdin (MBV) (Glazer & Wedemayer 1995, Wedemayer et al. 1992, Wedemayer et al. 1996) (Table 3.1) are unique to cryptophytes. DBV and MBV are precursors to PEB and PCB, respectively, in their biosynthetic pathway (Wedemayer et al. 1992, Frankenberg & Lagarias 2003). Bilin 584 and bilin 618 result from synthesis pathways that diverge from the pathways leading to PEB and PCB (Scholes et al. 2012). Both the composition of chromophores and the conformation of the bilin-protein complex affect the light absorption characteristics of Cr-PBPs (Wedemayer et al. 1996, Corbella et al. 2019, Michie et al. 2023).

To date, there are nine described Cr-PBPs, each named for the presence of a PEB or PCB on the β-Cys-82 binding site and for the wavelength of maximum absorption (Table 3.1). Cryptophyte phycoerythrins (Cr-PEs) are red in color, contain a PEB at β-Cys-82, and have a single absorption peak between 545 and 566 nm. Cryptophyte phycocyanins (Cr-PCs) are blue-green in color, contain a PCB at β-Cys-82, and often have two absorption peaks between 564 and 645 nm. The nine described Cr-PBPs are Cr-PE 545, Cr-PE 555, Cr-PE 566, Cr-PC 564, Cr-PC 569, Cr-PC 577, Cr-PC 612, Cr-PC 630, and Cr-PC 645 (Hoef-Emden 2008, Overkamp, et al. 2014, Magalhães et al. 2021).

Across the cryptophyte phylogeny, Cr-PE 545 is found in multiple clades and is thought to be the ancestral Cr-PBP (Greenwold et al. 2019). Cr-PE 566, on the other hand, is only found in freshwater species of *Cryptomonas* (Hill & Rowan 1989, Hoef-Emden 2008, Cunningham et al. 2019, Greenwold et al. 2019). *Hemiselmis* is the most diverse genus with respect to Cr-PBP type, containing species with one of multiple Cr-PEs or Cr-PCs (Hoef-Emden 2008, Cunningham et al. 2019, Greenwold et al. submitted). *Chroomonas* and *Komma* species group together and only ever have Cr-PC 630 or Cr-PC

645 (Hoef-Emden 2008, Cunningham et al. 2019, Greenwold et al. 2019). Historically scientists used color (appearance to the human eye), and later Cr-PBP type, as a way to classify cryptophytes (Hoef-Emden 2018). Problems with this quickly evolved (no pun intended) as the appearance of cryptophytes may change due to changes in light environment (Heidenreich & Richardson 2020, Spangler et al. 2022). While researchers usually bin Cr-PBPs into 9 general types according to the approximate wavelength of maximum absorption, there is remarkable variability within a Cr-PBP type with respect to wavelength of maximum absorption, the range and shape of the spectral absorption curve (here quantified as Full Width at Half Max; FWHM), and whether or not there is a detectable 'shoulder' (Fig. 3.1A).

Here, my objective was to quantify variability in spectral absorption across cryptophyte species with the same Cr-PBP type, with a view towards examining how this variability may inform our understanding of variability at the molecular level. I also aimed to determine a more precise standard for categorizing Cr-PBPs based on multiple criteria. Recognition of the physiological fluidity of spectral light absorption via chromatic acclimation helps predict potential effects of changes in water color on cryptophyte productivity. It also provides insight into possible steps in the evolution of the Cr-PBPs, and supports recent evidence that cryptophytes synthesize more than one type of Cr-PBP (Rathbone 2021).

Methods

I measured absorption spectra of extracted Cr-PBPs from 76 cryptophyte strains, representing at least 14 genera and 56 species (Table 3.1). Strains were maintained in batch culture at 4ºC, 15ºC, or 20ºC (depending on species preference) on a 12:12

light:dark cycle at an irradiance of 30-90 μmoles quanta m^{-2} s^{-1} with illumination provided from the side by Daylight Deluxe Arctic White 32-watt fluorescent lamps (Philips, Inc.). Stock cultures were transferred to fresh culture media while still in exponential phase and were swirled gently on a daily basis.

I used the freeze/thaw centrifugation method of Lawrenz et al. (2011) for Cr-PBP extractions. Aliquots (20-50 mL) of mid-exponential phase culture of each strain were sampled and then centrifuged at 2054 *g* for 10 minutes. The resulting supernatant was decanted, and the pellet re-suspended in 5 mL of 0.1M phosphate buffer (pH=6) and homogenized using a vortex. Samples were then placed at -20°C for at least 2 hours. Once frozen, samples were moved to 5°C to thaw for up to 24 hours. Thawed samples were centrifuged at 10,870 *g* for five minutes to remove excess cellular debris. The absorbance of each sample extract was measured from 400 to 750 nm at 1-nm intervals with a Shimadzu UV-VIS 2450 dual beam spectrophotometer using a 1-cm quartz glass cuvette against a phosphate buffer blank. Duplicate or triplicate measurements made from the same culture served as analytical replicates.

Spectra were analyzed using the 'pavo' package in R (Maia et al. 2019). To compare the shape of absorption curves, all spectra were scaled so that maximum absorption was equal to 1, and minimum absorption was equal to 0. Wavelength of highest absorption and full-width-at-half-maximum (FWHM) were determined for all extracted Cr-PBP spectra. FWHM is the width of the spectra at half of the maximum absorbance value. "Shoulders" were determined by finding the wavelength before or after a major peak where the slope of the spectrum changed noticeably.

Results

The spectra used include measurements from species with every known Cr-PBP type (Hoef-Emden et al. 2008, Magalhães et al. 2021). I characterized the spectra of each strain by considering the wavelength of maximum absorption, the peak shape, additional peaks and their heights relative to the primary peak, and the FWHM. By overlaying spectra of species with the same predominant Cr-PBP type, I could determine which Cr-PBP types had greater differences in shape, peak locations, and shoulders (Figure 3.2). I use the term "predominant Cr-PBP" to mean the Cr-PBP type that is most likely to be found in the largest quantity within the cell. This allows for the possibility that cryptophytes may have multiple Cr-PBPs, as was found in a strain of *H. andersenii* (CCMP 1180) in Rathbone (2021).

The wavelength of maximum absorption for purported Cr-PE 545 strains varied between 540 in *Proteomonas* sp. RCC 3072 and 554 nm in *Storeatula* sp. K-1488. The average maximum absorption peak for Cr-PE 545 spectra was located at 548 ± 2.5 nm. The average FWHM was 68.4 ± 4.3 nm. Despite their designated type, many purported Cr-PE 545-containing strains had spectra with an absorption maximum at or above 550 nm, including *R. reticulata* CCAP 995.2, *Rhodomonas falcata* NIES 702, and *Rhodomonas marina* K-0435. 19 strains out of 34 strains with Cr-PE 545 had a shoulder at approximately 564 nm. *Baffinella frigidus* Cr-PE 545 has a primary peak at 542 nm and two secondary peaks at 595 nm and 643 nm (Figure 3.1C). Hill and Rowan (1989) reported some strains with Cr-PE 545 as having primary peaks as low as 538 nm and some with secondary peaks at 645 nm, but this would be the first strain documented with 3 peaks.

Cr-PE 555-constaining strains had primary absorption peaks ranging from 548 nm in *Hemiselmis andersenii* CCMP 1180 to 555 nm in *Hemiselmis rufescens* CCMP 440. None of the Cr-PE 555 absorption spectra contained a noticeable shoulder. The average maximum absorption peak was located at 550 ± 3 nm. The average FWHM was 56.5 ± 3.7 nm.

There was some ambiguity when determining the Cr-PBP of Cr-PE-containing *Hemiselmis*. Although I observed that *H. andersenii* CCMP 1180 had its primary Cr-PBP peak at 548 nm, I categorized its predominant Cr-PBP as Cr-PE 555 due to its narrower FWHM (59 ± 3.13 nm). However, I found that a different Cr-PE-containing *Hemiselmis* species (RCC 2614) has both a primary peak location (551 nm) and FWHM (66 ± 5.03 nm) that fall within the same range as Cr-PE 545s. Taking these into account, I categorized its predominant Cr-PBP as Cr-PE 545. It is the only *Hemiselmis* strain we determined to have Cr-PE 545.

There was less variability among peak locations for strains with Cr-PE 566 than there was for Cr-PE 545 or Cr-PE 555. The average wavelength of the primary absorption peak for Cr-PE was 565 ± 0.5 nm. The average FWHM was 54.2 ± 3.2 nm. There were no noticeable shoulders in the Cr-PE 566 absorption spectra.

Hemiselmis aquamarina was the only cryptophyte with Cr-PC 564. Even so, there was some variability in the PBP absorption spectra. The Cr-PBP spectra were measured at two time points with n = 3 technical replicates in one set and n = 4 technical replicates in the other. The primary peak was located at 566 ± 1.9 nm, and the FWHM was 114 ± 4 nm. Similarly, *Hemiselmis cryptochromatica* was the only cryptophyte with Cr-PC 569. The absorption spectra were measured at two time points with n = 1 at one time point and

n = 4 at the other. The primary peak for *H. cryptochromatica* was located at 571± 1.1 nm with an FWHM of 105.5 ± 1.3 nm.

Hemiselmis tepida and *Hemiselmis virescens* were the two cryptophytes with Cr-PC 612. Although they're both categorized as Cr-PC 612, their absorption spectra slightly differed near the secondary peak leading to a ~11 nm difference in FWHM. *H. tepida* had a secondary peak at 570 nm and FWHM of 101 ± 0.58 nm. *H. virescens* had a secondary peak at 577 nm and FWHM of 90 ± 0.58 nm.

There was a wide range of primary peaks for Cr-PC 630 absorption spectra. *Chroomonas* sp. 0173B had its primary peak at 624 nm, and *Chroomonas* sp. K-1623 had its primary peak at 637 nm. In contrast, the secondary peak was consistently located at 583-585 nm. *Komma* sp. K-1622 had its primary peak at 582 nm and secondary peak at 631 but was categorized as having Cr-PC 630 as there was only 3% difference between its primary and secondary peak.

Lastly, the only cryptophytes with Cr-PC 645 were in the genus *Chroomonas*. The Cr-PC 645 spectra had a primary peak between 646-647 nm and a secondary peak at 584-586 nm. The FWHM averaged 103 ± 0.9 nm.

In general, Cr-PE 545 spectra had wider FWHMs (68.4 ± 3.6 nm) than Cr-PE 555 (56.5 ± 3.7 nm) or Cr-PE 566 (54.2 ± 3.2 nm). The FWHMs of Cr-PCs were considerably wider (92 – 118 nm) than those of Cr-PEs (54 – 68 nm) (Table 3.3).

Discussion

In this chapter, I aimed to explore the variation in spectral absorption characteristics within and across Cr-PBP types. I found that combining Cr-PBP primary peak location with FWHM allowed me to categorize Cr-PBP types with more confidence.

Although recent publications (e.g. Hoef-Emden et al. 2008, Cunningham et al. 2019, Greenwold et al. 2019) only report predominant Cr-PBP type without spectral data, my approach is not novel. Hill & Rowan (1989) provide primary peaks, secondary peaks, shoulders, and fluorescence emission peaks for 33 Cr-PE-containing cryptophyte strains and 22 Cr-PC-containing cryptophyte strains. A few of these strains were characterized by multiple authors and showed dramatic variation in spectral characteristics. For example, *Hemiselmis virescens* was sometimes characterized as having Cr-PC 615 (synonymous in the literature with Cr-PC 612; Ó hEocha & Raftery 1959, Ó hEocha et al. 1964, Glazer & Cohen-Bazire 1975, MacColl & Guard-Friar 1983) and sometimes as having Cr-PC 645 (Allen et al. 1959, Ó hEocha et al 1964, Glazer & Cohen-Bazire 1975). There was even variation within the same strain of *H. virescens* in where its secondary peak was located when the primary peak was at 612-615 nm—either at 577 nm (Ó hEocha & Raftery 1959, Glazer & Cohen-Bazire 1975) or at 585 nm (Ó hEocha et al. 1964, MacColl & Guard-Friar 1983).

This work demonstrates that there is variation within Cr-PBP types but raises the question of the underlying causes of the variation. I also show variation among Cr-PBPs from *Hemiselmis* species in particular. There was a wide range (548 nm – 555 nm) in peak locations for *Hemiselmis* with Cr-PE 555. The ambiguous peak height in *H. andersenii* CCMP 1180 Cr-PE 555 has led one author to consider it "PE 545/555" (Hoef-Emden 2008). *H. aquamarina* and *H. cryptochromatica* had differences in relative peak heights and peak locations when their respective Cr-PCs were measured at two different time points. Previous authors have been conflicted about whether *H. cryptochromatica* contains Cr-PC 630 (Lane and Archibald 2008) or Cr-PC 569 (Cunningham et al. 2019).

H. tepida and *H. virescens* are both categorized here and elsewhere (e.g. Cunningham et al. 2019, Richardson 2022, Michie et al. 2023) as having Cr-PC 612, but their secondary peaks differ by 7 nm. Perhaps not coincidentally, two Cr-PC-containing *Hemiselmis* have been shown to change their Cr-PBP absorption spectra when grown in different spectral environments (Heidenreich & Richardson 2020, Spangler et al. 2022). What is special about *Hemiselmis* Cr-PBPs that has allowed them to diversify so much and seems to allow them to change in different light environments?

Recent work shows that spectral variation in Cr-PBPs comes, not only from chromophore composition and "open" versus "closed" quaternary structure (Harrop et al. 2014, Corbella et al. 2019), but also from the amino acid sequences of α-subunits and how they interact with the chromophores (Michie et al. 2023). Unlike the β-subunit, which is encoded by a single gene on the plastid genome (Douglas 1992), the α-subunits are encoded by multiple genes, all of which are in the nuclear genome (Curtis et al. 2012). α-subunits control the quaternary structure of the Cr-PBPs, the ability of the Cr-PBP to move into the thylakoid, and even the orientation of chromophores on the β-subunit (Harrop et al. 2014, Michie et al. 2023). Although cryptophytes are thought to only have a single Cr-PBP type per species, some have been shown to express up to 20 distinct α-subunits (*Guillardia theta* in Kieselbach et al. 2018, multiple species in Michie et al. 2023). Michie et al. (2023) found that the β-subunits of *H. pacifica* and *H. virescens* were nearly identical in structure and sequence, but the α-subunits had little sequence similarity. They also found that 4 *Hemiselmis* species (*H. andersenii, H. rufescens, H. tepida, and H. virescens*) expressed genes for both closed-form and open-form α-

subunits. Differential expression of the α-subunit genes could potentially account for the spectral variability seen in Cr-PBPs, especially in *Hemiselmis*.

Like most measurements of Cr-PBP absorption spectra, I only measured the bulk Cr-PBP absorption from cryptophyte cultures. These methods are not sensitive enough to discern whether there are multiple α-subunits present or even multiple Cr-PBPs present. Rathbone et al. (2021) used more advanced methods to isolate multiple distinct Cr-PBPs from a single strain of *Hemiselmis andersenii* (CCMP 1180), including one with a primary peak at 560 nm and a secondary peak at 645 nm. This Cr-PBP, called *Ha*PE645 by Rathbone, contains both PEB and PCB chromophores on asymmetrical β subunits. This is the first time a cryptophyte has been found to 1) have multiple Cr-PBP types, 2) have both PEB and PCB in the same PBP molecule, and 3) have asymmetrical β subunits. These findings were prompted by curiosity surrounding unexpected peaks in extracted Cr-PBP spectra.

Given the amount of spectral variation within Cr-PBP types, spectral variation within Cr-PBP extracted from the same strain, and the expression of multiple distinct α-subunits, a very basic question is raised: what constitutes "a Cr-PBP type"? Are the cryptophytes that are expressing multiple α-subunits, which we know to be a major driver of changes to the Cr-PBP spectral characteristics, producing multiple Cr-PBPs? Have cryptophytes that changed their Cr-PBP absorption spectra in different light environments produced multiple Cr-PBPs (Heidenreich & Richardson 2020, Spangler et al. 2022)? Are the variations found in this paper evidence that there are far more than 9 Cr-PBPs? I believe that answering these questions could result in a paradigm shift that will lead to further inquiry into the molecular drivers of Cr-PBP spectral variation.

Tables

Table 3.1. Cr-PBP chromophore composition and absorption maxima in white light. Modified from Richardson 2022 with permission. Cr-PC 564 added from Magalhães et al. 2021. Bilin 618 on α-Cys-19 added from Wedemayer et al. 1992—some strains of *Cryptomonas ovata* have Bilin 584 in this position while others have Bilin 618 at this position. Chromophore on β-Cys-158 of Cr-PC 577 corrected to PCB based on Michie et al. 2023.

Cr-PBP	***Chromophore binding site***				***1° and 2° (if applicable) λ of maximum absorption (nm)***	***Species used***
	α-Cys-19	**β-Cys-50,61**	**β-Cys-82**	**β-Cys-158**		
Cr-PE 545	DBV	PEB	PEB	PEB	545	*Rhodomonas salina*
Cr-PE 555	PEB	DBV	PEB	PEB	555	*Hemiselmis rufescens*
Cr-PE 566	bilin 584 or bilin 618	bilin 584	PEB	bilin 584	566	*Cryptomonas ovata*
Cr- PC 564	Unknown	Unknown	Unknown	Unknown	564, 618	*Hemiselmis aquamarina*
Cr-PC 569	PCB	bilin 584	PCB	bilin 584	569, 625	*Falcomonas daucoides*
Cr-PC 577	PCB	DBV	PCB	DBV	577, 612	*Hemiselmis pacifica*
Cr-PC 612	PCB	DBV	PCB	PCB	612, 577	*Hemiselmis virescens*
Cr-PC 630	MBV	DBV	PCB	PCB	630, 583	*Chroomonas* sp.
Cr-PC 645	MBV	DBV	PCB	PCB	645, 585	*Chroomonas mesostigmatica*

Table 3.2. Cr-PBP absorption measurements for 76 cryptophyte strains.Strain source abbreviations: Spanish Bank of Algae (BEA); Central Collection of Algal Cultures at the University of Duisburg-Essen (CCAC); Scandinavian Culture Collection of Algae and Protozoa (CCAP); National Center for Marine Algae and Microbiota (NCMA, formerly CCMP); Canadian Phycological Culture Center (CPCC); Microbial Culture Collection at the National Institute for Environmental Studies (NIES); Norwegian Culture Collection of Algae (NIVA and K-); Culture Collection of Algae at the University of Texas at Austin (UTEX); and field isolations from: Baruch Marine Field Lab (BMFL), Charleston SC (CHAR), Battery Park in Charleston SC (CNOS), Winyah Bay SC (WNBY), and Congaree National Park in SC (ZIGY). Cr-PBP peaks and shoulders from extracted Cr-PBP spectra show absorption relative to the absorption of the primary peak. Peaks are shown in order of lowest wavelength to highest wavelength. Primary peaks (those with highest absorption) are shown in bold. Shoulders are shown in italics. Cr-PBP FWHM ± 1 standard deviation were determined based on extracted Cr-PBP spectra where possible. When there is an omission, FWHM could not be reliably determined due to noise in extracted PBP spectrum.

Strain	**Predominant Cr-PBP**	**n=**	**Peak wavelengths (nm) Relative abs.**	**Cr-PBP FWHM (nm) ± SD**
***Hemiselmis aquamarina* RCC 4102**	Cr-PC 564	7	**564** 617 **1** 0.89	114 ± 4.00
***Hemiselmis cryptochromatica* CCMP 1181**	Cr-PC 569	5	**572** 626 **1** 0.73	105.5 ± 1.3
***Hemiselmis pacifica* CCMP 706**	Cr-PC 577	5	**578** *613* **1** *0.85*	89 ± 1.8
***Hemiselmis tepida* CCMP 443**	Cr-PC 612	3	570 **612** 0.94 **1**	101 ± 0
***Hemiselmis virescens* RCC 3575**	Cr-PC 612	4	577 **614** 0.94 **1**	90 ± 0.58
***Chroomonas norstedtii* NIES 708**	Cr-PC 630	1	584 **637** 0.98 **1**	102 ± 0
***Chroomonas* sp. CCAC 0060**	Cr-PC 630	3	583 **633** 0.92 **1**	102 ± 1.15
***Chroomonas* sp. CCAC 0173B**	Cr-PC 630	2	585 **624** 0.93 **1**	117 ± 2.83
***Chroomonas* sp. K-1623**	Cr-PC 630	1	584 **637** 0.97 **1**	103 ± 0
***Chroomonas vectensis* K-0432**	Cr-PC 630	3	583 **631** 0.95 **1**	101 ± 1.73
***Komma sp.* K-1622**	Cr-PC 630	3	**582** 631 **1** 0.97	110 ± 0
***Chroomonas caudata* NIES 712**	Cr-PC 645	1	584 **647** 0.9 **1**	103 ± 0
***Chroomonas mesostigmatica* CCMP 1168**	Cr-PC 645	1	585 **646** 0.87 **1**	103 ± 0

Strain	Predominant Cr-PBP	n=	Peak wavelengths (nm) Relative abs.	Cr-PBP FWHM (nm) ± SD
Chroomonas sp. **CCAC 0059**	Cr-PC 645	3	585 **647** 0.9 **1**	103 ± 1
Chroomonas sp. **CCAC 2291**	Cr-PC 645	3	585 **647** 0.9 **1**	102 ± 1.53
***Chroomonas* sp.** **CCMP 1221**	Cr-PC 645	1	584 **647** 0.89 **1**	103 ± 0
***Chroomonas* sp.** **CCMP 270**	Cr-PC 645	1	586 **646** 0.87 **1**	103 ± 0
Baffinella frigidus **CCMP 2293**	Cr-PE 545	1	**542** 595 641 **1** 0.36 0.16	64 ± 0
Cryptomonas irregularis **NIES 698**	Cr-PE 545	1	**550** **1**	74 ± 0
Geminigera cryophila **CCMP 2564**	Cr-PE 545	1	546 *566* 1 *0.85*	70 ± 0
Guillardia theta **CCMP 327**	Cr-PE 545	4	**547** **1**	66 ± 4.96
Hanusia phi **CCMP 325**	Cr-PE 545	1	**546** **1**	
***Hemiselmis* sp.** **RCC 2614**	Cr-PE 545	3	551 1	66 ± 5.03
***Proteomonas* sp.** **RCC 1505**	Cr-PE 545	3	545 564 1 0.94	72 ± 4.51
Proteomonas sp. **CCMP 2715**	Cr-PE 545	1	545 *564* 1 *0.84*	70 ± 0
Proteomonas sp. **RCC 3072**	Cr-PE 545	1	540 1	
Proteomonas sulcata **CCMP 1175**	Cr-PE 545	1	548 *562* 1 *0.95*	65 ± 0
Rhinomonas reticulata **CCAP 995.2**	Cr-PE 545	1	**556** *560* **1** *0.98*	65 ± 0
Rhodomonas abbreviata **CCMP 1178**	Cr-PE 545	1	**550** **1**	66 ± 0
Rhodomonas atrorosea **CCAP 978.6A**	Cr-PE 545	1	**550** **1**	65 ± 0
Rhodomonas baltica **RCC 350**	Cr-PE 545	3	**548** **1**	
Rhodomonas chrysoidea **NIES 701**	Cr-PE 545	1	**549** *564* **1** *0.93*	66 ± 0
Rhodomonas falcata **NIES 702**	Cr-PE 545	1	**552** **1**	69 ± 0
Rhodomonas lens **CCMP 739**	Cr-PE 545	1	**548** *565* **1** *0.93*	65 ± 0
Rhodomonas marina **K-0435**	Cr-PE 545	3	**551** **1**	69 ± 4.04
Rhodomonas minuta **CPCC 344**	Cr-PE 545	1	551 *565* 1 *0.92*	67 ± 0
Rhodomonas salina **CCMP 1319**	Cr-PE 545	4	**548** *562* **1** *0.96*	70 ± 1.7
***Rhodomonas* sp.** **CCAC 6524B**	Cr-PE 545	3	**548** *564* **1** *0.94*	66 ± 1.2

Strain	Predominant Cr-PBP	n=	Peak wavelengths (nm) Relative abs.	Cr-PBP FWHM (nm) ± SD
Rhodomonas sp. **RCC 4444**	Cr-PE 545	3	**547** *565* **1** *0.91*	75 ± 1.5
***Storeatula* sp.** **CCMP 1868**	Cr-PE 545	1	**548** *564* **1** *0.93*	65 ± 0
***Storeatula* sp.** **K-1488**	Cr-PE 545	3	**553** **1**	67 ± 2.1
Teleaulax amphioxeia **K-1837**	Cr-PE 545	3	547 *563* 1 *0.9*	67.3 ± 0.58
Teleaulax sp. **RCC 4857**	Cr-PE 545	3	**550** *567* **1** *0.91*	68 ± 0.58
Unidentified sp. **CCMP 1179**	Cr-PE 545	1	550 *562* 1 *0.95*	67 ± 0
Unidentified sp. **CCMP 3175**	Cr-PE 545	1	545 *563* 1 *0.83*	71 ± 0
Unidentified sp. **CNOS 0001**	Cr-PE 545	3	**549** **1**	66 ± 0.58
Unidentified sp. **RCC 439**	Cr-PE 545	3	**549** **1**	
Unidentified sp. **RCC 4474**	Cr-PE 545	3	**547** *564* **1** *0.92*	71 ± 2.83
Unidentified sp. **RCC 4787**	Cr-PE 545	3	**547** *564* **1** *0.91*	68 ± 0.58
Unidentified sp. **RCC 4843**	Cr-PE 545	3	**548** *565* **1** *0.9*	70 ± 4.16
Urgorri complanatus **BEA 0603B**	Cr-PE 545	3	**547** **1**	66 ± 0
Hemiselmis andersenii **CCMP 1180**	Cr-PE 555	6	**548** **1**	59 ± 3.13
Hemiselmis andersenii **CCMP 644**	Cr-PE 555	1	**554** **1**	54 ± 0
Hemiselmis rufescens **CCMP 440**	Cr-PE 555	3	**555** **1**	53.3 ± 1.89
***Hemiselmis* sp.** **RCC 4116**	Cr-PE 555	3	**550** **1**	55.3 ± 3.2
Cryptomonas borealis **CCAC 0113B**	Cr-PE 566	3	**565** **1**	60.3 ± 3.51
Cryptomonas commutata **CCAC 0109B**	Cr-PE 566	1	**566** **1**	57 ± 0
Cryptomonas curvata **CCAC 0006**	Cr-PE 566	2	**565** **1**	55 ± 2.83
Cryptomonas curvata **CCAP 979.26**	Cr-PE 566	1	**566** **1**	54 ± 0
Cryptomonas erosa **CCAC 0740B**	Cr-PE 566	3	**565** **1**	52.7 ± 0.58
Cryptomonas loricata **CCAC 0189**	Cr-PE 566	3	**566** **1**	53.3 ± 0.58
Cryptomonas lucens **CCAC 1089B**	Cr-PE 566	3	**565** **1**	59 ± 2
Cryptomonas lucens **CCAP 979.35**	Cr-PE 566	1	**566** **1**	53 ± 0

Strain	Predominant Cr-PBP	n=	Peak wavelengths (nm) Relative abs.	Cr-PBP FWHM (nm) ± SD
Cryptomonas obovoidea **CCAC 0184B**	Cr-PE 566	3	**565** **1**	53 ± 1.79
Cryptomonas obovoidea **CCAC 1487B**	Cr-PE 566	3	**566** **1**	54.3 ± 1.15
Cryptomonas ovata **CCAC 1633B**	Cr-PE 566	3	**565** **1**	57.3 ± 4.16
Cryptomonas ovata **UTEX 2783**	Cr-PE 566	1	**566** **1**	55 ± 0
Cryptomonas phaseolus **CCAC 0182B**	Cr-PE 566	3	**565** **1**	53 ± 1.15
Cryptomonas pyrenoidifera **CCMP 1167**	Cr-PE 566	1	**566** **1**	53 ± 0
Cryptomonas **sp. CCAC 2298**	Cr-PE 566	3	566 1	54 ± 3
Cryptomonas **sp. CCAC 2770B**	Cr-PE 566	3	566 1	54.7 ± 2.52
Cryptomonas **sp. CCAC 3856B**	Cr-PE 566	3	566 1	52.7 ± 3.79
Cryptomonas **sp. CPCC 336**	Cr-PE 566	1	**565** **1**	54 ± 0
Cryptomonas tetrapyrenoidosa **CCAC 1800B**	Cr-PE 566	3	566 1	52.7 ± 0.58
Unidentified sp. BMFL 0001	Cr-PE 566	3	**566** **1**	49.3 ± 0.47
Unidentified sp. ZIGY 0001	Cr-PE 566	3	**565** **1**	53.3 ± 4.73

Table 3.3. Summary of average primary peaks ± 1 standard deviation from extracted Cr-PBP spectra with FWHM ± 1 standard deviation from extracted Cr-PBP spectra for each Cr-PBP type.

Cr-PBP type	**Average Extracted Cr-PBP Peak location (nm)**	**FWHM (nm)**
Cr-PE 545	548 ± 2.5	68.4 ± 4.3
Cr-PE 555	550 ± 3.0	56.5 ± 3.7
Cr-PE 566	565 ± 0.5	54.2 ± 3.2
Cr-PC 564	566 ± 1.9	114 ± 4.0
Cr-PC 569	571± 1.1	105.5 ± 1.3
Cr-PC 577	578 ± 0.45	92 ± 1.8
Cr-PC 612	613 ± 1.0	101 ± 0.6
Cr-PC 630	633 ± 4.3*	108 ± 8.6
Cr-PC 645	647 ± 0.37	103 ± 0.9

* 1 strain (*Komma* sp. K-1622) had its primary absorption peak at 582 nm, but its secondary peak was at 631. This strain was removed from this calculation.

Figures

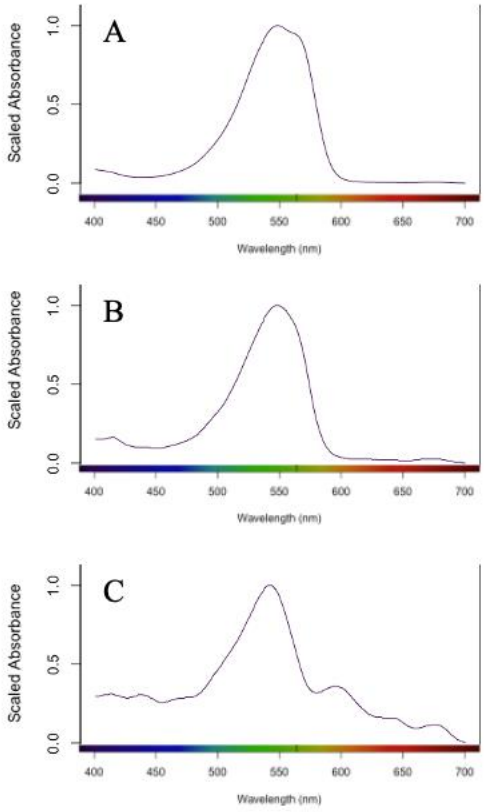

Figure 3.1. Extracted Cr-PBP spectra from 3 strains with Cr-PE 545: A) *Rhodomonas lens* CCMP 739, B) *Guillardia theta* CCMP 327, and C) *Baffinella frigidus* CCMP 229.

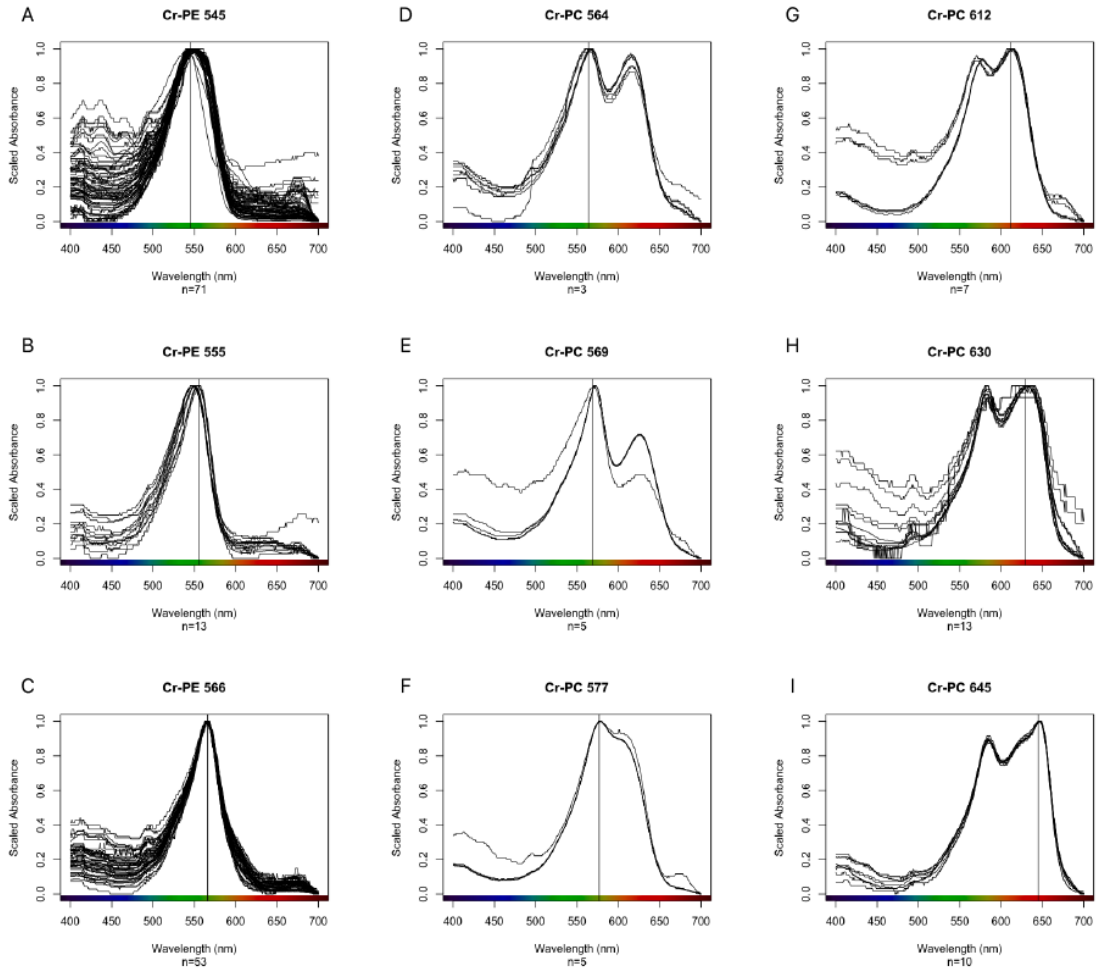

Figure 3.2. Scaled extracted Cr-PBP absorption spectra for all strains and replicates. For each Cr-PBP type, a vertical line is drawn at the wavelength for which the Cr-PBP is named (e.g. at 545 nm for Cr-PE 545). Number of total replicates is displayed under each spectrum. A shows all Cr-PE 545 spectra; B shows all Cr-PE 555 spectra; C shows all Cr-PE 566 spectra; D shows all Cr-PC 564 spectra; E shows all Cr-PC 577 spectra; F shows all Cr-PC 569 spectra; G shows all Cr-PC 612 spectra; H shows all Cr-PC 630 spectra; and I shows all Cr-PC 645 spectra.

CHAPTER 4

CRYPTOPHYTE PHOTOSYNTHESIS IN VARYING SPECTRAL ENVIRONMENTS

Abstract

The spectral quality of aquatic habitats varies widely across environments depending on the composition of the water. As depth increases, light intensity and spectral range of light decrease. Cryptophytes are often found in low light environments with a limited range of available wavelengths. In addition to Chl-*a*, cryptophytes contain cryptophyte-phycobiliprotein (Cr-PBP) pigments that capture wavelengths of light poorly absorbed by chlorophylls. Here, I determined photosynthesis parameters in green, red, and white light for 3 species of marine cryptophytes with different Cr-PBPs. I also explored the impact of historical light environment on photosynthesis in novel light environments by determining the same photosynthesis parameters for *Hemiselmis tepida* grown in green, red, and white light for 22 months. All 3 species had compensation irradiances (E_k) that were less than 100 μmol photons m^{-2} s^{-1}. *Chroomonas mesostigmatica* and *Proteomonas sulcata* showed no significant differences in maximum photosynthetic rate (P_{max}), photosynthetic efficiency at low light intensity (α), or E_k in green, red, and white light. *P. sulcata* and *H. tepida* previously grown in red or green light experienced photoinhibition in white light. While *H. tepida* grown in different colors of light showed different photosynthetic parameters in green, red, and white light, the effects of historical light

environment were difficult to predict. My results highlight the limitations of determining photosynthetic parameters only using algal stocks grown in white light.

Introduction

Cryptophytes are photosynthetic, microscopic algae found in a wide range of aquatic environments including chlorophyll-rich coastal waters (Kamiya & Miyachi 1984), chromophoric dissolved organic matter (CDOM)-rich estuaries (Gallegoes et al. 2009), and blue-water open ocean (Cotti-Rausch et al. 2016). They are often found in environments with low light intensity such as under ice (Kiili et al. 2009), deep water layers of lakes (Gervais 1997), and eutrophic ponds (Barone & Naselli-Flores 2003). They are small and easily digestible, so serve as valuable prey items for small grazing animals (Pedrós-Alió et al. 1995), ultimately supporting production at higher trophic levels.

The presence of cryptophytes in such a wide range of habitats is remarkable because the light environments of these habitats (both the intensity and color) vary greatly. Their success can be partly attributed to the diversity in their photosynthetic pigments. In addition to chlorophyll-*a* and chlorophyll-c_2 (which absorb blue and red light), cryptophytes also contain pigments called phycobiliproteins (Cr-PBPs) that absorb wavelengths of light poorly absorbed by chlorophylls (Haxo & Fork 1959). It's generally thought that cryptophytes have either phycocyanin (Cr-PC) or phycoerythrin (Cr-PE) as a Cr-PBP type, depending on the species (Hill & Rowan 1989). Cr-PCs allow absorption of yellow to red light (550-650 nm), while Cr-PEs allow absorption of green light (530-570 nm). Cr-PBPs are further categorized according to the wavelength where absorption is maximal (e.g. Cr-PE 545 is a phycoerythrin with an absorption peak at 545 nm).

Light is an important resource for all photosynthetic organisms, including cryptophytes, but light color and intensity in water are not uniform. The intensity of light decreases exponentially with depth, and, depending on the composition of the water, the color of light that penetrates to depth may differ greatly. In environments with high concentrations of colored dissolved organic matter (CDOM; e.g., humic acids and tannins from leaf litter), the light that will penetrate the deepest will be orange to red in color (Blough & del Vecchio 2002, Lawrenz et al. 2010). This is because CDOM absorbs blue light preferentially and leaves behind red light (Kirk 2011). In environments with high phytoplankton abundance, red and blue light are absorbed by chlorophylls leaving green light behind. A single body of water may have different light environments depending on location, season, or events that change the composition of the water (Lawrenz et al. 2010). As depth increases and light is attenuated, the spectral environment becomes increasingly monochromatic (Stomp et al. 2007b). Therefore, cryptophytes living at low depths of the euphotic zone experience not only low light intensity, but also a narrow range of wavelengths available for photosynthesis.

The color and intensity of light in many aquatic environments is changing due to the activities of humans (Beusen et al. 2016, Creed et al. 2018, Le Moal et al. 2019). Nutrient-rich runoff from agricultural operations, for example, can cause algal blooms in surface waters leading to green light environments. In Arctic and Antarctic environments, melting permafrost can increase CDOM inputs to lakes, resulting in more red light and lower light intensities at deeper depths (Roulet & Moore 2006). Increases in terrestrial vegetation due to changes in land use and increasing temperature also increase CDOM inputs into aquatic environments (Finstad et al. 2016).

Understanding how cryptophytes photosynthesize light of varying colors and intensities allows for better prediction of their growth and carbon fixation in different light environments and as light environments change. Historically, cryptophytes have been thought to be adapted for low light environments, using their Cr-PBPs to efficiently capture light in environments where light is scarce (Hoef-Emden & Archibald 2017). In recent years, however, cryptophyte blooms have been observed in surface waters, leading some to hypothesize that cryptophytes are actually adapted for high light intensities (Mendes et al. 2018). Previous studies designed to determine cryptophyte growth and photosynthesis parameters have been conducted only under full-spectrum fluorescent light (Gervais 1997, Hammer et al. 2002). While these methods shed some light on the relationship between irradiance and growth or photosynthesis, they do not adequately simulate realistic light environments at depths where cryptophytes are found.

Here I determined photosynthetic parameters for 3 cryptophyte species (*Chroomonas mesostigmatica*, *Hemiselmis tepida*, and *Proteomonas sulcata*) in white, green, and red light. By constructing photosynthesis versus irradiance (P vs E) curves, I determined the efficiency of photosynthesis at low light intensities (α), the light intensity at which irradiance is not limiting (E_k), the maximum rate of photosynthesis (P_{max}), and the slope of the photoinhibition parameter (β) (Platt et al. 1980) in each light color. The cryptophyte species used each has a different PBP (Figure 4.1): *P. sulcata* contains Cr-PE 545 (Cunningham et al. 2019); *H. tepida* contains Cr-PC 612 when grown in white or red light and an unnamed Cr-PC after 18 months of growth in green light (Figure 4.1B); and *C. mesostigmatica* contains Cr-PC 645 (Cunningham et al. 2019). *C. mesostigmatica* and *P. sulcata* were grown in white light for at least 5 years prior to the experiment. The *H.*

tepida cultures used were cultured in either white, green, or red light for 22 months prior to the experiment and allowed me to determine the effect of historical light environment on photosynthesis parameters.

I hypothesized that E_k for each cryptophyte in each light condition would be < 100 μmol photons m^{-2} s^{-1}, based on Gervais (1997), Hammer et al. (2002), and the light conditions where they are often found. I also hypothesized that cryptophytes would have highest P_{max} and α in colors of light efficiently captured by their Cr-PBPs compared to other colors. In Heidenreich and Richardson (2020), *P. sulcata* grew fastest in green light (the color best absorbed by its Cr-PE 545) compared to red and white light of similar intensity. *C. mesostigmatica* grew fastest in red light (the color best absorbed by its Cr-PC 645) (Heidenreich & Richardson 2020). When grown in white and red light, *H. tepida* contains Cr-PC 612, which has an absorption spectrum that is intermediate compared to that of Cr-PE 545 and Cr-PC 645. It had a similar growth rate in green and red light in Heidenreich and Richardson (2020). *H. tepida* grown in green light for 22 months has an unnamed Cr-PBP with an absorption maximum at 558 nm (Figure 4.1). While there are no published data regarding its growth rate in green, red, and white light, I predicted that it would have its highest P_{max} and α in green light based on where its Cr-PBP absorbs maximally. Finally, I hypothesized that *H. tepida* grown in a given color of light would have its highest α and lowest E_k in that light color.

Materials and Methods

Stock cultures. Cryptophyte strains were obtained from the National Center for Marine Algae and Microbiota (NCMA) at the Bigelow Laboratory for Ocean Sciences (ncma.bigelow.org): *C. mesostigmatica* (CCMP 1168), *H. tepida* (CCMP 443), and *P.*

sulcata (CCMP 1175). All cultures were grown in 250 mL Pyrex bottles with approximately 150 mL of culture medium and transferred in mid to late exponential stage. *C. mesostigmatica* and *P. sulcata* were grown in a reach-in incubator at 20 °C on a 12: 12 h light: dark cycle of ~30 μmol photons m^{-2} s^{-1} PAR of full-spectrum white light as measured with a Biospherical Instruments QS 2101 light meter with a 4π sensor (Biospherical Instruments, Inc., San Diego, CA, USA) just outside culture containers. *C. mesostigmatica* and *P. sulcata* were both grown in f/2 – Si culture medium.

H. tepida was grown in a Conviron walk-in incubator (Controlled Environments, Inc., Manitoba, Canada) set to 20 °C on a 12: 12 h light: dark cycle. Cultures were placed in white, green, or red light (Figure 4.2, Figure 4.3B) all with irradiance of ~25 μmol photons m^{-2} s^{-1} PAR also measured with a Biospherical Instruments QS 2101 light meter. *H. tepida* was grown in L1 + NH_4 culture medium. Cultures were grown in their respective light conditions for 22 months prior to photosynthesis experiments.

Whole cell absorption spectra. Whole cell absorption spectra were obtained before P vs E experiments took place. Absorption spectra were acquired with a Shimadzu dual-beam UV/VIS 2450 spectrophotometer using the filter pad technique (Shibata 1958, Roesler 1998). For each species in each growth environment, 10 mL of sample was filtered onto a Whatman GF/C filter. A blank GF/C, through which only culture medium was filtered, served as reference. All samples were stored at -80°C until analysis. Samples were scanned from 400 to 800 nm at 1 nm intervals. Spectral data were analyzed using the 'pavo' package in R (Maia et al. 2019). To compare the shape of absorption curves, all spectra were scaled so that maximum absorption is equal to 1, and minimum absorption is equal to 0.

Photosynthesis versus Irradiance. The P vs E relationships were determined using ^{14}C-based primary productivity measurements in cultures incubated under white, green, and red light according to Lewis and Smith (1983). For every combination of species, growth light treatment, and photosynthesis light treatment, three P vs E experiments were conducted. For *C. mesostigmatica* and *P. sulcata*, technical replicates were used (i.e., 1 semicontinuous batch culture of each species was used and sampled from on different days). *H. tepida* experiments were conducted on biological replicates (i.e., 3 independently maintained cultures from each growth light treatment were tested in each photosynthesis light treatment.)

All P vs E experiments were carried out in a dark room to minimize effects of ambient light. 55 mL of culture was spiked with approximately 50 μCi of ^{14}C in the form of sodium bicarbonate. 1 mL of spiked culture was added to each of 48 scintillation vials, which were placed in the photosynthetron. 1 mL of spiked culture was added to each of 3 vials containing 50 μL of buffered formalin (T_0) to correct for ^{14}C label uptake that occurred prior to incubation. 3 total count (T_c) samples were prepared by adding 20 μL of spiked sample to 200 μL of monoethanolamine (MEA) and 5 mL of Ecolume scintillation cocktail. Incubations in the photosynthetron were performed for 30 minutes at 20 °C. Immediately following incubation, 50 μL of buffered formalin was added to each vial. Samples were then placed on a shaker table and acidified with 200 μL 50% HCl and left overnight to purge unincorporated ^{14}C label. The next day 5 mL of Ecolume scintillation cocktail was added to all experimental vials and T_0 vials. Counts per minute were

enumerated using a Beckman Coulter LS 6500 scintillation counter and converted to disintegrations per minute by dividing by count efficiency of a known ^{14}C standard.

Irradiance in each position of the photosynthetron was measured using a Biospherical Instruments QS 2101 light meter with a 4π sensor (Biospherical Instruments, Inc., San Diego, CA, USA) inserted into a scintillation vial and held at the approximate height of 1 mL of water. A range of irradiances from 0-2700 µmol photons m^{-2} s^{-1} for white light, 0-1450 µmol photons m^{-2} s^{-1} for green light, and 0-1350 µmol photons m^{-2} s^{-1} for red light was provided from underneath the vials. Green light and red light were supplied by placing a green or red tinted film between the light source in the photosynthetron and the vials. Temperature was held at 20 °C using a circulating water bath. Spectral irradiances of white, green, and red light were measured using a StellarNet BLUE-Wave miniature spectrometer with a 2π sensor (StellarNet, Inc., Tampa, FL USA) inserted into a scintillation vial and held at the approximate height of 1 mL of water in one position of the photosynthetron (Figure 4.3A). Spectral data were analyzed using the 'pavo' package in R (Maia et al. 2019). To compare the shape of irradiance curves, all spectra were scaled so that maximum absorption is equal to 1, and minimum absorption is equal to 0.

Photosynthesis rates were normalized to chlorophyll-*a* (Chl-*a*). Chl-*a* concentrations were determined using HPLC according to the procedure of Pinckney et al. (1996). 5 mL of culture from each P vs E experiment was filtered onto a 25 mm Whatman GF/C filter (GE LifeSciences, Buckinghamshire, UK) in triplicate immediately before the P vs E experiment and stored at -80 °C.

Results of these experiments were modeled using the equation of Platt et al. (1980):

$$P^B = P_s^B(1 - e^{-a})e^{-b}$$

Where P^B (μgC μgChl^{-1} h^{-1}) is the observed rate of photosynthesis per unit biomass at irradiance E (μmol photons m^{-2} s^{-1}), P_s^B is the maximum photosynthesis rate in the absence of photoinhibition (μgC μgChl^{-1} h^{-1}), $a = \alpha E / P_s^B$, α [(μgC μgChl^{-1} h^{-1}(μmol photons m^{-2} s^{-1})$^{-1}$] is the slope of the linear portion of the curve below E_k (μmol photons m^{-2} s^{-1}), $b = \beta E / P_s^B$, and β [(μgC μgChl^{-1} h^{-1}(μmol photons m^{-2} s^{-1})$^{-1}$] is the slope of the linear portion of the curve above E_k and characterizes photoinhibition. Curves were fit to P vs E data using 'nlsLM' function from the 'minipack.lm' package in R, which fits the data using the Levenberg-Marquardt nonlinear least-squares algorithm (Elzhov et al. 2022). Values for P_{max} and E_k were calculated by the method of Platt et al. (1980) from values of P_s^B, α, and β determined from the curve fits. β with values below zero were considered to equal 0, indicating no photoinhibition.

Statistics. P_{max}, α, and E_k for each tested combination of species, growth color, and photosynthetron color were tested for normality using the Shapiro-Wilk normality test with the hypothesis of normality rejected at *P*-values < 0.05. For normally distributed data, significant differences in photosynthesis parameters within species across light treatments were determined by a one-way ANOVA with Tukey post-hoc test ($P < 0.05$). Data that were not found to be normally distributed were compared to parameters within species across light treatments using the Kruskal-Wallis test. As these data were not

significantly different after applying the Kruskal-Wallis test ($P > 0.05$), no post-hoc test was performed. All analyses were conducted using R.

Results

C. mesostigmatica had α values ranging from 0.31 ± 0.08 (μgC μgChl^{-1} h^{-1}(μmol photons m^{-2} s^{-1})$^{-1}$ in white light to 0.39 ± 0.14 (μgC μgChl^{-1} h^{-1}(μmol photons m^{-2} s^{-1})$^{-1}$ in red light (Table 4.1). These values were not statistically significantly different across light treatments. The P_{max} values were very similar across light treatments with a range of 17.73 ± 3.68 in red light to 20.10 ± 4.80 μgC μgChl^{-1} h^{-1} in white light. The compensation irradiances for *C. mesostigmatica* were 63.48 ± 4.60 μmol photons m^{-2} s^{-1} in green light, 49.62 ± 18.39 μmol photons m^{-2} s^{-1} in red light, and 65.04 ± 2.27 μmol photons m^{-2} s^{-1} in white light. These values were not statistically significantly different. Overall, there was no photoinhibition across light treatments.

P. sulcata α values across light treatments were very similar with a range of 0.19 ± 0.09 (μgC μgChl^{-1} h^{-1}(μmol photons m^{-2} s^{-1})$^{-1}$ in red light to 0.23 ± 0.15 (μgC μgChl^{-1} h^{-1}(μmol photons m^{-2} s^{-1})$^{-1}$ in green light (Table 4.1). P_{max} values were also similar, ranging from 12.14 ± 4.94 μgC μgChl^{-1} h^{-1} in green light to 13.20 ± 6.35 μgC μgChl^{-1} h^{-1} in white light. The values for E_k ranged from 57.54 ± 14.74 μmol photons m^{-2} s^{-1} in green light to 75.50 ± 18.74 μmol photons m^{-2} s^{-1} in white light and were not statistically significantly different across light treatments. Unlike *C. mesostigmatica*, *P. sulcata* photosynthesis was inhibited in white light (β = 0.0080 ± 0.0021 (μgC μgChl^{-1} h^{-1}(μmol photons m^{-2} s^{-1})$^{-1}$) and green light (0.0007 ± 0.0009 (μgC μgChl^{-1} h^{-1}(μmol photons m^{-2} s^{-1})$^{-1}$). Photoinhibition in white light was significantly higher than in green or red light ($P < 0.05$) (Figure 4.4).

H. tepida grown in varying light environments had very similar values for α, P_{max}, and E_k when photosynthesizing in green light (Figure 4.5 and Table 4.1). When photosynthesizing in red light, α was significantly greater for *H. tepida* grown in white light than for *H. tepida* grown in green or red light. However, E_k similar across growth treatments when photosynthesizing in red light (26.41 ± 2.51 μmol photons m^{-2} s^{-1} for *H. tepida* grown in green light to 30.81 ± 7.50 μmol photons m^{-2} s^{-1} for *H. tepida* grown in white light). *H. tepida* grown in green light and photosynthesizing in white light had significantly higher P_{max} and E_k values than *H. tepida* grown in white light. There was also greater variation in photosynthesis parameters for *H. tepida* grown in green light and photosynthesizing in white light than in any other combination of growth light treatment and photosynthesis light treatment. Photoinhibition was only observed in *H. tepida* grown in green or red light and photosynthesizing in white light.

Discussion

I set out to determine whether cryptophytes are low light adapted, whether they photosynthesize more efficiently in colors of light that are maximally absorbed by their Cr-PBP, and whether the historical light environment gives cryptophytes an advantage in similar light environments. The low E_k values for all tested combinations of species (<100 μmol photons m^{-2} s^{-1}), light color in photosynthetron, and light color in growth chamber led me to conclude that cryptophytes are adapted for low light environments. However, the lack of photoinhibition in the red and green light treatments and for *C. mesostigmatica* indicate that cryptophytes are not restricted to only low light environments in most circumstances. *P. sulcata* experienced photoinhibition in white light, but white light is generally only available at the surface of water due to rapid

attenuation of certain wavelengths of light (depending on water composition). Future studies should include a blue light treatment to explore the possibility of photoinhibition in clearer waters such as oligotrophic ocean environments. It's possible that the higher energy wavelengths in blue light would have more of an inhibitory effect than the lower energy wavelengths in this study. The only *H. tepida* cultures that experienced photoinhibition were those that were grown in red or green light and photosynthesizing in white light. Therefore, lack of inhibition for cultures grown in white light might not rule out the possibility of photoinhibition for natural populations.

I hypothesized that cryptophytes would have their highest P_{max} and α in colors of light that are most efficiently absorbed by their Cr-PBPs. There were no significant differences for *C. mesostigmatica* and *P. sulcata* P_{max} and α when photosynthesizing in green, red, or white light. Although *H. tepida* with "Cr-PC 558" did not have its highest P_{max} and α in green light, it did have its lowest P_{max} and α in red light—the color least absorbed by its Cr-PBP (Figure 4.1B). *H. tepida* with Cr-PC 612 did not have a consistent response. After growth in red light, *H. tepida* did not have any significant differences in P_{max} and α across photosynthesis light treatments. After growth in white light, however, *H. tepida* had its highest α in red light which is the color best absorbed by Cr-PC 612 (Figure 4.1B). The difference in response between *H. tepida* grown in white light and *H. tepida* grown in red light may be attributed to the larger contribution of Cr-PC 612 to the whole cell absorption spectrum after growth in white light (Figure 4.1).

I wanted to know how historical light environment affected photosynthesis in new light environments. I hypothesized that *H. tepida* grown a color of light would have its highest α and lowest E_k when photosynthesizing in the same light color. Only *H. tepida*

grown in red light had its lowest E_k value in the color of light it was grown in. However, this E_k value was not significantly different from *H. tepida* grown in green or white light. The light conditions that resulted in the highest values for α did not correspond with the light environments where *H. tepida* was grown.

While the results of the *H. tepida* growth experiments did not match my predictions, they do show that there are effects of historical light environment on photosynthesis parameters in new light environments. There were significant differences in P_{max} and E_k between *H. tepida* grown in different light environments when photosynthesizing in white light. This shows that P vs E experiments conducted in white light from laboratory stocks that were also grown in white light are likely to respond differently than natural populations that have acclimated in other light environments.

There was more variation in *H. tepida* grown in green light and photosynthesizing in white light than other combinations of growth environment and photosynthesis light color. Because these were biological replicates kept in green light for 18 months, it's possible that the individual replicate cultures adapted to their light environment differently. There was little variability in E_k for cultures grown in green light and photosynthesizing in green light, but white light revealed differences among the cultures. More technical replication for each biological replicate may have elucidated these differences more clearly. Given the changes in Cr-PBP absorption in green light and the increased variation in photosynthesis in white light, it is surprising that *H. tepida* had remarkably similar photosynthesis parameters when photosynthesizing in green light regardless of historical light environment. This could be due to the photosynthetron light

spectra being generally red shifted compared to the growth chamber light spectra (Figure 4.3).

Overall, my results indicate that cryptophytes are adapted to low light environments in that they do not benefit photosynthetically at irradiances greater than 100 μmol photons m^{-2} s^{-1}. I showed that *P. sulcata* experiences photoinhibition in white light and *H. tepida* experiences photoinhibition in white light if grown in a spectrally limited light environment. There are likely differences in photoinhibition responses across the cryptophyte phylogeny, as demonstrated by the lack of photoinhibition in *C. mesostigmatica*. Lack of photoinhibition coupled with increased nutrient runoff from melting glaciers may explain the presence of cryptophytes in surface waters in Antarctica found by Mendes et al. (2018). My study also shows that the impact of changing light environments on CO_2 fixation from photosynthesis is difficult to predict. More studies on photosynthetic rates in different colors of light using natural phytoplankton populations will be needed to accurately model the effects of brownification and eutrophication on CO_2 fixation.

Table

Table 4.1. Results of the photosynthesis versus irradiance experiments in green, red, and white light. α [(μgC μgChl^{-1} h^{-1}(μmol photons m^{-2} s^{-1})$^{-1}$], β [(μgC μgChl^{-1} h^{-1}(μmol photons m^{-2} s^{-1})$^{-1}$], P_{max} (μgC μgChl^{-1} h^{-1}), and E_k (μmol photons m^{-2} s^{-1}) values ± 1 standard deviation for *C. mesostigmatica* and *P. sulcata* grown in white light and for *H. tepida* grown in green, red, or white light were calculated from the P vs E model of Platt et al. 1980.

Grown in	**Photosynthesizing in**	**α**	**β**	**P_{max}**	**E_k**
		C. mesostigmatica			
White	Green	0.32 ± 0.09	0	20.10 ± 4.17	63.48 ± 4.60
	Red	0.39 ± 0.14	0	17.73 ± 3.68	49.62 ± 18.39
	White	0.31 ± 0.08	0	20.10 ± 4.80	65.04 ± 2.27
		P. sulcata			
White	Green	0.23 ± 0.15	0.0007 ± 0.0009	12.14 ± 4.94	57.54 ± 14.74
	Red	0.19 ± 0.09	0	12.66 ± 3.29	70.76 ± 20.34
	White	0.20 ± 0.15	0.0080 ± 0.0021	13.20 ± 6.35	75.50 ± 18.74
		H. tepida			
Green	Green	0.16 ± 0.04	0	7.59 ± 1.82	46.91 ± 1.15
	Red	0.05 ± 0.02	0	1.37 ± 0.62	27.00 ± 3.50
	White	0.22 ± 0.14	0.0034 ± 0.0027	17.62 ± 13.25	71.10 ± 15.14
Red	Green	0.17 ± 0.03	0	8.00 ± 1.00	48.09 ± 6.80
	Red	0.16 ± 0.04	0	4.39 ± 1.36	26.41 ± 2.51
	White	0.12 ± 0.02	0.0005 ± 0.0002	6.79 ± 1.52	54.13 ± 7.43
White	Green	0.18 ± 0.04	0	8.40 ± 1.20	48.09 ± 6.80
	Red	0.35 ± 0.06	0	11.08 ± 4.10	30.81 ± 7.50
	White	0.10 ± 0.02	0	3.71 ± 1.39	36.28 ± 6.54

Figures

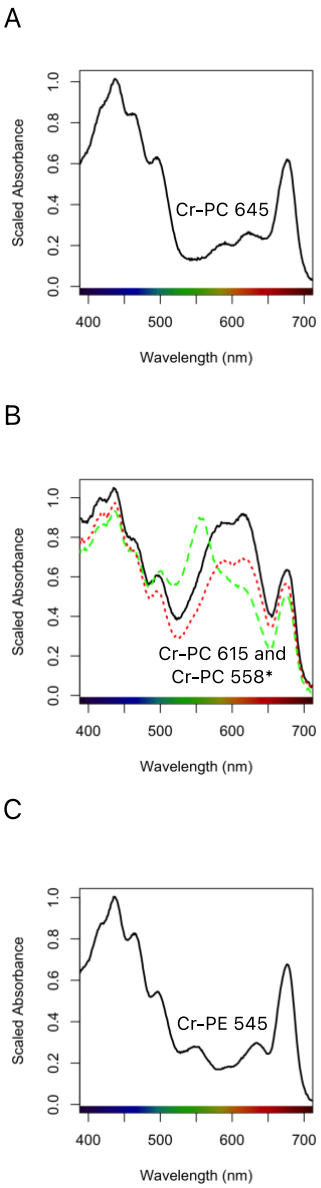

Figure 4.1. Whole cell absorption spectra of A) *Chroomonas mesostigmatica* grown in white light; B) *Hemiselmis tepida* grown in white (solid black line), green (dashed green line), and red light (dashed red line) for 18 months; and C) *Proteomonas sulcata* grown in white light. Cr-PBP peaks are labeled according to their classification based on wavelength of maximum PBP absorption. *H. tepida*'s Cr-PBP peak changed after 18 months of growth in green light. There is not an existing Cr-PBP that has a similar peak shape, so it is labeled "Cr-PC 558" as it has a primary absorption peak at 558 nm and a shoulder at 612 nm.

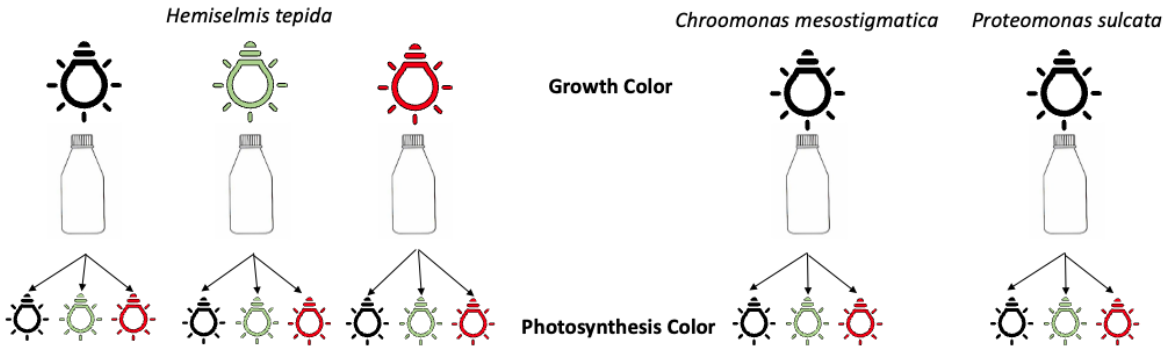

Figure 4.2. Schematic of experimental design. *H. tepida* was grown in white, green, and red light for 22 months prior to P vs E experiments. *H. tepida* from each growth treatment was tested in white, green, and red light in the photosynthetron. *C. mesostigmatica* and *P. sulcata* were only grown in white light before being tested in white, green, and red light in the photosynthetron.

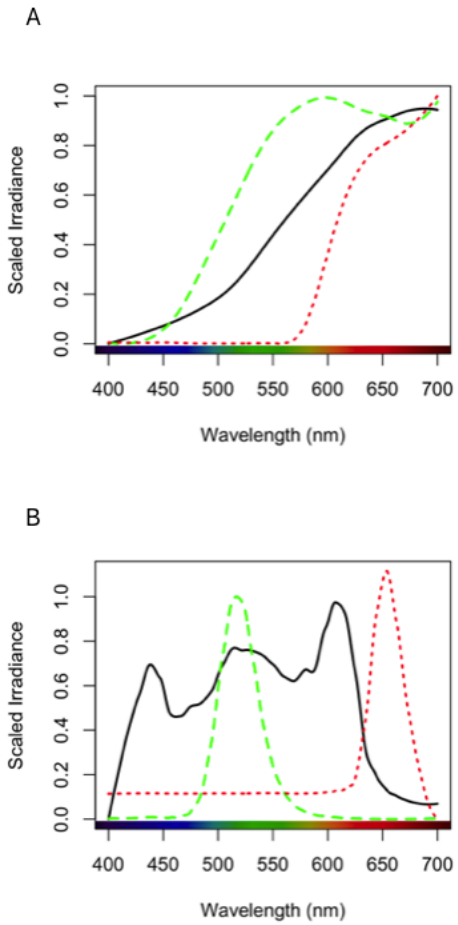

Figure 4.3. Emission spectra of green (green dashed line), red (red dotted line), and white (black solid line) light in photosynthetron (A) and *H. tepida* growth chamber (B).

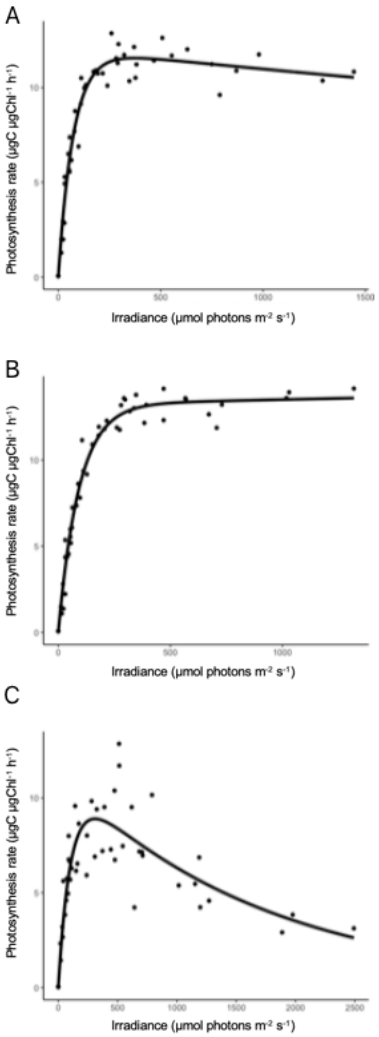

Figure 4.4. Representative P vs E curves from *P. sulcata* photosynthesizing in green light (A), red light (B), and white light (C). Note slight photoinhibition in green light, no photoinhibition in red light, and strong photoinhibition in white light.

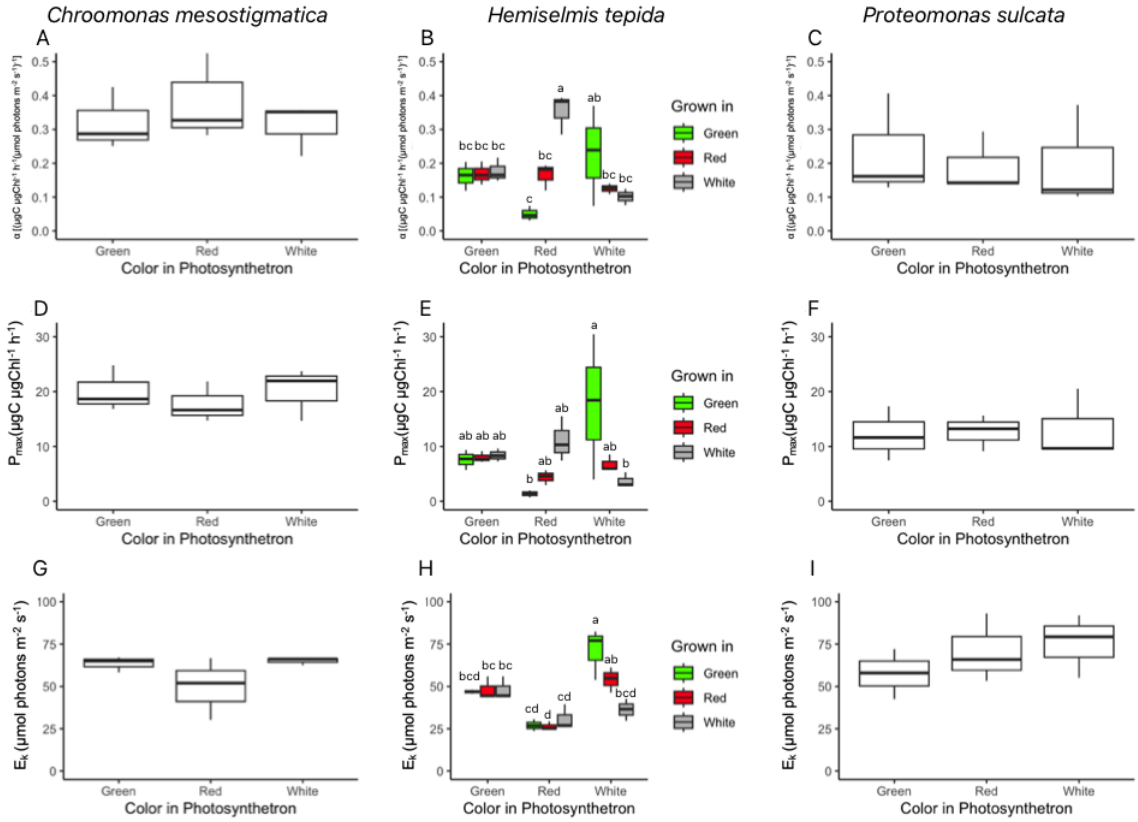

Figure 4.5. α values for *C. mesostigmatica* (A) grown in white light; *H. tepida* (B) grown in green, red, or white light; and *P. sulcata* (C) grown in white light and photosynthesizing in green, red, and white light. P_{max} values for *C. mesostigmatica* (D) grown in white light; *H. tepida* (E) grown in green, red, or white light; and *P. sulcata* (F) grown in white light and photosynthesizing in green, red, and white light. E_k values for *C. mesostigmatica* (G) grown in white light; *H. tepida* (H) grown in green, red, or white light; and *P. sulcata* (I) grown in white light and photosynthesizing in green, red, and white light. In B, E, and H, the colors of light the cultures were grown in are always presented in the order: green, red, white. Also in B, E, and H, values are statically significantly different ($P < 0.05$) if they do not have a letter in common. Values for P_{max}, α, and E_k were not significantly different in green, red, and white light compared within species for *C. mesostigmatica* and *P. sulcata*.

CHAPTER 5

EXPERIMENTAL EVOLUTION OF PHENOTYPIC PLASTICITY IN ALGAL PIGMENT MAY SHED LIGHT ON ORIGIN OF SPECTRAL VARIATION OF CRYPTOPHYTE ALGAE

Abstract

Heterogeneity of light color in water divides underwater habitats into distinct spectral niches. Absorption of different wavelengths of light depends on the light absorption characteristics of algal pigments. Cryptophytes are an algal group that uses pigments called cryptophyte phycobiliproteins. The evolutionary origins of cryptophyte phycobiliprotein diversity and phenotypic plasticity in the genus *Hemiselmis* are unknown. I grew two *Hemiselmis* species with different phycobiliprotein types in white, blue, green, and red light for 2 and 3 years to determine whether they could change their pigmentation in novel light environments. *Hemiselmis rufescens*, which uses cryptophyte phycoerythrin 555, had little change in phycobiliprotein absorption after 3 years in each light condition. *Hemiselmis tepida*, which uses cryptophyte phycocyanin 612, showed no change in phycobiliprotein absorption after 2 years in white, blue, and red light. In green light, however, it evolved to use a novel pigment that resembles cryptophyte phycoerythrin 555 and the ability to switch between the novel pigment and the ancestral phycocyanin depending on spectral environment. I propose a model for *Hemiselmis* evolution that involves a phenotypically plastic ancestor that diverged and evolved

fixation of cryptophyte phycoerythrin in the ancestor of *H. rufescens* and cryptophyte phycocyanin in the ancestor of *H. tepida*.

Introduction

In "Paradox of the Plankton," Hutchinson (1961) seeks to understand the nature of diversity of phytoplankton in a seemingly homogenous environment. Ultimately, he concludes that from the perspective of phytoplankton, water is both spatially and temporally heterogenous in terms of nutrient and light availability. This heterogeneity carves the water column into distinct niches.

Depth, particulate organic matter, and colored dissolved organic matter (CDOM) change both the amount and spectrum of light available (Kirk 2011). As depth increases, both the intensity and range of wavelengths of light available for photosynthesis decrease (Lawerenz et al. 2010, Stomp et al. 2007b). Blue light reaches the lowest depths of the photic zone in clear, oligotrophic environments, while red light reaches the lowest in CDOM-rich waters (Kirk 1994, Blough and Del Vecchio 2002, Lawrenz et al. 2010). In eutrophic environments, green light reaches the lowest depths of the photic zone. Differences in light spectra is one way that the water column is partitioned into many niches (Stomp et al 2007b).

Cryptophytes are a group of phytoplankton that can be found in many aquatic and marine environments with low light intensity that differ greatly in light color. They evolved as a result of secondary endosymbiosis in which an unknown eukaryotic ancestor engulfed a eukaryotic red algal cell (Archibald & Keeling 2002). From this merger, cryptophytes ended up with 4 genomes: their one nuclear and mitochondrial genomes, a nucleomorph genome from the red algal nucleus, and a plastid genome from the red algal

plastid (Douglas et al 2001, Keeling 2004). They also gained photosynthesis and modified the red algal phycobiliprotein (PBP) pigment to form a novel cryptophyte (Cr)-PBP-based light-harvesting antenna. Structurally, the Cr-PBPs are made up of 2 α-subunits that each bind a single chromophore and 2 β-subunits that each bind 3 chromophores at conserved locations (Glazer & Wedemayer 1995, Guard-Friar & MacColl 1986). The β-subunits are derrived from red algal phycoerythrin (PE) β-subunits (Apt et al. 1995). They are highly conserved and encoded by a single gene located in the plastid genome (Douglas 1992). In contrast, α-subunits are unrelated to red algal α-subunits and are encoded by multigene families located in the nucleus (Wilk et al. 1999, Doust et al. 2004, Curtis et al. 2012).

Cr-PBPs are remarkably diverse compared to PBPs of red algae, and this diversity has allowed cryptophytes to occupy a wide range of spectral niches. Cr-PBP color and spectral absorption characteristics are the result of their chromophore composition (Glazer & Wedemayer 1995, Wedemayer et al. 1992, Wedemayer et al. 1996), the overall shape of the protein component (Harrop et al. 2014, Corbella et al. 2019), and the interaction of amino acid side chains on the α-subunits with the chromophores (Michie et al. 2023). To date, there have been 9 described Cr-PBPs, which are cateorized as either cryptophyte-phycoerythrin (Cr-PE) or cryptophyte-phycocyanin (Cr-PC) and named for the approximate wavelength of maximum absorption (Hoef-Emden 2008, Overkamp et al. 2014, Magalhães et al. 2021). Cr-PEs give cryptophytes a pink to orange color and facilitate absorption of green light, while Cr-PCs give cryptophytes a bluish green color and facilitate absorption of orange to red light. Cr-PEs have a single absorption peak, but Cr-PCs typically have two peaks—a major peak for which they are named and a minor

peak. Historically cryptophytes have been thought to only have a single Cr-PBP type per species (Hill & Rowan 1989, Wedemayer et al. 1996).

To determine how Cr-PBPs evolved, several phylogenies have been constructed which match cryptophyte species to their Cr-PBP (Hoef-Emden 2008, Cunningham et al. 2019, Greenwold et al. 2019). The true topography of the cryptophyte phylogeny is currently unknown as there are few genetic tools available for cryptophytes (Archibald 2020) and there has been extensive intracellular horizontal gene transfer between the 4 cryptophyte genomes (Douglas et al. 2001, Keeling 2004). The cryptophyte phylogenies we do have (e.g. Hoef-Emden 2008, Greenwold et al. 2019) imply multiple switches between Cr-PBP types. The most diverse cryptophyte genus with regard to Cr-PBP type is *Hemiselmis* (Hoef-Emden 2008, Cunningham et al. 2019, Greenwold et al. 2019). Of the 9 named Cr-PBPs, 5 are only found in *Hemiselmis*: Cr-PE 555, Cr-PC 564, Cr-PC 569, Cr-PC 577, and Cr-PC 612 (Cunningham et al. 2019, Magalhães et al. 2021). According to one phylogeny, the Cr-PBP in *Hemiselmis* underwent multiple state reversals (Cr-PE to Cr-PC and Cr-PC to Cr-PE) (Greenwold et al. 2019). How did *Hemiselmis* become so diverse?

Although Cr-PBP type is generally considered a fixed trait by scientists who study cryptophytes, some species in the genus *Hemiselmis* have shown phenotypic plasticity in Cr-PBP absorption spectrum. *Hemiselmis cryptochromatica* has been described as having Cr-PC 630 by Lane and Archibald (2008) or Cr-PC 569 (with a minor peak at 630 nm) by Cunningham et al. (2019). As it turns out, the peak wavelength for *H. cryptochromatica* depends on its light environment (Heidenreich & Richardson 2020). *Hemiselmis virescens* uses Cr-PC 612, but its minor absorption peak has been reported as either 577

or 585 nm (Hill and Rowan 1989). Spangler et al. (2022) found that the absorption spectrum of Cr-PC 577 from *Hemiselmis pacifica* also changed when *H. pacifica* is grown in green light. Although Heidenreich & Richardson (2020) tested the phenotypic plasticity of cryptophytes from 6 genera when grown in white, blue, green, and red light, they only found *H. cryptochromatica* to be capable of altering its Cr-PBP absorption spectrum.

Hemiselmis is both uniquely evolutionarily labile and has species which demonstrate a high degree of phenotypic plasticity with regard to Cr-PBP absorption characteristics. Given this, I wanted to determine the long-term response of two *Hemiselmis* species when grown for 2-3 years in four light environments: white (full spectrum), blue, green, and red light with similar light intensities. Blue, green, and red light were chosen to simulate oligotrophic ocean, a eutrophic water body, and an environment with high CDOM inputs, respectively. White light was used as a control as the stock cultures used had been maintained in a lab in white light for 30+ years prior to the experiment. I used two closely related *Hemiselmis* species that use different Cr-PBP types: *Hemiselmis rufescens* CCMP 440 with Cr-PE 555 and *Hemiselmis tepida* CCMP443 with Cr-PC 612. I hypothesized that over a long period of time, *Hemiselmis* species living in a light color that is not well-absorbed by their Cr-PBP would be able to adapt their Cr-PBP absorption spectrum complementarily to their light environment.

Methods

Stock cultures. *Hemiselmis rufescens* CCMP 440 and *Hemiselmis tepida* CCMP 443 were obtained from the National Center for Marine Algae and Microbiota (NCMA) at the Bigelow Laboratory for Ocean Science. 32 replicate cultures of each species were started

with approximately 6 million cells each from a single laboratory stock culture. Cultures were grown in L1 + NH_4 culture medium in 250 mL Pyrex bottles. Approximately 5 million cells were transferred every 9-14 days (while cultures were in mid to late exponential phase). Cultures were maintained as separate lines throughout the experiment. Cultures that died were not replaced. Volume of culture transferred was determined using cell counts from a Beckman Coulter Z2 culture particle count and size analyzer (Beckman Coulter, Inc., Atlanta, GA, USA), with the particle size measurement set from 3 to 8 μm. Volume of culture inoculum plus volume of fresh culture medium was equal to 150 mL for every transfer. Cultures were grown in a Conviron walk-in incubator (Controlled Environments, Inc., Manitoba, Canada) set to 20 °C on a 12: 12 h light: dark cycle. 8 cultures of each species were placed in white, green, or red light, each of which had an irradiance of ~25 μmol photons m^{-2} s^{-1} photosynthetically available radation (PAR) measured with a Biospherical Instruments QS 2101 light meter. Blue and red light were provided by LumiBar Pro LED light strips (LU50001; Lumigrow, Emeryville, CA, USA). Green light was provided by an Even-Glow RGB LED panel set to green output only (superbrightleds.com). Spectral irradiances of white, blue, green, and red light were measured using a StellarNet BLUE-Wave miniature spectrometer with a 2π sensor (StellarNet, Inc., Tampa, FL USA) through a 250 mL Pyrex bottle and held at the approximate height of 150 mL of culture (Figure 5.1). Every day cultures were gently swirled by hand. *H. rufescens* cultures were maintained in their light conditions for 3 years (~370 – 540 generations, depending on light color). *H. tepida* cultures were maintained in their respective light conditions for 2 years (~240 – 320 generations, depending on light color).

Phenotypic measurements. Phenotypic measurements included growth rate during exponential phase, Cr-PBP absorption spectrum, whole cell absorption spectrum, and photosynthetically usable radiation (PUR) in each culture's respective light treatment. Measurements were taken at 1, 6, 12, 19, 24, and 30 months for *H. rufescens* and 1, 6, 12, 18, and 24 months into the experiment for *H. tepida*. Cr-PBP absorption spectra and whole cell absorption spectra were taken in triplicate from the original stock culture before the start of the evolution experiment.

Growth rate. Growth rate was determined using cell counts from a Beckman Coulter Z2 particle counter, with the particle size measurement set from 3 to 8 μm. Cell counts were taken at 2-day intervals starting 2 days after inoculation and continuing until the culture reached stationary phase. Ln(cell counts) were plotted with time, and data were fit with a linear curve according to the equation:

$$Ln(N_T) = \mu * T + Ln(N_0)$$

where μ is growth rate (day^{-1}), T is time (days), and N_0 is the initial cell concentration (cell * mL^{-1}).

Cr-PBP absorption spectra. Cr-PBP extractions were carried out using the freeze/thaw centrifugation method of Lawrenz et al. (2011). 20 mL aliquots of mid-exponential phase cultures were centrifuged at 2054 *g* for 10 minutes. The supernatant was then decanted, and the pellet was re-suspended in 5 mL of 0.1 M phosphate buffer (pH = 6) and homogenized using a vortex. Samples were placed at -20°C for at least 12 hours. After freezing, samples were moved to 5°C to thaw for up to 24 hours. Thawed samples were centrifuged at 10,870 *g* for 5 minutes to remove excess cellular debris. The absorbance of

each sample extract was measured from 400 to 750 nm at 1-nm intervals with a Shimadzu UV-VIS 2450 dual beam spectrophotometer using a 1-cm quartz glass cuvette against a phosphate buffer blank.

Whole cell absorption spectra. Absorbance spectra for each cryptophyte strain were obtained with a Shimadzu dual-beam UV/VIS 2450 spectrophotometer (Shimadzu Corporation, Japan) using the filter pad technique (Shibata 1958, Roesler 1998). For each replicate, 5 mL of sample was filtered onto a 25 mm Whatman GF/C filter. A blank GF/C, through which only culture medium was filtered, served as reference. All samples were stored at -80°C until analysis. Samples were analyzed at wavelengths from 400 to 800 nm at 1 nm intervals. Pigments were then extracted from the filters overnight using 10 mL of 100% methanol and placing in a -20°C freezer. Filters were then re-run to allow for correction for CDOM absorption. Spectra were scatter corrected by subtracting the average absorbance from 730 to 750 nm. Absorption was calculated using the following formula:

$$a^{Chl}(\lambda) = \frac{2.303 * A(\lambda)}{L * \beta * N}$$

where $A(\lambda)$ = the wavelength-dependent absorbance, L = the optical path length of the particles on the filter (i.e., the sample volume divided by clearance area of the filter), N = the concentration of chl-*a* in the culture, and β = the path length amplification factor. Because the filters had a high particle load, a β correction factor of 2.0 was used (Roesler 1998).

Photosynthetically Usable Radiation (PUR). We calculated PUR (μmol photons m^{-2} s^{-1}) for cultures in their respective light environments as:

$$PUR = \int_{400}^{700} PAR\ (\lambda)\bar{A}\,(\lambda)$$

where the weighting function $\bar{A}(\lambda)$ represents the probability that a photon with a given wavelength is absorbed by the cell (Morel 1978). It is derived from the whole cell absorption spectrum (described above) normalized to its maximum absorption (a_{max}^{Chl}). Percent light use was determined by dividing total PUR by total PAR in the appropriate spectral environment.

Spectral data analysis. Cr-PBP spectra were analyzed using the 'pavo' package in R (Maia et al. 2019). Cr-PBP spectra were scaled so that the maximum absorption is equal to 1, and minimum absorption is equal to 0. This allowed us to compare the overall shape of the Cr-PBP absorption spectra and relative difference in Cr-PBP peak heights. Wavelength of highest absorption (λ_{max}) and full-width-at-half-maximum were determined for extracted Cr-PBP spectra. FWHM is the width of the spectrum at half of the maximum absorbance value. Scaled absorption at 612 nm (Abs_{612}) was also determined for *H. tepida*'s Cr-PBP. When $Abs_{612} = 1$, 612 nm is equal to the maximum Cr-PBP absorption peak. When $Abs_{612} < 1$, Abs_{612} represents the relative contribution to Cr-PBP absorption spectrum as compared to the primary Cr-PBP peak at λ_{max}.

Reciprocal transplants. Starting at 22 months, *H. tepida* cultures grown in green light were used to create cultures that were then grown in white or red light. At the same time, *H. tepida* cultures grown in white light and cultures grown in red light were used to start cultures that were then grown in green light. Cr-PBP absorption spectra were taken from parent cultures on the day new cultures were made. Cr-PBP spectra were then taken in mid to late exponential phase following the initial transplant and following one to two transfers (approximately 4 generations in between transfers; green to white was

transferred twice after the initial transplant; all others were transferred once after the initial transplant). After this, cultures that came from green light and were placed in white or red light were returned to green light for another ~ 8 -12 generations. Cr-PBP absorption spectra were taken from these cultures at approximately 4, 8, and 12 generations (4 and 8 for those coming from white light and 4, 8, and 12 generations for those coming from red light).

Statistics. Growth rate, λ_{max}, FWHM, Abs_{612} (as applicable), and percent light use for cultures in each light treatment across each time point (excluding reciprocal transplants) were tested for normality using the Shapiro-Wilk normality test with the hypothesis of normality rejected at *P*-values < 0.05. Abs_{612} and λ_{max} in white, blue, and red light were too often identical across all replicates for any further analysis. For normally distributed data, significant differences within light treatments across time were determined by a one-way ANOVA with Tukey post-hoc test ($P < 0.05$). For data that were not normally distributed, significant differences were determined using the Kruskal-Wallis test with Dunn's post-hoc test with Bonferroni *P*-adjustment ($P < 0.05$). Only λ_{max}, FWHM, and Abs_{612} were determined for the reciprocal transplants. All analyses were conducted using R.

Results

H. rufescens' growth rate in white, blue, and green light was consistent over the course of 3 years apart from a significantly decreased growth rate in green light at 24 months (Table 5.1). In red light, *H. rufescens* had a significant increase in growth rate from 1-11 months before stabilizing. Percent light use fluctuated over time with no clear trend in any light treatment (Table 5.2). *H. tepida*'s growth rate did not differ

significantly with time in any of the light treatments (Table 5.1), but growth rate in blue light was significantly higher than in any of the other light colors (P <0.005) across all time points. Percent light use fluctuated over time with no clear trend in white, blue, and red light, but increased significantly from 27.05% ± 0.88 at 1 month to 34.45% ± 0.21 after 24 months in green light (Table 5.2). This increase is due to the changes in Cr-PBP absorption in green light.

Figure 5.2 shows the scaled overlay plot of every extracted Cr-PBP absorption spectrum from each light treatment over 2 years for *H. tepida* and 3 years for *H. rufescens*. The general shape of *H. rufescens*' extracted Cr-PBP absorption spectrum remained similar (λ_{max} of 555 nm) in all 4 light treatments, although λ_{max} was slightly more variable in green light with a range of 552-555 nm. FWHM across all light treatments and time points ranged from 55 – 57 nm.

For *H. tepida*, the shape of the extracted Cr-PBP absorption spectrum remained remarkably similar in white, blue, and red light for 2 years (a minor peak at 570 nm with relative absorption of ~0.85-0.95, λ_{max} of 612, FWHM of 90-92 nm). However, it changed dramatically when *H. tepida* was grown in green light (Figure 5.2G). Within 1 month, λ_{max} switched from 612 nm to the peak at 568 nm (previously at 570 nm). Over time, the new primary peak both increased in magnitude compared to the peak at 612 nm and shifted towards the spectral output of the green light (Figure 5.1, Figure 5.3, Table 5.1). FWHM was initially larger than that of *H. tepida* grown in other light colors, ranging from 99-107 nm until 18 months. At 18 months, the primary peak had an absorbance that was more than double the absorbance of the trough separating the two peaks. As a result, the FWHM at 18 months dropped to 56 ± 2 nm, similar to that of *H.*

rufescens. At 18 months, changes to the Cr-PBP were visible in the extracted Cr-PBP absorption spectrum (Figure 5.4B), in cell cultures (Figure 5.4C), and on glass fiber filters with 10 mL of cell culture (Figure 5.4D). By 2 years, the Cr-PBP spectrum from *H. tepida* grown in green light had λ_{max} at approximately 558 nm. One culture ended with FWHM of 60 nm, λ_{max} at 556 nm, and Abs_{612} of only 0.37. The λ_{max} for this culture is within a normal range for a cryptophyte with Cr-PE 555, such as *H. rufescens.* In fact, the visual appearance of this culture is more similar to *H. rufescens* than to *H. tepida* grown in other colors of light. (Figure 5.6).

Reciprocal transplant experiments were conducted at 20 months to determine whether changes to *H. tepida*'s Cr-PBP in green light were permanent. When green-evolved *H. tepida* cultures were placed in white or red light, the Cr-PBP absorption spectra reverted to their ancestral state before the first transfer (~ 4 generations) (Figure 5.5, Table 5.4). λ_{max} reverted to the peak near 612 nm, so $Abs_{612} = 1$. However, when these cultures were returned to green light, their Cr-PBP absorption spectra switched back to the green-evolved phenotype within 1 or 2 transfers (~ 4 generations in white light and ~8 generations in red light). The green-evolved cultures that were in red light took more time in green light to revert to the green-evolved phenotype than those that were placed in white light. Surprisingly, the extracted Cr-PBP absorption spectra only shared characteristics with the ancestral Cr-PBP spectrum or the green-evolved Cr-PBP spectrum—i.e. no intermediate phenotype or indication that the population was heterogenous was detected. There were no noticeable changes to the Cr-PBP spectra from white or red-evolved cultures when placed in green light for 29-30 days (~8-10 generations).

Discussion

I aimed to determine whether two cryptophyte species, *H. rufescens* and *H. tepida*, could adapt their Cr-PBP absorption spectra when grown in a novel light environment over hundreds of generations. I found that Cr-PE 555 from *H. rufescens* showed little to no change in absorbance characteristics across the light environments tested. In contrast, *H. tepida* grown in green light not only evolved to use a Cr-PBP with spectral characteristics more similar to Cr-PE 555 than to its ancestral Cr-PC 612—it could switch between the two depending on its spectral environment. The ancestral *H. tepida* appeared to be able to subtly change the absorbance of the peak in the 565-570 nm region of the Cr-PBP spectrum over 1 month (Figure 5.3B), but not to the extent that the green-evolved *H. tepida* could. I observed no difference in absorption characteristics of red- or white-evolved *H. tepida* Cr-PBP when grown in green light. Therefore, I believe *H. tepida* evolved phenotypic plasticity in green light.

For both *Hemiselmis* species tested here as well as *H. cryptochromatica* (Heidenreich & Richardson 2020) and *H. pacifica* (Spangler et al. 2022), green light elicited the most pronounced changes in Cr-PBP absorption spectrum. While some changes were subtle (*H. rufescens* here and *H. pacifica* in Spangler et al. 2022), it does show the potential for green light to reveal phenotypic plasticity in cryptophytes. A possible explanation is that the blue and red lights used here and in Heidenreich & Richardson (2020) are absorbed so efficiently by chlorophyll that there's no selection pressure on cryptophytes to modify their Cr-PBP as a response.

Cryptophytes are generally thought to only use one Cr-PBP per species, but here we show that *H. tepida* can produce at least two spectroscopically distinct Cr-PBPs after

2 years in green light. In fact, based on criteria used recently to define a novel Cr-PBP type (Magalhães et al. 2021), I could argue that *H. tepida* synthesized at least 3 distinct Cr-PBPs: Cr-PC 612, Cr-PC 564 (6-12 months—Figure 5.3C & D), and the novel Cr-PBP at 18-24 months. However, based on the gradual increase in magnitude and leftward shift of the peak in the 555-570 nm range, I propose that Cr-PBP absorption is a more continuous trait than a categorical one. At the very least, bulk Cr-PBP absorption measurements, as were done here and are typical (Hoef-Emden 2008, Cunningham et al. 2019, Magalhães et al. 2021), should be seen as continuous traits.

Two important limitations of this study are that I was not able to sequence the genomes of the *H. rufescens* and *H. tepida* cultures used and that I was not able to determine chromophore composition and Cr-PBP protein structures. Therefore, the discussion regarding potential changes to the Cr-PBP absorption spectrum from green-evolved *H. tepida* is limited to evidence from other *Hemiselmis* species.

Recent studies have demonstrated the potential for some *Hemiselmis* species to produce multiple Cr-PBP types. Rathbone (2021) isolated and characterized 3 spectrally distinct Cr-PBPs from a strain of *Hemiselmis andersenii* (CCMP 1180). One of these Cr-PBPs contained both phycoerythrobilin (characteristic of Cr-PEs) and phycocyanobilin (characteristic of Cr-PCs) as chromophores. In this particular Cr-PBP, which Rathbone calls *Ha*645, there are two absorption peaks—one at 560 nm and the other at 645 nm. This is relevant to *H. tepida*'s green-evolved Cr-PBP because its two peaks (556-558 nm and 612 nm) appear to be the results of both phycoerythrobilin and phycocyanobilin. However, unlike Ha645, which was only barely detectable in bulk Cr-PBP absorption measurements, green-evolved *H. tepida* produced enough of the novel Cr-PBP (or

combination of Cr-PBPs) to yield two clear peaks in bulk measurements. Prior to Rathbone in 2021, there was no account of a Cr-PBP binding both phycoerythrobilin and phycocyanobilin. When chromophore composition has been determined for Cr-PBPs, there haven't been any documented Cr-PBPs with absorption peaks below 560 nm that don't contain phycoerythrobilin and nor any Cr-PBPs with absorption peaks above 600 nm that don't contain phycocyanobilin (see Table 1 in Richardson 2022).

Michie et al. (2023) demonstrated that much of the absorption characteristics of Cr-PBPs comes from the interaction between the α-subunits and the chromophores. Specifically, they demonstrated that 6 amino acid substitutions on the α-subunit of Cr-PC 577 from *Hemiselmis pacifica* compared to that of the Cr-PC 612 from *Hemiselmis virescens* account for the increased magnitude of the 577 nm peak compared to the peak at 612 nm (which becomes the shoulder in Cr-PC 577). They also demonstrated, along with earlier work (Kieselbach et al. 2018), that between 9-20 different α-subunits are expressed at a time by cryptophyte species across the phylogeny. In fact, 4 *Hemiselmis* species (including the strain of *H. tepida* used here) expressed α-subunits that would produce both open and closed forms of the Cr-PBP quaternary structure (Michie et al. 2023). The increased magnitude of the peak in the 556-570 nm range for our green-evolved Cr-PBP could, therefore, be the result of a substituted α-subunit. The primary α-subunit used could have evolved *de novo* or could have been expressed in smaller quantities previously.

When I began this experiment, I hypothesized that I would observe permanent shifts in Cr-PBP absorption spectra. I did not predict that we would see both a large, complementary shift in the absorption spectrum AND that *H. tepida* would be able to

rapidly shift between the ancestral form of Cr-PC 612 and the novel Cr-PBP. At that time, there was little to suggest that cryptophytes could produce multiple Cr-PBPs in a single species. Since then, research has shown that other *Hemiselmis* species have been found to express multiple α-subunits (Michie et al. 2023) and even multiple Cr-PBPs with different chromophore compositions (Rathbone 2021). Given that all *H. tepida* replicate cultures had shifts in Cr-PBP absorption spectrum, it seems most likely that the green-evolved *H. tepida* did not evolve an entirely new Cr-PBP—it evolved the ability to express a more useful Cr-PBP or combination of Cr-PBPs. It also appears to have evolved the ability to shift between Cr-PBP types in fewer than 10 generations the way *H. cryptochromatica* is able to (Heidenreich & Richardson 2020).

The evolution of phenotypic plasticity in Cr-PBP absorption would potentially allow *H. tepida* to thrive in a variety of spectral niches. Since light color in water is spatially and temporally variable, it seems intuitive that phenotypic plasticity in light absorption would afford phytoplankton an advantage over phytoplankton with fixed light absorption characteristics. It's long been known that many cyanobacteria demonstrate plasticity in their PBP absorption spectra when their light environments change (e.g. Gaiducov 1902, Tandeau de Marsac 1977). Stomp et al. (2008) demonstrated the competitive advantange cyanobacteria with plasticity in PBP abpsorption have over cyanobacteria with fixed PBP absorption. They showed that a cyanobacterial species that can change PE: PC ratios competitively excluded species that primarily use PE or PC, even in fixed light regimes and light regimes that fluctuated faster than the plastic species could adjust its PBP absorption. This raises a few questions regarding cryptophyte Cr-PBP plasticity: 1) why aren't more cryptophytes capable of phenotypic plasticity? and 2)

how does our understanding of Cr-PBP evolution in *Hemiselmis* change if we consider Cr-PBP plasticity as a trait that can be evolved or lost?

Although it's unknown why early authors began stating that cryptophytes only have a single Cr-PBP in a species, a possible explanation is that most cryptophytes do not appear to have a plastic Cr-PBP phenotype. However, there are hints and direct observations in the literature that suggest that *Hemiselmis* species with Cr-PCs have some degree of Cr-PBP plasticity (Hill & Rowan 1989, Heidenreich & Richardson 2020, Spangler et al. 2022). Here I show the evolution of plasticity in *H. tepida* over 2 years, but there was very little change in *H. rufescens* over 3 years. Additionally, Heidenreich and Richardson (2020) saw no change in Cr-PBP absorption when *Hemiselmis andersenii* (another *Hemiselmis* species with Cr-PE 555) was grown in white, blue, green, and red light.

One possibility explaining why *Hemiselmis* species can have a plastic Cr-PBP phenotype but other genera don't seem to is that the evolution of the open form α-subunit and maintenance of the closed form α-subunit in *Hemiselmis* allowed these species to tune at least part of their absorption spectrum to complement their environment. It's conceivable that these species express different forms of the α-subunit to different extents in varying spectral environments. Future work should determine whether the transcriptomes of Cr-PC containing *Hemiselmis* express different ratios of open-form: closed-form α-subunits in varying spectral environments.

Why don't Cr-PE-containing *Hemiselmis* species show more plasticity in Cr-PBP absorption? The main chromophore in Cr-PE 555 is phycoerythrobilin, and the main chromophore in Cr-PC 612 is phycocyanobilin (Wemmer et al. 1993, Wedemayer et al.

1996). These two chromophores are isomers of each other, and phycoerythrobilin is the precursor to phycocyanobilin in one of two phycocyanobilin biosynthesis pathways (Beale 1993). Hoef-Emden (2008) suggested that the switch from an ancestral *Hemiselmis* species that uses Cr-PC 612 to a line of decendents that use Cr-PE 555 could be due to a mutation leading to a defect of the isomerase that converts phycoerythrobilin to phycocyanobilin. Perhaps *Hemiselmis* species with Cr-PC are capable of synthesizing phycoerythrobilin as well as phycocyanobilin, but species with Cr-PE have lost the ability to synthesize meaningful amounts of phycocyanobilin.

The evolution of plasticity and a novel Cr-PBP that causes *H. tepida* to look more like *H. rufescens* than like its ancestor (Figure 5.6) suggests that the ancestor to both species may have had a plastic Cr-PBP phenotype before fully shifting to Cr-PE 555 or Cr-PC 612. The Baldwin effect refers to increased survivability of phenotypically plastic individuals in novel environments (Baldwin 1902, Simpson 1953). Organisms with a wide range of phenotypic responses to different environments are able to explore a range of adaptive strategies. If there is a good fit between part of a range of phenotypic responses and the environment and there are costs to maintain plasticity, what was part of a plastic response may become a fixed trait (Price et al. 2003, Crispo 2007). I can imagine a scenario where an organism with the Cr-PBPs and plasticity of our green-evolved *H. tepida* persisted in an environment dominated by green light for long enough that it lost the ability to synthesize phycocyanobilin and, therefore, Cr-PC.

The fact that increases in percent light use did not correspond with significant increases in growth rate for green-evolved *H. tepida* (Tables 5.1 and 5.2) suggests there may be fitness costs associated with maintaining phenotypic plasticity. These costs could

be related to synthesis of phycoerythrobilin-to-phycocyanobilin isomerase, maintenance and regulation of multiple α-subunits, and/or maintenance of the ability to sense the spectral environment. In contrast, *H. rufescens*, which had a similar growth rate to *H. tepida* in white light throughout the experiment, had a considerably higher growth rate in green light than the green-evolved *H. tepida*, despite having a similar Cr-PBP.

Here I showed the evolution of a novel Cr-PBP and phenotypic plasticity in *H. tepida* and contrasted it with *H. rufescens*, a closely related species whose Cr-PBP absorption spectrum remained remarkably fixed. I propose a model for the evolution of these two species that involves an ancestor with a plastic Cr-PBP absorption spectrum that diverged into separate lineages: one that uses Cr-PE primarily and one that uses Cr-PC primarily. A phenotypically plastic ancestor would have been able to explore varying spectral environments and a variety of Cr-PBP compositions before arriving at a more fixed Cr-PBP phenotype. More work should be done to determine the costs and mechanisms of phenotypic plasticity in Cr-PBP absorption spectra in *Hemiselmis*.

Tables

Table 5.1. Average growth rate (day^{-1}) for *H. rufescens* and *H. tepida* grown in white, blue, green, and red light over time. Errors are standard deviations of 4-8 measurements. Superscript letters represent significant differences within a species and light treatment across time points (i.e., if superscript letters within a species/light treatment match, they are not significantly different with a $P < 0.05$). Where there are no superscript letters, there was no significant difference in growth rate within species and light treatment across time points.

		White	**Blue**	**Green**	**Red**
H. rufescens	1 month	0.23 ± 0.04	0.44 ± 0.04	0.43 ± 0.03^{a}	0.14 ± 0.06^{c}
	6 months	0.25 ± 0.05	0.46 ± 0.02	0.40 ± 0.02^{ab}	0.23 ± 0.02^{ab}
	11 months	0.23 ± 0.03	0.42 ± 0.02	0.41 ± 0.03^{a}	0.27 ± 0.02^{a}
	24 months	0.30 ± 0.11	0.47 ± 0.05	0.33 ± 0.06^{b}	0.21 ± 0.05^{abc}
	30 months	0.23 ± 0.05	0.44 ± 0.02	0.41 ± 0.02^{a}	0.18 ± 0.07^{bc}
H. tepida	1 month	0.24 ± 0.03	0.35 ± 0.05	0.24 ± 0.03	0.21 ± 0.05
	12 months	0.26 ± 0.04	0.35 ± 0.02	0.27 ± 0.02	0.24 ± 0.02
	18 months	0.26 ± 0.03	0.37 ± 0.05	0.25 ± 0.01	0.24 ± 0.02
	24 months	0.25 ± 0.03	0.30 ± 0.08	0.28 ± 0.07	0.23 ± 0.03

Table 5.2. Average percent light use (photosynthetically usable radiation/photosynthetically available radiation) for *H. rufescens* and *H. tepida* grown in white, blue, green, and red light over time. Errors are standard deviations of 4-8 measurements. Superscript letters represent significant differences within a light treatment across time points (i.e., if superscript letters within a light treatment match, they are not significantly different with a $P < 0.05$)

		White	**Blue**	**Green**	**Red**
H. rufescens	1 month	37.8 ± 1.60^{c}	45.8 ± 0.24^{ab}	39.9 ± 1.11^{ad}	10.9 ± 1.90^{bcd}
	6 months	45.4 ± 1.97^{ab}	46.2 ± 0.39^{a}	43.2 ± 0.95^{ab}	16.1 ± 0.37^{ac}
	11 months	39.0 ± 1.84^{bc}	45.5 ± 0.42^{b}	38.3 ± 2.23^{bcd}	10.0 ± 1.90^{bd}
	19 months	54.1 ± 3.30^{a}	45.9 ± 1.08^{ab}	45.2 ± 3.41^{a}	23.0 ± 7.18^{a}
	24 months	43.2 ± 3.60^{ac}	45.8 ± 0.14^{ab}	35.8 ± 1.38^{d}	15.6 ± 0.54^{ad}
	30 months	43.7 ± 3.84^{ac}	46.1 ± 0.19^{a}	42.7 ± 0.88^{ac}	16.7 ± 2.18^{ac}
	36 months	40.4 ± 4.03^{bc}	46.0 ± 0.19^{ab}	41.3 ± 4.04^{ad}	17.2 ± 4.35^{ab}
H. tepida	1 month	46.5 ± 1.60^{c}	45.0 ± 0.40^{ab}	27.1 ± 0.88^{c}	19.0 ± 1.01^{c}
	6 months	53.6 ± 1.66^{a}	45.4 ± 0.21^{a}	33.3 ± 0.73^{ab}	23.9 ± 0.98^{a}
	12 months	51.7 ± 1.22^{a}	45.4 ± 0.18^{ab}	31.0 ± 0.95^{bc}	22.6 ± 1.11^{ab}
	18 months	43.1 ± 1.46^{d}	45.3 ± 0.17^{ab}	35.5 ± 1.19^{a}	23.2 ± 0.76^{ab}
	24 months	49.2 ± 0.55^{b}	44.9 ± 0.21^{b}	34.5 ± 0.21^{ab}	21.5 ± 0.66^{b}

Table 5.3. Average wavelength of maximum absorption (λ_{max}) and absorption at 612 nm (Abs_{612}) for *H. tepida* grown in green light for 0, 1, 6, 12, 18, and 24 months. Errors are standard deviations of 3-8 measurements. Superscript letters represent significant differences within a treatment across time points (i.e., if superscript letters within a treatment match, they are not significantly different with a $P < 0.05$).

	λ_{max} (nm)	Abs_{612}
0 months (before)	612 ± 0^{a}	1 ± 0^{ab}
1 month	568 ± 0^{b}	0.99 ± 0.01^{a}
6 months	567 ± 0.92^{bd}	0.98 ± 0.02^{a}
12 months	562 ± 1.51^{bc}	0.80 ± 0.06^{ac}
18 months	558 ± 0.74^{c}	0.54 ± 0.03^{c}
24 months	558 ± 1.73^{cd}	0.58 ± 0.18^{bc}

Table 5.4. Average wavelength of maximum absorption (λ_{max}) and absorption at 612 nm (Abs_{612}) for *H. tepida* reciprocal transplants. Days are measured from the start of the reciprocal transplant. Where evolved light color is the same, there were replicates created from the same cultures (e.g. cultures grown in green light were used for inoculations for cultures that were transplanted to red or white light). Red to green light and white to green light transplants were ended after 30 and 29 days, respectively. Green to red light cultures were grown in red light for 33 days before being placed back in green light for an additional 42 days. Green to white light cultures were grown in white light for 40 days before being placed back in green light for an additional 24 days. Errors are standard deviations of 3-8 measurements.

Evolved light color	**Transplant light color**	**Days since 1st transplant**	**λ_{max} (nm)**	**Abs_{612}**
Green	Red	0	558 ± 0.82	0.56 ± 0.05
Green	Red	18	613 ± 0.71	1.00 ± 0.01
Green	Red	33	614 ± 1.00	1.00 ± 0
Green	Red → Green	47	613 ± 0.50	1.00 ± 0
Green	Red → Green	61	557 ± 1.00	0.56 ± 0.04
Green	Red → Green	75	557 ± 0.6	0.56 ± 0.03
Green	White	0	558 ± 0.82	0.56 ± 0.05
Green	White	13	612 ± 0.55	1 ± 0
Green	White	25	614 ± 0.84	1 ± 0
Green	White	40	612 ± 0.45	1 ± 0.01
Green	White → Green	48	558 ± 0.58	0.58 ± 0.04
Green	White → Green	64	558 ± 0.84	0.52 ± 0.03
Red	Green	0	613 ± 0.41	1 ± 0
Red	Green	16	613 ± 0	1 ± 0
Red	Green	30	613 ± 0.41	1 ± 0
White	Green	0	613 ± 0.82	1 ± 0
White	Green	15	613 ± 0.75	1 ± 0
White	Green	29	613 ± 0.98	1 ± 0.01

Figures

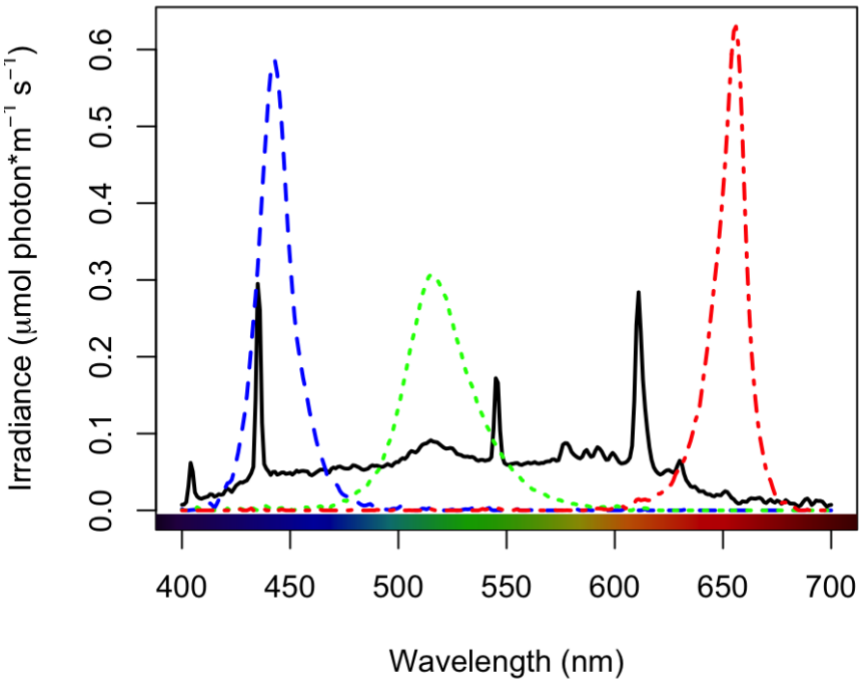

Figure 5.1. Spectral irradiance of white (solid black line), blue (dashed blue line), green (dotted green line), and red (dot-dash red line) light in incubator.

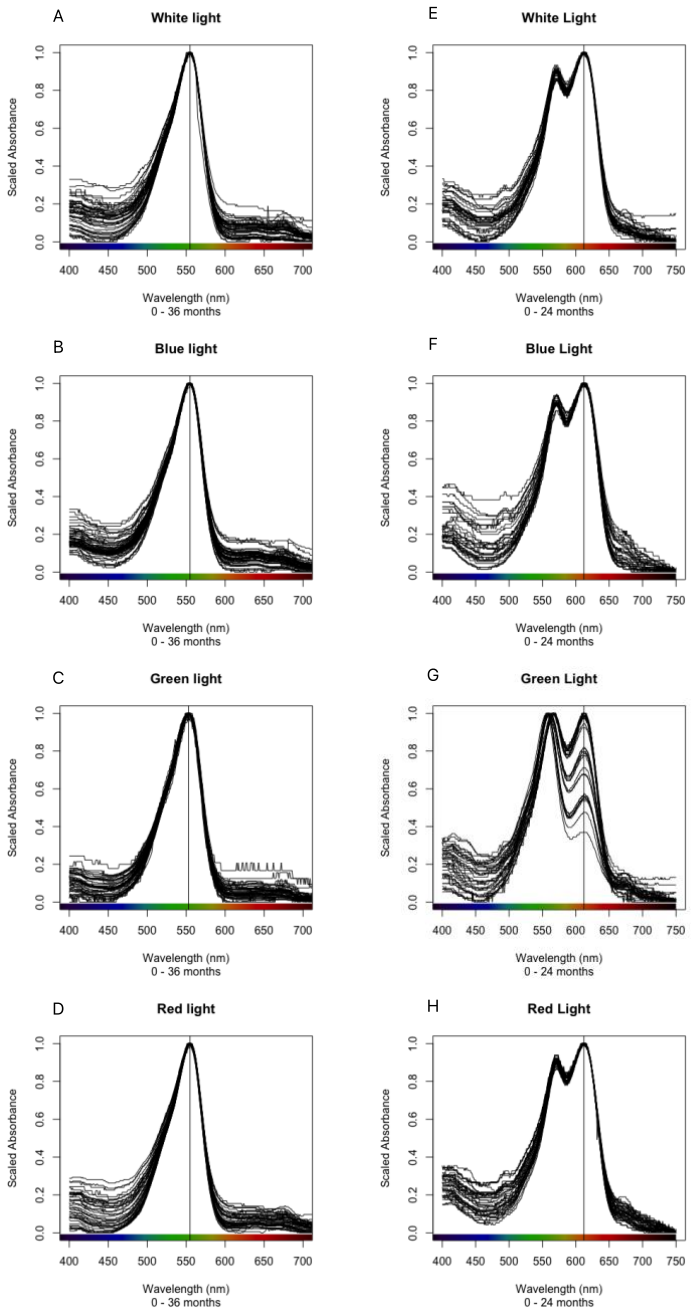

Figure 5.2. Overlay plots of extracted Cr-PBP spectra scaled from 0 – 1 (0 = minimum absorbance, 1= maximum absorbance) from *H. rufescens* grown in white (A), blue (B), green (C), and red (D) light for 0 - 36 months and *H. tepida* grown in white (E), blue (F), green (G), and red (H) light for 0 – 24 months. For each combination of species and light color at each time point, 3-8 cultures were sampled. Vertical line on each plot indicates the wavelength of maximum absorption in the ancestral culture grown in white light (555 nm for *H. rufescens* and 612 nm for *H. tepida*).

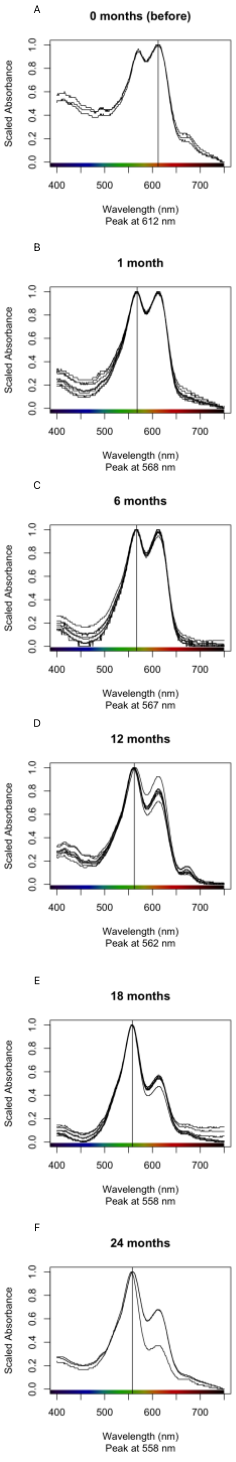

Figure 5.3. Overlay plots of extracted Cr-PBP spectra scaled from 0 – 1 (0 = minimum absorbance, 1= maximum absorbance) from *H. tepida* in white light before start of experiment (A) and in green light at 1 month (B), 6 months (C), 12 months (D), 18 months (E), and 24 months (F). Vertical line indicates wavelength of maximum absorption.

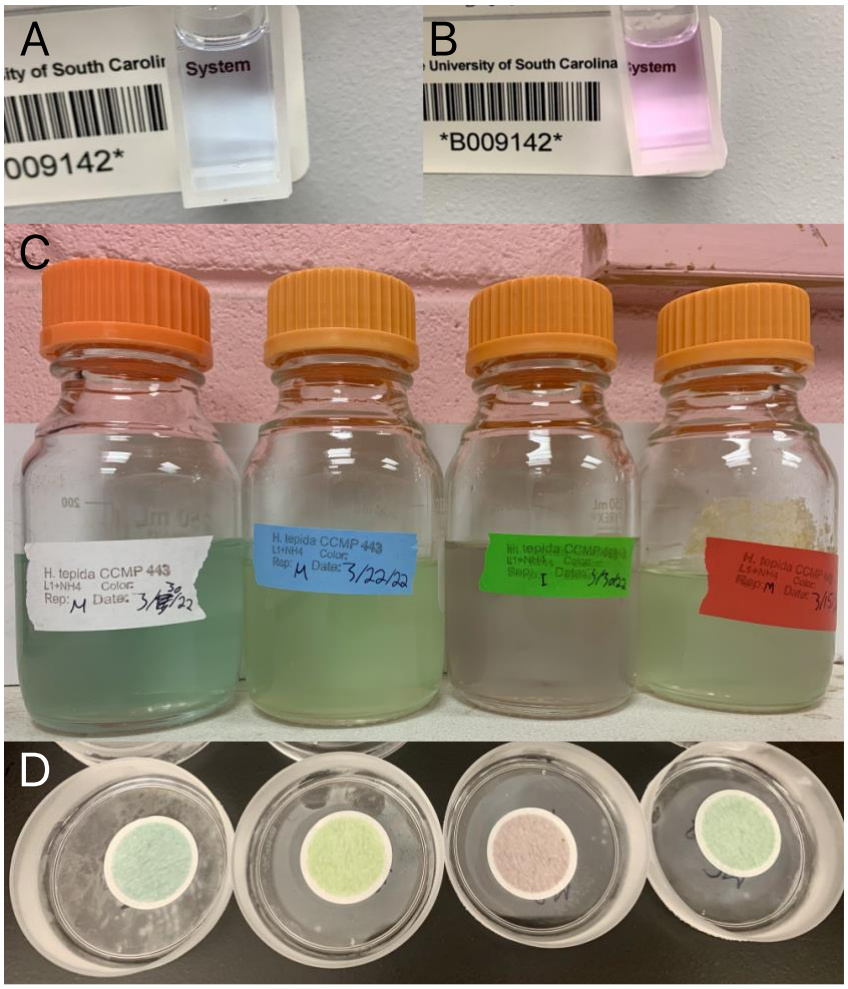

Figure 5.4. Visible color differences at 18 months. A shows a cuvette containing extracted Cr-PBP from *H. tepida* grown in white light. B shows a cuvette containing extracted Cr-PBP from *H. tepida* grown in green light. C shows dense cultures of *H. tepida* grown in (from left to right) white, blue, green, and red light. D shows glass fiber filters with cells from 10 mL of cultures grown in (from left to right) white, blue, green, and red light.

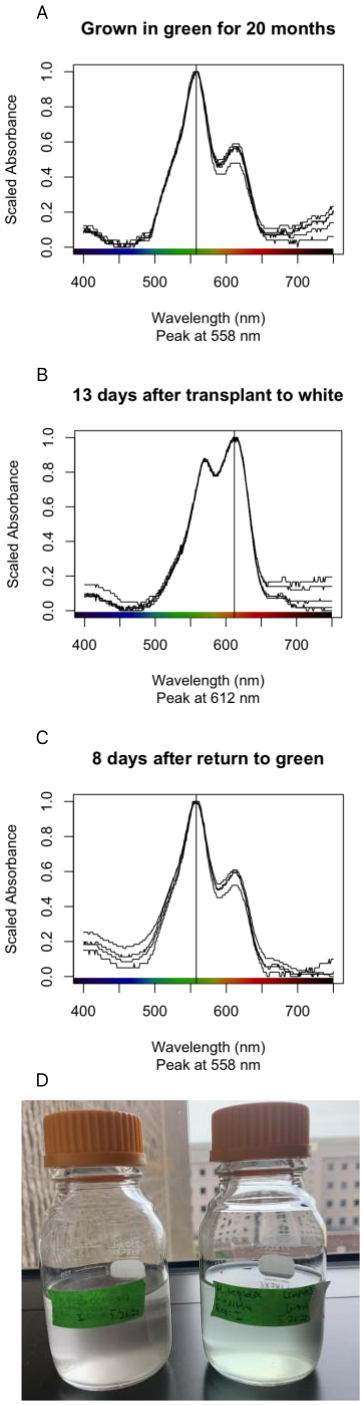

Figure 5.5. A-C: Overlay plots of extracted Cr-PBP spectra scaled from 0 – 1 (0 = minimum absorbance, 1= maximum absorbance) from *H. tepida* grown in green light for 20 months (A), then transplanted to white light for 13 days (B) and grown in white for an additional 27 days and returned to green light for 8 days. D shows two cultures that were both created 13 days earlier from the same parent culture that had been grown in green light for 20 months. The culture on the left stayed in green light, but the culture on the right was transplanted to white light.

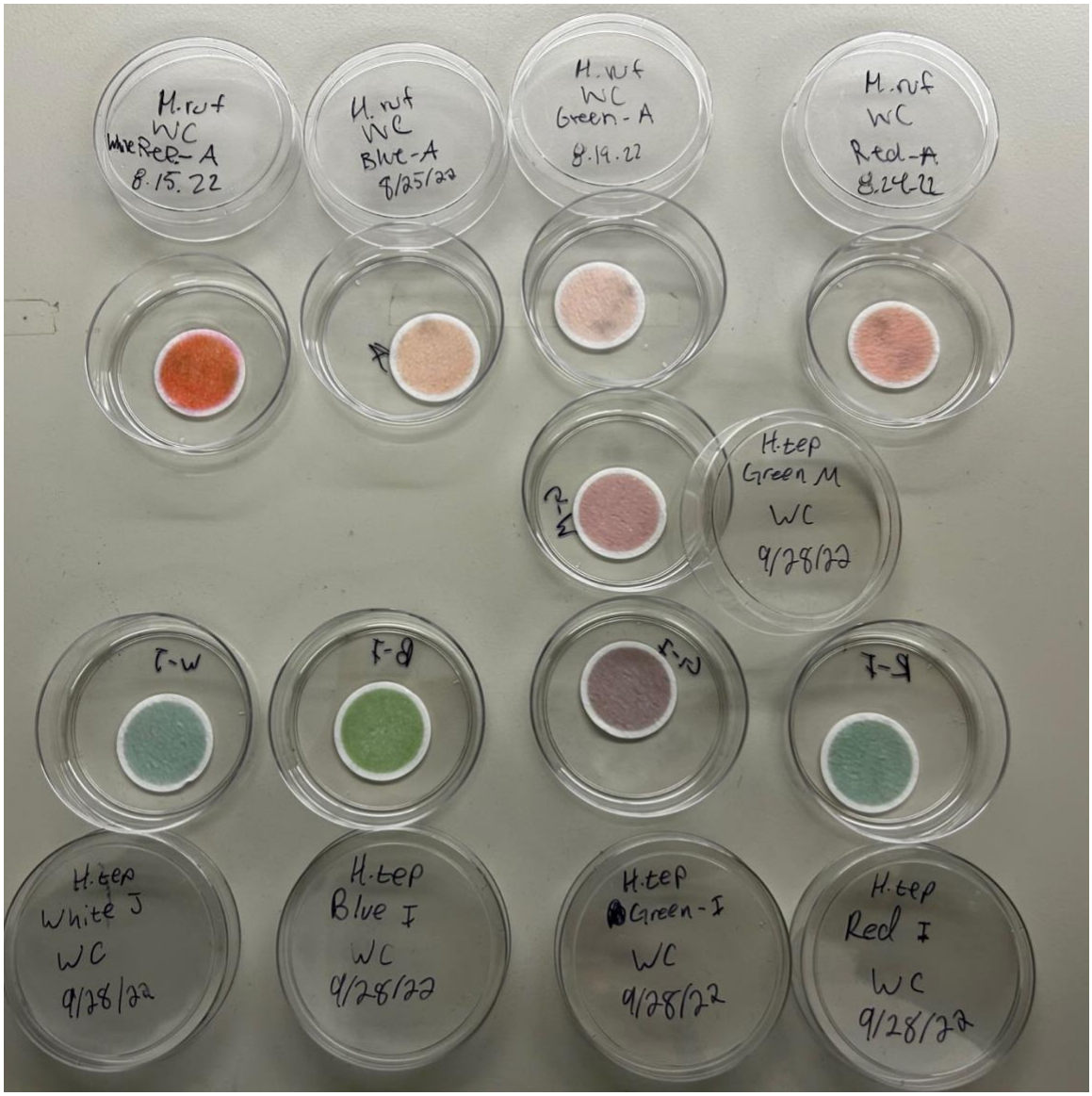

Figure 5.6. Comparison of visual appearance of *H. rufescens* (top row) on glass fiber filters grown in (left to right) white, blue, green, and red light for 3 years versus *H. tepida* (bottom row) on glass fiber filters grown in (left to right) white, blue, green, and red light for 2 years. The filter in the middle is from a single replicate culture of *H. tepida* grown in green light whose Cr-PBP λ_{max} was 556 nm.

CHAPTER 6

CONCLUSION

“And [the teacher] said...

Flowers are red young man and

Green leaves are green

There's no need to see flowers any other way

Than they way they always have been seen

But the little boy said...

There are so many colors in the rainbow

So many colors in the morning sun

So many colors in a flower and I see every one”

Harry Chapin 1978

As scientists, there’s a dangerous tendency to assume that we are less likely than the average person to cling to paradigms that aren’t supported by evidence. We imagine that we are purely rational so the assumptions that we make about the systems we study are likely true. Not recognizing and questioning the dogmas around which we build our

scientific frameworks can steer us away from asking basic questions that could further our understanding of the natural world.

One example of the way scientific dogmas can cloud our judgement is the story of how we came to accept the theory of endosymbiosis as the origin for mitochondria and plastids. The idea that plastids originated from an ancient endosymbiosis event dates back to 1883 and comes from a footnote from a paper on plastids by German botanist, Andreas Schimper. Schimper (1883) wrote that if plastids are not produced *de novo* in plant egg cells, it could be evidence of a symbiotic relationship between the chloroplast and the host cell. Despite the testability of this hypothesis, the idea gained little traction for another twenty years. At the time, the accepted theory for the appearance of chloroplasts in the cell was that they were differentiated within the cytoplasm (Mereschkowsky 1905).

Mereschkowsky (1905) pointed out that there's no evidence of differentiation of chloroplasts from cytoplasm and no reason to believe cells were ever capable of creating chloroplasts *de novo*. In fact, it was observed that plastids only ever arose through division of preexisting plastids. He also argued that organs must necessarily originate from germ plasm and be heritable. If the plastids are not and have never been organs, they must be symbionts. As evidence of plastid independence, he points out that when the nucleus is removed from a plant cell, plastids continue to function while organelles shut down with lack of synthetic morphological processes usually initiated by the nucleus. Mereschkowsky goes on to hypothesize that plastids came specifically from blue-green cyanophyceae, now known as cyanobacteria, and even demonstrates instances of cyanophytes invading eukaryotic algal cells.

Despite the apparent evidence for the endosymbiotic theory, it was again largely dismissed for decades until Lynn Sagan promoted the idea of a unifying theory for the origin of eukaryotic cells in 1967. In addition to the chloroplast, she also theorized that the mitochondria of eukaryotic cells were the descendants of an ancient aerobic bacterium (Sagan 1967). Like Mereschkowsky, Sagan also pointed to cyanobacteria as the ancestor of the chloroplast. She pointed to naturally occurring counterparts to the plastid and mitochondria and the fact that these organelles have their own genomes as evidence.

The theory of endosymbiosis drew controversy from some because it seemingly sidestepped a difficult issue in considering the gradual evolution of organelles (Uzzell and Spolsky 1974). The prevailing dogma at the time was that evolution only occurred gradually so the structures we observe today must have arisen through small steps and minor modifications rather than in large leaps. Critics of the endosymbiotic theory called it "retrogressive" and argued that the criteria to consider organelles as having an endosymbiotic origin were insufficient to rule out evolutionary origins. Uzzell and Spolkey argue that similarity between organelles and prokaryotes could simply reflect the primitive character state of the common ancestor of eukaryotic organisms rather than endosymbiotic origin. Before organellar genomes were sequenced, they said that if organellar genomes are similar to eukaryotic nuclei, then that's evidence they evolved without endosymbiosis. However, they also make the argument that if organellar genomes are similar to prokaryotic genomes, it could be due to retention of primitive genes. It's hard to imagine that they would make such a "heads, I win; tails, you lose"

argument if they weren't so attached to the idea that evolution can only progress gradually.

Eventually, Gray & Doolittle (1982) identified potential forms of proof for the endosymbiotic theory: 1) evolutionary histories of nuclear genomes are shown to be distantly removed before the date of the formation of the first eukaryotic cell; 2) the nuclear genome is clearly descended from a different lineage other than that of the mitochondria and plastid; and 3) if the nuclear genome had only one ancestor, but plastids of different eukaryotic groups had different ancestors. Observation of plastid genomes across green algae and higher plants revealed similarities between plastid DNA and bacterial DNA such as circular DNA and absence of histones (Gray & Doolittle 1982). Size and G+C content was also very consistent across plastids from green algae and higher plants. Plastid DNA and bacterial DNA also both had very few repeated sequences, unlike nuclear DNA. Even the structure and function of plastid ribosomes more closely aligns with bacteria than eukaryotic cytoplasmic ribosomes. Further exploration showed that nuclear, mitochondrial, and plastid genomes had distinct lineages independent of each other save for a few genes that could have been transferred horizontally following an endosymbiosis event.

Almost a century passed between initial observations that suggested plastids arose via endosymbiosis and acceptance of the endosymbiotic theory. We now recognize the importance of endosymbiosis in the evolution of all eukaryotic life and can ask important questions about the consequences and mechanisms of endosymbiosis. For example: what are the effects of intracellular horizontal gene transfer following endosymbiosis? In Chapter 2 of this dissertation, I point out that the cryptophyte phycobiliprotein (Cr-PBP)

β-subunit is highly conserved and encoded by a single plastid gene (Douglas 1992). In contrast, the α-subunits are nuclear-encoded and form a large gene family that appears to be the result of a series of duplications and divergences (Curtis et al. 2012, Michie et al. 2023). As Gray & Doolittle (1982) found, unlike nuclear DNA, plastid DNA tends to have very few repeated sequences. The transfer of linker protein genes from cyanobacteria to the red algal nucleus allowed these genes to diversify (Lee et al. 2019). It's possible that one of these genes that evolved in red algae moved to the cryptophyte nucleus following endosymbiosis and went through a series of duplications and divergences to eventually become the diverse gene family that encodes for the cryptophyte α-subunits (Rathbone et al. 2021).

When I started my PhD, the consensus among cryptophyte researchers was that cryptophytes are only capable of producing one Cr-PBP per species. It still is not clear to me exactly how this consensus was reached. The earliest papers stating that cryptophytes only produce a single Cr-PBP do not explain how they came to this conclusion. I learned that Cr-PBPs were named for the wavelength where their absorption is maximal, but I didn't understand why many Cr-PBPs had absorption maxima that were different than their name would imply (e.g. Cr-PE 555 from *Hemiselmis andersenii* has an absorption maximum at 548 nm, so why isn't it Cr-PE 545?). When the post-doctoral fellow in our cryptophyte research group published a cryptophyte phylogeny with ancestral state reconstructions, it implied that the ancestry leading to the diverse *Hemiselmis* clade switched between cryptophyte phycoerythrin (Cr-PE) and cryptophyte phycocyanin (Cr-PC) multiple times (Greenwold et al. 2019). When I assisted the previous graduate student with her data collection, we saw that *Hemiselmis cryptochromatica* had

drastically different Cr-PBP absorption characteristics when grown under different colors of light (Heidenreich & Richardson 2020). Its wavelength of maximum absorption differed by 57 nanometers when grown in red light versus green light, but we still asked how it changed its (singular) Cr-PBP.

Fortuitously, in 2021, my advisor served on the committee of a PhD student in Australia who was studying Cr-PBPs. This researcher was also troubled by clues in the Cr-PBP literature that don't make sense under the single Cr-PBP per species framework (Rathbone 2021). By growing large-volume cultures and separating Cr-PBPs using mass spectrometry he showed that *H. andersenii* CCMP 1180 contains multiple spectrally distinct Cr-PBPs. More recently, structural and transcriptomic work showed that 1) amino acids on α-subunits can tune the chromophores on Cr-PBPs to the extent that they result in different Cr-PBP types, and 2) cryptophytes transcribe as many as 23 different α-subunits (Michie et al. 2023). These findings aligned so much better with my observations of spectral variation within "Cr-PBP types" (Chapter 3) and previous observations of phenotypic plasticity in *H. cryptochromatica* (Heidenreich & Richardson, 2020).

Breaking from the single Cr-PBP per species paradigm and observing the evolution of a phenotypically plastic Cr-PBP spectrum in *Hemiselmis tepida* (Chapter 5), I began to incorporate phenotypic plasticity into a potential model for the evolution of Cr-PBP diversity in *Hemiselmis*. Instead of forcing *Hemiselmis* species with multiple Cr-PBP spectra into a single category based on the Cr-PBP types defined by literature, I considered a range of phenotypic plasticity (Figure 6.1). I also compared *H. tepida*'s Cr-PBP absorption spectra at different time points when evolving in green light (Chapter 5)

to Cr-PBP absorption spectra of other *Hemiselmis* grown in white light in the Richardson lab (Figure 6.2). Finally, I considered the current knowledge regarding α-subunit sequence and structure in *Hemiselmis* and the *Chroomonas/Komma* clade (Michie et al. 2023).

I found that the Cr-PBP absorption spectrum from *Hemiselmis aquamarina* appears to be an intermediate form of the Cr-PBP absorption spectrum of *H. tepida* grown in green light at 6 and 12 months (Figure 6.2 A-C). In fact, the spectrum of a single *H. tepida* culture in green light for 12 months has its maximum absorption at 565 nm, which would not be unexpected for a measurement of *H. aquamarina*'s Cr-PC 564. The Cr-PBP spectrum of *Hemiselmis rufescens* resembles that of the primary Cr-PBP absorption peak from *H. tepida* grown in green light for 24 months (Figure 6.2 D & E).

An amino acid insertion on the α-subunit changes the quaternary form of the Cr-PBP $\alpha_1\alpha_2\beta\beta$ dimer from a tightly packed "closed" conformation to a donut-shaped "open" conformation (Harrop et al. 2014). This insertion is characteristic *Hemiselmis* species but found not in any other cryptophyte species (Harrop et al. 2014). Michie et al. (2023) found that *Hemiselmis* species transcribe multiple sequences of both open and closed form α-subunits. I think this insertion and the maintenance of multiple forms of α-subunits is what set *Hemiselmis* on a separate evolutionary path from *Chroomonas/Komma* (Figure 6.3). I hypothesize that the ancestor to all the *Hemiselmis* species had a high degree of plasticity and primarily used Cr-PCs, as seen in *H. cryptochromatica* (Figure 6.4). After *H. cryptochromatica* diverged from the rest of the *Hemiselmis*, I think the ancestor to the rest had a phenotypically plastic Cr-PBP composition that included Cr-PC 615 (equivalent to Cr-PC 612 in the literature).

A phenotypically plastic ancestor to extant *Hemiselmis* species may have occupied a variety of spectral niches and diverged into multiple lines that arrived at different end points for Cr-PBP absorption spectra that vary as to the degree of phenotypic plasticity. Phenotypes that were once part of a range of phenotypically plastic responses may become more fixed set points in stable environments, especially if maintaining phenotypic plasticity is costly (Crispo 2007). Perhaps the ancestor *Hemiselmis* species that primarily use Cr-PE lived in green light for long enough that the maintenance of PEB to PCB isomerase was too costly or a defect in the gene coding for this enzyme was not detrimental (Hoef-Emden 2008). Even though Stomp et al. (2008) demonstrated that a cyanobacterial species phenotypically plastic Cr-PBP absorption has an advantage in most light environments over species with fixed Cr-PBP absorption, there may be costs of phenotypic plasticity that are specific to cryptophytes.

By critically examining and even overturning the dogma that cryptophytes only have a single Cr-PBP per species, we can investigate the mechanistic underpinnings of phenotypic plasticity in Cr-PBP absorption in cryptophytes. We may also be able to ask more informed questions about why so many cryptophytes do not appear to be able to change their Cr-PBP absorption spectrum although they express so many distinct α-subunits (Kieselbach et al. 2018, Michie et al. 2023). We may be better able to model light transfer from Cr-PBPs to photosystems within the thylakoid (Rathbone 2021). It's natural to rely on existing frameworks when studying a complex system. However, scientific frameworks are only as good as the evidence upon which they are built. As scientists we need to remember to constantly evaluate our underlying assumptions based

on existing evidence. Strict adherence to a particular paradigm can cause us to overlook and underreport contradictory evidence, impeding scientific progress.

Figures

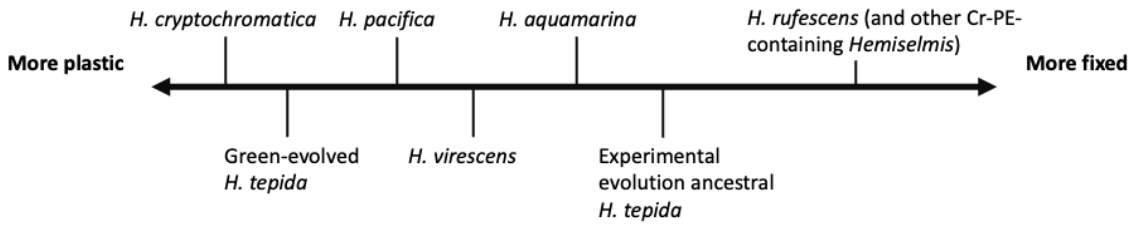

Figure 6.1. A conceptual phenotypic plasticity scale for Cr-PBP absorption spectrum. Exact distances are arbitrary here. *H. cryptochromatica* is on the extreme plastic side of the scale because it changes its Cr-PBP absorption drastically in white, blue, green, and red light within 10 generations (Heidenreich & Richardson 2020). Green-evolved *H. tepida* is next because it switches between a novel Cr-PBP spectrum in green light to a typical Cr-PC 612 in white and red light within 4-5 generations (Chapter 5). Spangler et al. 2022 show modest, reversible changes in *H. pacifica* Cr-PBP absorption, but an undergraduate researcher in the Richardson lab has shown substantial phenotypic plasticity in Cr-PBP absorption (Jin, 2023). *H. virescens* and *H. aquamarina* are next because, although we don't have studies showing their spectra in different light environments, their major Cr-PBP peaks change in location and relative height (even within a strain and within the same lab—Hill & Rowan 1989, Chapter 3). The ancestor to the *H. tepida* cultures I used for Chapter 5 are next because they showed modest changes to relative peak height (i.e., the minor peak having the same scaled absorption as the major peak) after 10 generation in green light. *H. rufescens* and other *Hemiselmis* species with Cr-PE are on the more fixed end of the scale because there hasn't been a change of more than 5 nm in Cr-PBP major peak location in any light color studied by me or Heidenreich & Richardson 2020.

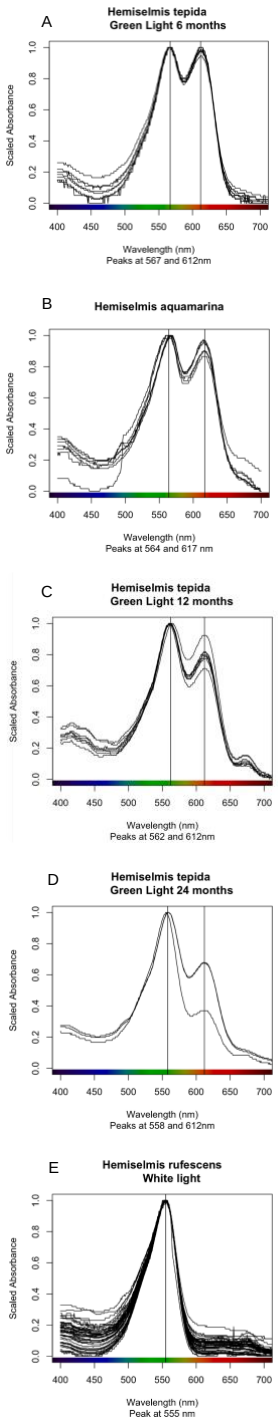

Figure 6.2. Comparison of Cr-PBP absorption spectra from *H. tepida* grown in green light for 6 months (A), 12 months (C), and 24 months (D) versus *H. aquamarina* (B) and *H. rufescens* (E) both grown in white light.

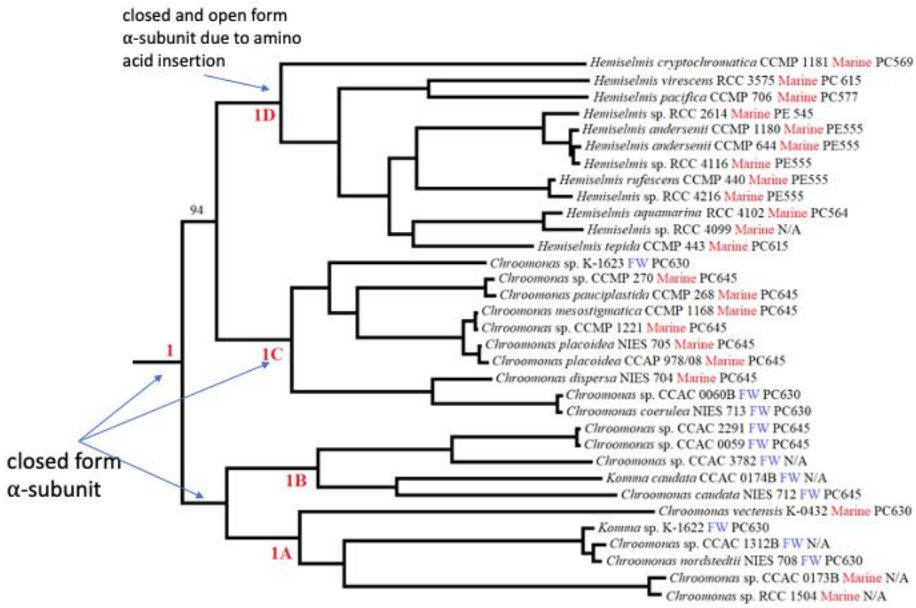

Figure 6.3 A cropped version of maximum likelihood cryptophyte phylogeny based on ultra-conserved elements from nuclear, nucleomorph, and plastid genomes (Greenwold et al. 2023, submitted; used with permission). Strains are labeled based on habitat (marine or FW=freshwater) and predominant Cr-PBP inferred from extracted Cr-PBP absorption spectra when grown in white light. Arrows indicate my hypothesis for the ancestral state of the α-subunit at each node.

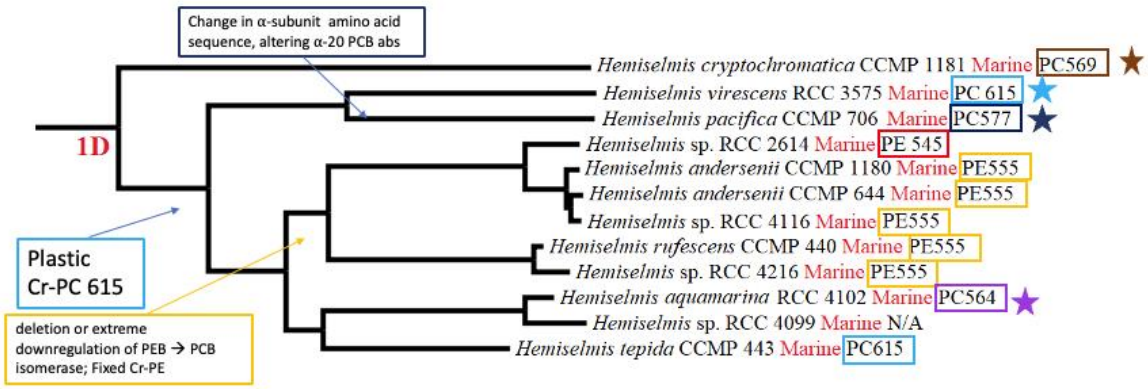

Figure 6.4. A cropped version of maximum likelihood cryptophyte phylogeny based on ultra-conserved elements from nuclear, nucleomorph, and plastid genomes (Greenwold et al. 2023, submitted; used with permission). Strains are labeled based on habitat (marine or FW=freshwater) and predominant Cr-PBP inferred from extracted Cr-PBP absorption spectra when grown in white light. Stars indicate *Hemiselmis* species with evidence of plasticity in the literature. Boxes and arrows indicate my hypotheses for ancestral states at particular nodes.

REFERENCES

Adolf JE, Bachvaroff T, Place AR (2008) Can cryptophyte abundance trigger toxic *Karlodinium veneficum* blooms in eutrophic estuaries? Harmful Algae 8: 119-128.

Allen MB, Dougherty EC, McLaughlin JJA (1959) Chromoprotein pigments of some cryptomonad flagellates. Nature 184:1047-1049.

Apt KE, Collier JL, and Grossman AR (1995) Evolution of the Phycobiliproteins. J Mol Biol 248 (1): 79-96.

Archibald JM, and Keeling PJ (2002) Recycled plastids: a "green movement" in eukaryotic evolution. Trends Genet 18 (11): 577-584.

Archibald JM (2020) Cryptomonads. Curr Biol 30: R1114-6.

Baldwin JM (1902) Development and evolution. MacMillan Co., London.

Barone, R & Naselli-Flores, L (2003) Distribution and seasonal dynamics of cryptomonads in Sicilian water bodies. Hydrobiologia 502: 325-329.

Beale SI (1993) Biosynthesis of phycobilins. Chem Rev 93: 785-802.

Beusen AHW, Bouwman AF, Van Beek LPH, Mogollón JM, & Middelburg JJ (2016) Global riverine N and P transport to ocean increased during the 20th century despite increased retention along the aquatic continuum. Biogeosciences 13: 2441–2451.

Blough NV, del Vecchio R (2002) Chromophoric DOM in the Coastal Environment. In: Hansell, D.A., Carlson, C.A. [Eds.], Biochemistry of Marine Dissolved Organic Matter. Elsevier Science, pp. 509-546.

Brocks JJ, Buick R, Summons RE, Logan GA (2003) A reconstruction of Archean biological diversity based on molecular fossils from the 2.78 to 2.45 billion-year-old Mount Bruce Supergroup, Hamersly Basin, Western Austrailia. Geochim Cosmochim Ac 67 (22): 4321-4335.

Buick R (1992) The Antiquity of Oxygenic Photosynthesis: Evidence from Stromatolites in Sulphate-Deficient Archaean Lakes. Science 255 (5040): 74-77.

Corbella M, Cupellini L, Lipparini F, Scholes GD, Curutchet C (2019) Spectral variability in phycocyanin cryptophyte antenna complexes is controlled by changes in the α-polypeptide chains. Chem Photo Chem 3 (9): 945-956

Cotti-Rausch BE, Lomas MW, Lachenmyer EM, Goldman EA, Bell DW, Goldberg SR, Richardson TL (2016) Mesoscale and sub-mesoscale variability in phytoplankton community composition in the Sargasso Sea. Deep-Sea Res. Pt I 56: 106-122.

Creed IF, Bergström A, Trick CG, Grimm NB, Hessen DO, Karlsson J, et al. (2018) Global change-driven effects on dissolved organic matter composition: implications for food webs of northern lakes. Glob. Change Biol. 24: 3692-3714.

Crispo E (2007) The Baldwin effect and genetic assimilation: revisiting two mechanisms of evolutionary change mediated by phenotypic plasticity. Evolution 61: 832-841.

Cunningham BR, Greenwold MJ, Lachenmyer EM, Heidenreich KM, Davis AC, Dudycha JL, Richardson TL (2019) Light capture and pigment diversity in marine and freshwater cryptophytes. J Phycol 55(3), 552–564.

Curtis BA, Tanifuji G, Burki F, Gruber A, Irimia M, Maruyama S et al. (2012) Algal genomes reveal evolutionary mosaicism and the fate of nucleomorphs. Nature 492: 59-65.

de Marsac NT, Cohen-Bazire G (1977) Molecular composition of cyanobacterial phycobilisomes. Proc Natl Acad Sci USA 74 (4), 1635-1639.

Des Marais DJ (2000) When did photosynthesis emerge on Earth? Science 289: 1703-1705. PMID: 11001737

Douglas SE (1992) Eukaryote-eukaryote endosymbioses: insights from studies of a cryptomonad alga. Biosystems 28: 57-68.

Douglas SE, Zauner S, Fraunholz M, Beaton M, Penny S, Deng L, et al. (2001) The highly reduced genome of an enslaved algal nucleus. Nature 410, 1091–1096.

Doust AB, Marai CNJ, Harrop SJ, Wilk KE, Kurmi PMG, Scholes GD (2004) Developing a structure–function model for the cryptophyte phycoerythrin 545 using ultrahigh resolution crystallography and ultrafast laser spectroscopy. J Mol Biol 344, 135–153.

Doust AB,Wilk KE, Curmi PMG, Scholes GD (2006) The photophysics of cryptophyte light harvesting. J Photochem Photobiol 184, 1–17.

Dutkiewicz A, Volk H, George SC, Ridley J, and Buick R (2006) Biomarkers from Huronian oil-bearing fluid inclusions: An uncontaminated record of life before the Great Oxidation Event. Geology 34 (6): 437-440.

Engelmann TW (1902) Untersuchungen über die qualitativen Beziehungen zwieschen Absorbtion des Lichtes und Assimilation in Pflanzenzellen. I. DasMikrospectraphotometer, ein Apparat zur qualitativen Mikrospectralanalyse. II.

Experimentelle Grundlangen zur Ermittelung der quantitativen Beziehungen zwieschen Assimilationsenergie und Absorptiongrösse. III. Bestimmung der Vertheilung der Energie im Spectrum von Sonnenlicht mittels Bacterien-methode und quantitativen Mikrospectralanalyse. Bot Z 42:81–105.

Elzhov TV, Mullen KM, Speiss A-N, Bolker B. minpack.lm: R Interface to the Levenberg-Marquardt nonlinear least-squares algorithm found in MINPACK, plus support for bounds. https://cran.r-project.org/web/packages/minpack.lm/minpack.lm.pdf Accessed May 15, 2023.

Finstad A, Andersen T, Larsen S, Tominaga K, Blumentrath S, de Wit HA, et al. (2016) From greening to browning: Catchment vegetation development and reduced S-deposition promote organic carbon load on decadal time scales in Nordic lakes. *Sci Rep* 6, 31944.

Förster T (1948) Intermolecular energy migration and fluorescence. Ann Phys 437 (1-2) 55-75. https://doi.org/ Foerster, T. (1948). Intermolecular energy migration and fluorescence. Annals Of Physics, 437(1-2), 55–75.

Frankenberg N, Mucougawa K, Kohchi T, Lagarias JC (2001) Functional genomic analysis of the HY2 family of ferredoxin-dependent bilin reductases from oxygenic photosynthetic organisms. Plant Cell 13 (4) 965-978.

Frankenberg N, Lagarias JC (2003) Phycocyanobilin:ferredoxin oxidoreductase of Anabaena sp. PCC 7120: biochemical and spectroscopic characterization. J Biol Chem 278 (11) 9219-9226.

Gaidukov N (1902) Über den Einfluss farbigen Lichts auf die Färbung lebender Oscillarien. Abh Preuss Akad Wiss 5:1–36

Gaidukov N (1903) Die farbervonderung bei den prozessen der komplementoren chromatischen adaptation. Ber Dtsch Bot Ges 21:517–22

Gallegos CL, Jordan TE, Hedrick SS (2009) Long-term dynamics of phytoplankton in the Rhode River, Maryland (USA). Estuar. Coast 33: 471-484.

Gervais F (1997) Light-dependent growth, dark survival, and glucose uptake by cryptophytes isolated from a freshwater chemocline. J. Phycol. 33:18–25.

Gantt E, Edwards MR, Provasoli L (1971) Chloroplast structure of the Cryptophyceae: evidence for phycobiliproteins within intrathylakoidal spaces. J. Cell Biol., 48, 280–290.

Gantt E, Lipschultz CA (1972) Phycobilisomes of *Porphyridium cruentum*. J Cell Biol 54 (2): 313-324.

Glazer AN, Cohen-Bazire G (1975) A comparison of cryptophycean phycocyanins. Arch Microbiol 104: 29-32.

Glazer AN, Apell GS, Hixon CS, Bryant DA, Rimon S, Brown DM (1976) Biliproteins of cyanobacteria and Rhodophyta: homologous family of photosynthetic accessory pigments. Proc Natl Acad Sci USA 73 (2) 428-431.

Glazer AN, Williams RC, Yamanaka G, Schachman, HK (1979) Characterization of cyanobacterial phycobilisomes in zwitterionic detergents. Proc Natl Acad Sci USA 76 (12) 6162-6166.

Glazer AN (1989) Light Guides: directional energy transfer in a photosynthetic antenna. J Biol Chem 264 (1): 1-4.

Glazer AN, Wedemayer GJ (1995) Cryptomonad biliproteins– an evolutionary perspective. Photosynth Res 46, 93–105.

Granick, S (1965) Evolution of Heme and Chlorophyll. In: Bryson V and Vogel HJ (eds) Evolving Genes and Proteins. Academic Press, New York.

Gray MW, Doolittle WF (1982) Has the Endosymbiont Hypothesis Been Proven? Microbiol Rev 46 (1): 1-42.

Green B (2019) What happened to the phycobilisome? Biomolecules 9(11): 748.

Greenwold MJ, Cunningham BR, Lachenmyer EM, Pullman JM, Richardson TL, Dudycha JL (2019) Diversification of light capture ability was accompanied by the evolution of phycobiliproteins in cryptophyte algae. Proc. R. Soc. B 286: 20190655.

Guard-Friar D, MacColl R (1986) Subunit separation (α,α',β) of cryptomonad biliproteins. Photochem Photobio S 43(1): 81-85.

Guglielmi G, Cohen-Bazire G, Bryant DA (1981) The structure of *Gleobacter violaceus* and its phycobilisomes. Arch Microbiol 129: 181-189.

Hammer A, Schumann R, Schubert H (2002) Light and temperature acclimation of *Rhodomonas salina* (Cryptophyceae): photosynthetic performance. Aquat. Microb. Ecol. 29: 287-296.

Harrop SJ, Wilk KE, Dinshaw R, Collini E, Mirkovic T, Teng CY, et al. (2014) Single-residue insertion switches the quaternary structure and exciton states of cryptophyte light-harvesting proteins. Proc Natl Acad Sci U S A 111:E2666-75

Haxo FT, Fork DC (1959) Photosynthetically active accessory pigments of cryptomonads. Nature 184: 1051-1052.

Heidenreich KM, Richardson TL (2020) Photopigment, absorption, and growth responses of marine cryptophytes to varying spectral irradiance. J Phycol 56, 507–520.

Hill DRA, Rowan KS (1989) The biliproteins of the Cryptophyceae. Phycologia 28:455-463.

Hiller RG, Scaramuzzi CD, Breton J (1992) The organization of photosynthetic pigments in a cryptophyte alga: a linear dichroism study. Biochim Biophys Acta 1102 (3) 360–364.

Hoef-Emden K (2008) Molecular phylogeny of phycocyanin containing cryptophytes: evolution of biliproteins and geographical distribution. J. Phycol., 44, 985–993.

Hoef-Emden K, Archibald JM (2017). Cryptophyta (Cryptomonads). In: Archibald, J., Simpson, A., Slamovits, C. (eds) Handbook of the Protists. Springer, Cham.

Hoef-Emden (2018) Revision of the genus *Chroomonas* HANSGIRG: the benefits of DNA-containing specimens. Protist 169: 662-681.

Hutchinson GE (1961) The paradox of the plankton. Am Nat 95(882): 137-145.

Kamiya A, Miyachi S (1984) Effects of light quality on formation of 5-aminolevulinic acid, phycoerythrin and chlorophyll in *Cryptomonas* sp. cells collected from the subsurface chlorophyll layer. Plant & Cell Physiol. 25 (5): 831-839.

Keeling PJ (2004) Diversity and evolutionary history of plastids and their hosts. Am J Bot 91(10): 1481–1493.

Kehoe DM, Gutu A (2006) Responding to color: the regulation of complementary chromatic adaptation. Annu Rev Plant Biol 57: 127-150.

Kieselbach T, Cheregi O, Green BR, Funk C (2018) Proteomic analysis of the phycobiliprotein antenna of the cryptophyte alga *Guillardia theta* cultured under different light intensities. Photosynth Res 135:149-163.

Kiili M, Pulkkanen M, Salonen K (2009) Distribution and development of under-ice phytoplankton in 90-m deep water column of Lake Päijänne (Finland) during spring convection. Aquat. Ecol. 43:707–13.

Kirk JTO (2011) Light and Photosynthesis in Aquatic Ecosystems, 3rd edition. Cambridge University Press.

Klaveness D (1989) Biology and ecology of the cryptophyceae: status and challenges. Biol Oceanog 6: 257-270.

Klotz AV, Glazer AN (1985) Characterization of the bilin attachment sites in R-phycoerythrin. J Biol Chem 260 (8) 4856-4863.

Lane CE, Archibald JM (2008) New marine members of the genus *Hemiselmis* (Cryptomonadales, Cryptophyceae). J Phycol 44: 439–450.

Latsos C, van Houcke J, Blommaert L, Verbeeke GP, Kromkamp J, Timmermans KR (2021) Effect of light quality and quantity on productivity and phycoerythrin concentration in the cryptophyte *Rhodomonas* sp. J Appl Phycol 33: 729-741.

Lawrenz E, Pinckney JL, Ranhofer ML, MacIntyre HL, Richardson TL (2010) Spectral irradiance and phytoplankton community composition in a blackwater-dominated estuary, Winyah Bay, SC, USA. Estuar Coast 33(5): 1186-1201.

Le Moal M, Gascuel-Odoux C, Ménesguen A, Souchon Y, Étrillard C, Levain A, et al. (2019) Eutrophication: a new wine in an old bottle? Sci. Total Environ. 651: 1-11.

Ledermann B, Béjà O, Frankenberg-Dinkel N (2016) New biosynthetic pathway for pink pigments from uncultured oceanic viruses. Environ Microbiol 18 (12) 4337-4347.

Lee J, Kim D, Bhattacharya D, Yoon HS (2019) Expansion of phycobilisome linker gene families in mesophilic red algae. Nat. Commun. 10, 4823.

Lewis MR, Smith JC (1983) A small volume, short-incubation-time method for measurement of photosynthesis as a function of incident irradiance. Mar. Ecol. Prog. Ser. 13: 99-102.

Liu LN, Chen XL, Zhang YZ, Zhou BC (2005) Characterization, structure and function of linker polypeptides in phycobilisomes of cyanobacteria and red algae: an overview. Biochim Biophys Acta 1708:133–142.

Ma J, You X, Sun S, Wang X, Qin S, Sui S (2020) Structural basis of energy transfer in Porphyridium purpureum phycobilisome. Nature 579: 146–151.

MacColl R, Guard-Friar D (1983) Phycocyanin 612: a biochemical and photophysical study. Biochemstry-US 22(24): 5568-5572.

MacColl R, Guard-Friar D (1987) Phycobiliproteins. Boca Raton, FL

MacColl R (1998) Cyanobacterial Phycobilisomes. J Struct Biol 124 (2-3): 311-334.

Magalhães K, Santos AL, Vaulot D, Oliveira MC (2021) *Hemiselmis aquamarina* sp. nov. (Cryptomonadales, Cryptophyceae), a cryptophyte with a novel phycobilin type (Cr-PC 564). Protist 172: 125832.

Maia R, Gruson H, Endler JA, White TE (2019) pavo 2: new tools for the spectral and spatial analysis of colour in R. Methods in Ecol. Evol. 10(7).

Mauzerall, D (1962) The Photoreduction of Porphyrins: Structure of the Products. J Am Chem Soc 84 (12): 2437-2445.

Mendes CRB, Tavano VM, Dotto TS, Kerr R, de Souza MS, Garcia CAE, Secchi ER (2018) New insights on the dominance of cryptophytes in Antarctic coastal waters: A case study in Gerlache Strait. *Deep-Sea Res.Pt II* 149: 161-170.

Mereschkowsky C (1905) Uber Natur ued Ursprung der Chromatophoren im Pflanzenreiche. Biologisches Centralblatt 25: 593-604.

Michie KA, Harrop SJ, Rathbone HW, Wilk KE, Teng CY, Hoef-Emden K, et al. (2023) Molecular structures reveal the origin of spectral variation in cryptophyte light harvesting antenna proteins. Protein Sci 32: e4586.

Nagy JO, Bishop JE, Klotz AV, Glazer AN, Rapoport H (1985) Bilin attachment sites in the α, β, and γ subunits of R-Phycoerythrin: structural studies on singly and doubly linked phycourobilins. J Biol Chem 260 (8) 4864-4868.

Ó hEocha C, Raftery M (1959) Phycoerythrins and phycocyanins of cryptomonads. Nature 184: 1049-1051

Ó hEocha C, Ó Carra PO, Mitchell D (1964) Biliproteins of cryptomonad algae. Proc Roy Irish Acad 63B: 191-200.

Oborník M (2019) Endosymbiotic evolution of algae, secondary heterotrophy and parasitism. Biomolecules 9 (7): 266.

Ojala A (1993) The influence of light quality on growth and phycobiliprotein/chlorophyll a fluorescence quotients of some species of freshwater algae in culture. Phycologia, 32, 22–28.

Ong L, Glazer AN (1987) R-phycocyanin II, a new phycocyanin occurring in marine Synechococcus species: identification of the terminal energy acceptor bilin in phycocyanins. J Biol Chem 262 (13) 6323-6327.

Ong L, Glazer AN (1991) Phycoerythrins of marine unicellular cyanobacteria: bilin types and locations and energy transfer pathways in Synechococcus spp. Phycoerythrins. J Biol Chem 266 (15) 9515-9527.

Overkamp KE, Langklotz S, Aras M, Helling S, Marcus K, Bandow JE, Hoef-Emden K and Frankenberg-Dinkel N (2014) Chromophore composition of the phycobiliprotein Cr-PC577 from the cryptophyte *Hemiselmis pacifica*. Photosynth Res 122: 293–304.

Pastoureaud A, Dupuy A, Chrétiennot-Dinet MJ, Lantoine F, Loret P (2003) Red coloration of oysters along the French Atlantic coast during 1998 winter season: implication of nanoplanktonic cryptophytes. Aquaculture 228: 225-235.

Pedrós-Alió C, Massana R, Latasa M, García-Cantizano J, Gasol JM (1995) Predation by ciliates on a metalimnetic Cryptomonas population: feeding rates, impact and effects of vertical migration. J. Plankton Res. 17:2131–54.

Pinckney JL, Millie DF, Howe KE, Paerl HW, Hurley JP (1996) Flow scintillation counting of ^{14}C-labeled microalgal photosynthetic pigments. J. Plankton Res. 18:1867-80.

Platt T, Gallegos CL, Harrison WG (1980) Photoinhibition of photosynthesis in natural assemblages of marine phytoplankton. J. Mar. Res. 38: 687-701.

Price TD, Qvarnström A, Irwin DE (2003) The role of phenotypic plasticity in driving evolution by genetic assimilation. Proc R Soc Lond B 270: 1433-1440.

Rathbone HW (2021) Tracing the evolutionary history of the cryptophyte light harvesting antenna: a structural perspective. Dissertation, School of Physics, UNSW, Sydney.

Rathbone HW, Michie KA, Landsberg MJ, Green BR, and Curmi PMG (2021) Scafolding proteins guide the evolution of algal light harvesting proteins. Nat Commun 12, 1890.

Richardson TL (2022) The colorful world of cryptophyte phycobiliproteins. J Plankton Res 44(6): 814-826

Roulet N, Moore TR (2006) Browning the waters. Nature 444: 283-284.

Roesler CS (1998) Theoretical and experimental approaches to improve the accuracy of particulate absorption coefficients derived from the quantitative filter technique. Limnol. Oceanogr. 43:1649–60.

Sagan L (1967) On the origin of mitosing cells. J Theor Biol 14: 225-274.

Sanfilippo JE, Garczarek L, Partensky F, Kehoe DM (2019) Chromatic Acclimation in Cyanobacteria: A Diverse and Widespread Process for Optimizing Photosynthesis. Annu Rev Microbiol 73:407-433.

Schimper AFW (1883) Uber die Entwicklung der Chlorophyllkorner and Farbkorper. Botanische Zeitung 41: 105-113.

Scholes GD, Mirkovic T, Turner DB, Fassioli F, Buchleitner A (2012) Solar light harvesting by energy transfer: from ecology to coherence. Energy Environ Sci 5: 9374.

Shibata BYK (1958) Spectrophotometry of intact biological materials. J. Biochem. 45:599–624.

Shih PM, Matzke J (2013) Primary endosymbiosis events date to the later Proterozoic with cross-calibrated phylogenetic dating of duplicated ATPase proteins. Proc Natl Acad Sci USA 110:12355–12360.

Simpson GG (1953) The Baldwin effect. Evolution 7:110-117.

Six C, Thomas JC, Garczarek L, Ostroski M, Dufresne A, Blot N, et al. (2007) Diversity and evolution of phycobilisomes in marine Synechococcus spp.: a comparative genomics study. Genome Biol 8, R259.

Spangler LC, Yu M, Jeffrey PD, Scholes GD (2022) Controllable phycobilin modification: an alternative photoacclimation response in cryptophyte algae. ACS Cent. Sci, 8, 340–350.

Stadnichuk IN (1995) Phycobiliproteins: determination of chromophore composition and content. Phytochem Analysis 6: 281-288.

Stadnichuk IN, Tropin IV (2014) Antenna replacement in the evolutionary origin of chloroplasts. Microbiology 83 (4): 385-402.

Stadnichuk IN, Krasilnikov PM, Zlenko DV (2015) Cyanobacterial Phycobilisomes and Phycobiliproteins. Microbiology 84 (2): 101-111.

Stomp M, Huisman J, de Jongh F, Veraat AJ, Gerla D, Rijkeboer M, et al. (2004) Adaptive divergence in pigment composition promotes phytoplankton diversity. Nature 432: 104-107.

Stomp M, Huisman J, Vörös L, Pick FR, Laamanen M, Haverkamp T, Stal LJ (2007a) Colorful coexistence of red and green picocyanobacterial in lakes and seas. Ecol Lett. 10(4): 290-298.

Stomp M, Huisman J, Stahl LJ, Matthijs HCP (2007b) Colorful niches of phototrophic microorganisms shaped by vibrations of the water molecule. ISME J, 1, 271–282.

Stomp M, van Dijk MA, van Overzee HMJ, Wortel MT, Sigon CAM, Egas M, et al. (2008) The timescale of phenotypic plasticity and its impact on competition in fluctuating environments. Am Nat. 172(5): 169-185

Sui SF (2021) Structure of Phycobilisomes. Annu Rev Biophys 50, 53–72.

Uzzell T, Spolsky C (1974) Mitochondria and Plastids as Endosymbionts: A Revival of Special Creation? The similarities between cellular organelles and prokaryotes are probably primative features retained independently from a common ancestor. Am Sci 62 (3): 334-343

Van der Weij-De Wit CD, Doust AB, van Stokkum IHM, Dekker JP, Wilk KE, Curmi PMG, van Grondelle R (2008) Phycocyanin sensitizes both photosystem I and photosystem II in cryptophyte *Chroomonas* CCMP270 cells. Biophys J 94: 2423–2433.

Vesk M, Jeffrey SW (1977) Effect of blue-green light on photosynthetic pigments and chloroplast structure in unicellular marine algae from six classes. J Phycol 13: 280–288.

Watanabe M, Ikeuchi M (2013) Phycobilisome: architecture of a light-harvesting supercomplex. Photosyn Res 116: 265-276.

Wedemayer GJ, Kidd DG, Wemmer DE, Glazer AN (1992) Phycobilins of cryptophycean algae: Occurrence of dihydrobiliverdin and mesobiliverdin in cryptomonad biliproteins. J Biol Chem 267(11):7315–7331

Wedemayer GJ, Kidd DG, Glazer AN (1996) Cryptomonad biliproteins: Bilin types and locations. Photosyn Res 48: 163-170.

Wemmer DE, Wedemayer GJ, Glazer AN (1993) Phycobilins of the cryptophycean algae: novel linkage of dihydrobiliverdin in a phycoerythrin 555 and a phycocyanin 645. J Biol Chem 268(3): 1658-1669.

Westermann M, Wehrmeyer W (1995) A new type of complementary chromatic adaptation exemplified by *Phormidium* sp. C86: changes in the number of peripheral rods and in the stoichiometry of core complexes in phycobilisomes. Arch Microbiol 164: 132-141.

Wilk KE, Harrop SJ, Jankova L, Edler D, Keenan G, Sharples F, et al. (1999) Evolution of a light-harvesting protein by addition of new subunits and rearrangement of conserved elements: crystal structure of a cryptophyte phycoerythrin at 1.63-A resolution. Proc Natl Acad Sci USA 96(16), 8901–8906.

Zhang J, Ma J, Liu D, Qin S, Sun S, Zhao J, Sui S (2017) Structure of phycobilisome from the red alga *Griffithsia pacifica*. Nature 551: 57–63.